INFORMATION TO USERS

This was produced from a copy of a document sent to us for microfilming. While the most advanced technological means to photograph and reproduce this document have been used, the quality is heavily dependent upon the quality of the material submitted.

The following explanation of techniques is provided to help you understand markings or notations which may appear on this reproduction.

1. The sign or "target" for pages apparently lacking from the document photographed is "Missing Page(s)". If it was possible to obtain the missing page(s) or section, they are spliced into the film along with adjacent pages. This may have necessitated cutting through an image and duplicating adjacent pages to assure you of complete continuity.
2. When an image on the film is obliterated with a round black mark it is an indication that the film inspector noticed either blurred copy because of movement during exposure, or duplicate copy. Unless we meant to delete copyrighted materials that should not have been filmed, you will find a good image of the page in the adjacent frame.
3. When a map, drawing or chart, etc., is part of the material being photographed the photographer has followed a definite method in "sectioning" the material. It is customary to begin filming at the upper left hand corner of a large sheet and to continue from left to right in equal sections with small overlaps. If necessary, sectioning is continued again—beginning below the first row and continuing on until complete.
4. For any illustrations that cannot be reproduced satisfactorily by xerography, photographic prints can be purchased at additional cost and tipped into your xerographic copy. Requests can be made to our Dissertations Customer Services Department.
5. Some pages in any document may have indistinct print. In all cases we have filmed the best available copy.

University
Microfilms
International

300 N. ZEEB ROAD, ANN ARBOR, MI 48106
18 BEDFORD ROW, LONDON WC1R 4EJ, ENGLAND

7923764

PRYSTOWSKY, MICHAEL BENNETT
INHIBITION OF THE CLASSICAL COMPLEMENT PATHWAY BY
SYNTHETIC PEPTIDES FROM THE C(GAMMA)2 DOMAIN OF
IMMUNOGLOBULIN G.

CITY UNIVERSITY OF NEW YORK, PH.D., 1978

University
Microfilms
International 300 N. ZEEB ROAD, ANN ARBOR, MI 48106

INHIBITION OF THE CLASSICAL COMPLEMENT PATHWAY BY SYNTHETIC PEPTIDES FROM THE $C_{\gamma}2$ DOMAIN OF IMMUNOGLOBULIN G

by

MICHAEL B. PRYSTOWSKY

A dissertation submitted to the Graduate Faculty in Biomedical Sciences in partial fulfillment of the requirements for the degree of Doctor of Philosophy, The City University of New York.

1978

This manuscript has been read and accepted for the Graduate Faculty in Biomedical Science in satisfaction of the dissertation requirement for the degree of Doctor of Philosophy.

9/12/78
Date

Chairman of Examining Committee

9/12/78
Date

Executive Officer

Doris J. Bucher

James G Wetmur

Jerome L Schulman

P G Katsoyannis

H. G. Kunkel

Bruce W Erickson

The
City University
of
New York

Abstract

INHIBITION OF THE CLASSICAL COMPLEMENT PATHWAY BY SYNTHETIC PEPTIDES FROM THE $C_{\gamma}2$ DOMAIN OF IMMUNOGLOBULIN G

by

MICHAEL B. PRYSTOWSKY

Advisers: Professors Bruce W. Erickson and J. Michael Kehoe

The C1-binding site of immunoglobulin G is thought to reside in the $C_{\gamma}2$ domain. Previous studies by other groups have implicated the presence of a tryptophan residue and cationic residues at or near this site. Since these residues may be necessary for binding to C1q, likely peptide segments from $C_{\gamma}2$ containing such residues were synthesized and examined for their ability to interact with C1q.

Three segments from the $C_{\gamma}2$ domain of the gamma chain of IgG1 (residues 275-290) were synthesized by the solid-phase method and purified to homogeneity using reverse-phase high-pressure liquid chromatography. The following seven peptides were examined for inhibition of the classical complement pathway: a hexadecapeptide (16) consisting of γ-chain residues 275-290 (Phe-Asn-Trp-Tyr-Val-Asp-Gly-Val-Gln-Val-His-Asn-Ala-Lys-Thr-Lys), which contained Trp-277 and the cationic residues His-285, Lys-288, and Lys-290; an N^{i}-formyl derivative of peptide 16

(16F); a decapeptide (10) comprising the γ-chain residues 281-290 and including the three cationic residues; an N^{α}-acetylpentapeptide (A5) consisting of the γ-chain residues 275-279 and containing the hydrophobic region around Trp-277; an N^{i}-formyl derivative of peptide A5 (A5F); $\underline{N}^{\alpha}$-acetyl-glutamyl-tryptophanyl-tyrosyl-glutamyl-arginyl-glycine (A6J), which in the unacetylated form has been shown by Johnson and Thames to inhibit complement fixation; and phenylalanyl-glycyl-leucyl-alanyl-arginine (FR5), an unrelated hydrophobic peptide.

When these peptides were assayed in a hemolytic C1 inhibition assay, four peptides exhibited the following molar inhibitory activities relative to monomeric human IgG taken as 100%: 16F = 50%, 10 = 40%, A6J = 50%, and A5F = 2700%. Inhibition of the classical complement pathway in this assay could be achieved by blocking the action of C1q, C1r, C1s, or C4. Peptide A5F was a potent inhibitor of the classical complement pathway. It showed 50% inhibition at a concentration of 3 micromolar and thus was 27 times more active than monomeric IgG. When the formyl group was removed from the indole nitrogen of tryptophan, inhibitory activity decreased at least tenfold.

When examined by equilibrium dialysis, none of the inhibitory peptides showed detectable binding to C1q under conditions where 5% binding would have corresponded to an association constant of 1×10^4 l.mol^{-1}. If A5F inhibits through binding to C1q, it should have shown an association constant for C1q of at least 4×10^5 l.mol^{-1}. Thus the C1q-binding site of IgG does not include the tryptophan residue at position 277. Since the expected association constants for peptides 16F, 10, and A6J were 1×10^4 l.mol^{-1} or less, these equilibrium dialysis results neither support nor preclude the binding of these peptides to C1q. While the 5-residue hydrophobic segment containing tryptophan-277 does not bind to C1q, the adjacent 10-residue cationic segment containing histidine-285, lysine-288, and lysine-290 may be a part of the C1q-binding site of IgG.

ACKNOWLEDGMENTS

I am grateful to both of my mentors: Dr. Bruce Erickson for his help, enthusiasm, and direction in the execution of this project and Dr. J. Michael Kehoe for the initiation of this project and for his guidance throughout it.

Many other people have generously given their advice and assistance. I am grateful to Dr. Bruce Merrifield and the Merrifield group for helpful discussions on the solid-phase method, to Dr. Stanford Moore and Dr. Peter Blackburn for their help and advice in performing amino acid analyses, to Dr. Robert Winchester and Dr. Henry Kunkel for providing Fc and monomeric IgG proteins and for their helpful discussions on immune aggregates and C1q isolation, and to Dr. James Wetmur for many enlightening discussions and for the sedimentation analysis of IgG1 Pen.

In addition, I wish to thank Dr. David Cowburn and William Wittbold for their help with the NMR spectroscopy of peptide A5F; Erdwin Chua, Ray Martin, and Dr. John Thornton for their help with the computer graphics of IgG; Mark Fulk for the computer program to analyze the C1 inhibition assay data and for his help with the UNIX text editor; my wife, Janet Hill Prystowsky, for her advice and help with the oral and written presentations of this project; Dr. Rochelle Seide-Kehoe for her help in preparing IgG1 Pen; Dr. Ann

Erickson for her assistance with the polyacrylamide gel electrophoresis; and Dr. Cecille Unson for a sample of the pure synthetic peptide FR5.

Finally, I am pleased to acknowledge the financial support of the Biomedical Sciences Program of The City University of New York and The Department of Microbiology at The Mount Sinai School of Medicine.

DEDICATION

This thesis is dedicated to my wife
JANET HILL PRYSTOWSKY
and to my parents
DRS. MILTON AND ROSE PRYSTOWSKY
for their continuing support throughout
each phase of my education.

CONTENTS

CHEMICAL AND IMMUNOLOGICAL ABBREVIATIONS

AcOH	acetic acid
Aoc	*tert*-isoamyloxycarbonyl
Boc	*tert*-butyloxycarbonyl
Bzl	benzyl
BuOH	1-butanol
$C_\gamma 2$	second constant homology region (domain) from the γ-chain of IgG; similarly $C_\gamma 1, C_\gamma 3, C_\mu 4, C_L$
C1	first component in the classical complement pathway; a trimolecular complex composed of C1q, C1r, and C1s
Cn	the n-th protein component of the serum complement cascade
C-EDTA	functionally complement proteins C3-C9
3-ClZ	3-chlorobenzyloxycarbonyl
2,6-Cl_2 Bzl	2,6 dichlorobenzyl
DCC	*N*,*N*'-dicyclohexylcarbodiimide
DIEA	*N*,*N*-diisopropylethylamine
DMF	*N*,*N*-dimethylformamide
DNA	deoxyribonucleic acid
DNase I	deoxyribonuclease I
Dnp	2,4-dinitrophenyl
EAC4	sheep erythrocytes coated with immunoglobulin G and human C4

EDTA	*N*,*N*,*N'*,*N'*-ethylenediaminetetraacetic acid
EtOAc	ethyl acetate
Fab	amino-terminal half of the immunoglobulin molecule containing the antigen-binding region
Facb	immunoglobulin G lacking the $C_{\gamma 3}$ domains
Fc	carboxyl-terminal half of the immunoglobulin molecule containing the biological effector functions
$(Fc)_{5}\mu$	the 5 covalently linked Fc regions of immunoglobulin M
For	formyl
^{3}H	radioisotopic hydrogen, tritium
HOBt	1-hydroxybenzotriazole
HPLC	high-pressure liquid chromatography
^{125}I	radioisotopic iodine
I_{50}	50% inhibition of C1-mediated hemolysis
IgG	immunoglobulin class G; similarly IgM
IgG1	IgG subclass 1; similarly 2,3, and 4
K_{ass}	association constant
k'	number of column volumes that a compound is retained during HPLC

$\underline{M}_{\underline{r}}$	molecular weight ratio relative to hydrogen
N^{α}	alpha-amino nitrogen
N^{i}	indole nitrogen
NMP	*N*-methyl-2-pyrrolidinone
NMR	nuclear magnetic resonance
PBS	phosphate buffered saline
PBSA	PBS containing azide
OBzl	benzyl ester
Pyr	pyridine
Ⓡ	resin
$\underline{R}_{\underline{f}}$	retardation factor; ratio of compound migration to solvent front migration
SGVB	veronal-buffered saline containing sucrose and gelatin
TFA	trifluoroacetic acid
TLC	thin-layer chromatography
TLE	thin-layer electrophoresis
Tos	4-toluensulfonyl (tosyl)
UV	ultraviolet
Z	benzyloxycarbonyl

AMINO ACID ABBREVIATIONS

A, Ala	alanine
B, Asx	asparagine or aspartic acid
C, Cys	cysteine
D, Asp	aspartic acid
E, Glu	glutamic acid
F, Phe	phenylalanine
G, Gly	glycine
H, His	histidine
I, Ile	isoleucine
K, Lys	lysine
L, Leu	leucine
M, Met	methionine
N, Asn	asparagine
P, Pro	proline
Q, Gln	glutamine
R, Arg	arginine
S, Ser	serine
T, Thr	threonine
V, Val	valine
W, Trp	tryptophan
Y, Tyr	tyrosine
Z, Glx	glutamine or glutamic acid

TITLES OF TABLES

TITLES OF FIGURES

INTRODUCTION

A. Immunoglobulin and Complement

The immunoglobulin (Ig) molecule can be divided functionally into two regions (Fig. 1) . The amino-terminal half of the immunoglobulin molecule contains the antigen-binding region (Fab), which binds to substances (antigenic determinants) that the host recognizes as being foreign. The carboxyl-terminal half (Fc) of the immunoglobulin molecule initiates a variety of biological effector functions, including recruitment of the complement system, binding to specific cell-surface proteins, and binding to staphylococcal protein A. This thesis is concerned with the interaction between immunoglobulin and complement, two groups of serum proteins that comprise the major humoral host defense system.

In the normal homeostatic state, binding of the Fab region to a multivalent antigen leads to aggregation of Fc regions and to activation of the classical complement pathway. When activation of the complement system is directed at an invading microorganism, this usually leads to the destruction and clearance of that organism. The ability of immunoglobulin to recognize an invading organism and initiate its destruction through activation of the complement system provides a powerful and vital function in the host immune response (Fig. 2).

Activation of the complement system by immune complexes is not always benficial to the host. Destruction of host tissue can result from complement activation by extensive formation of immune complexes or by autoimmune recognition. In immune-complex glomerulonephritis (1) and in the vasculitis associated with hepatitis B antigenemia (2), the host is overwhelmed by the amount of immune complexes formed and is unable to clear them effectively. The immune injury associated with rheumatoid arthritis (3) and Hashimoto's thyroiditis (4) results from recognizing an altered or native host IgG (5 and 6) or a previously hidden host thyroglobulin (7) as being foreign. Autoimmune diseases and immune complex diseases, such as anti-glomerular basement membrane glomerluonephritis (1) and systemic lupus erythematosus (8), can produce systemic lesions attributable to an autoimmune response.

The pathophysiological mechanism of host tissue destruction probably results from the following series of events (9): immune complex activation of the classical complement pathway, production of anaphylatoxins and chemotactic factors, release of vasoactive amines, tissue deposition of immune complexes, inflammation, and tissue destruction resulting from cellular invasion and release of cellular lysosomal enzymes. This immunopathological mechanism is initiated by the binding of immune complexes to C1q, a subcomponent of the first component of serum complement. Specific inhibition of immune complex-activation of C1 would diminish the occurrence of this immunopathogenic mechanism and the extent to which lesions are formed in the diseases just mentioned. One approach to obtain a specific inhibitor of the IgG-C1 interaction is to study the biochemical nature of this interaction and to define its structural requirements.

The general approach of localizing particular structure-function correlates in proteins has been well documented for staphylococcal nuclease and ribonuclease A (reviewed in (10)). Both of these enzymes have been enzymatically degraded and the fragments necessary for activity have been isolated and characterized (11-14). Since the enzymatic fragments could be noncovalently associated with recovery of enzymatic activity, it was initially assumed and subsequently demonstrated that synthetic peptides could be associated with inactive enzyme fragments to produce enzymatic activity (15-17). By making amino acid substitutions in the synthetic peptides, the residues essential for enzymatic activity were determined and the active site of each enzyme was defined (18-21).

During the past three decades, many investigators have attempted to define the portion of the IgG molecule that binds to the first component of serum complement (C1). This thesis has explored the structural requirements for the binding of IgG to C1 using synthetic peptide segments derived from an IgG1 myeloma protein.

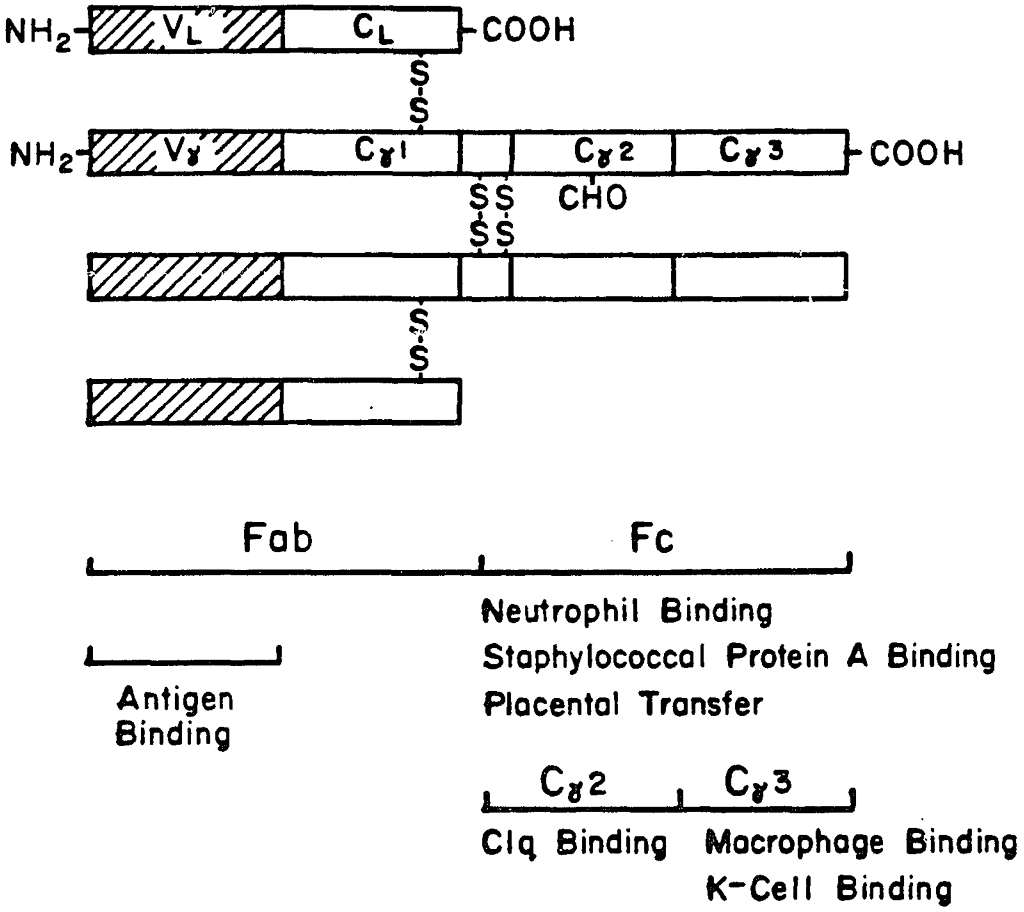

Fig. 1. Structure and function of immunoglobulin G. IgG is comprised of four disulfide bonded chains, two light chains consisting of two domains (V_L and C_L) and two heavy chains consisting of four domains (V_γ, $C_\gamma 1$, $C_\gamma 2$, and $C_\gamma 3$). Each heavy chain also contains an oligosaccharide (CHO) covalently linked to the $C_\gamma 2$ domain. The variable domains (V) in the Fab region function as a receptor for antigens. The Fc region contains most of the effector functions of IgG. Neutrophil binding, staphylococcal protein A binding, and placental transfer all require an intact Fc region, whereas C1q binding only requires the $C_\gamma 2$ domain and macrophage and cytotoxic K cell binding only require the $C_\gamma 3$ domain.

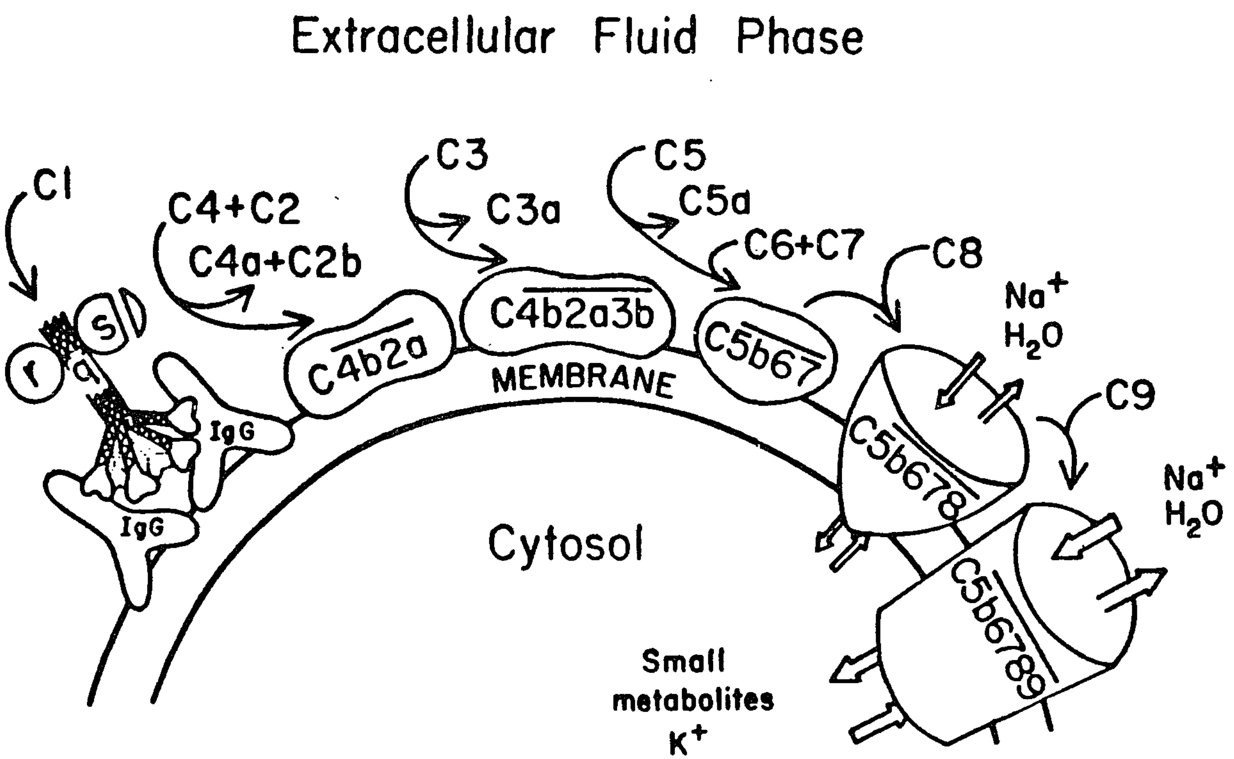

<u>Fig</u>. <u>2</u>. Membrane attack through the classical complement pathway. The binding of C1q to immune complexes leads to the autoactivation of C1r and subsequent activation and cleavage of C1s. C$\overline{1s}$ activates C4 and C2 through enzymatic cleavage to form the classical C3 convertase, C$\overline{4b2a}$. By cleaving C3 and incorporating C3b, C3 convertase becomes C5 convertase, C$\overline{4b2a3b}$. After cleavage of C5, components C5b through C9 are inserted into the plasma membrane in stages to produce a transmembrane channel, C5b-9. This channel disrupts the normal electrochemical equilibrium across the membrane by reversing the net ion fluxes to Na$^+$ in and K$^+$ out. Cell death probably results from this and the loss of small energy (ATP) and intermediary (monosaccharide) metabolites.

B. C1-Binding Site of Immunoglobulin G

The interaction of immunoglobulin with serum complement was described as early as 1899 by Morgenroth and Ehrlich (22). In order to localize the complement binding site on IgG, it was necessary to obtain reproducible methods for fragmenting the immunoglobulin molecule. Enzymatic digestion of IgG antibodies using papain was first described by Pope (23,24) in 1939 and confirmed by Peterman in the 1942 and 1946 (25,26). A refined version of this method and a thorough description of the fragments produced was obtained by Porter in 1959 for rabbit IgG (27) and by Kunkel and coworkers in 1960 for human IgG (28). Porter found that enzymatic digestion of immunoglobulin G using crystalline papain produced an antigen-binding region (Fab) and a crystalline region (Fc) that contained most of the antigenic determinants. In 1962 Ishizaka et al. (29) discovered that the Fc region of IgG was responsible for the passive cutaneous anaphylaxis reaction and complement activation. Studies by Utsumi (30) using progressive enzyme degradation of the Fc region demonstrated that as the amino-terminal portion of Fc was lost, complement binding also disappeared.

In 1969 Kehoe et al. (31) showed that the amino-terminal portion of Fc contained the complement-binding site. By treating a murine myeloma protein with cyanogen bromide, they produced a 62-residue fragment which corresponded to the amino-terminal half of the $C_{\gamma}2$ domain. When bound to latex particles, this fragment was able to activate complement. However, this assay could not differentiate between the activation of complement through the classical pathway and activation through the alternative pathway. More convincing evidence that the $C_{\gamma}2$ domain was the binding site for the first component of serum complement was subsequently provided by other laboratories. Colomb and Porter (32) used IgG molecules lacking the $C_{\gamma}3$ domain (Facb) and Yasmeen et al. (33) used isolated $C_{\gamma}2$ domains to show that these IgG fragments could bind to C1 and inhibit the classical complement pathway. These investigators did not demonstrate the direct binding of the IgG fragments to C1q. Even though these studies are not conclusive they are consistent with the hypothesis that immunoglobulin domains form functional units (34) and that if one domain is required for a particular function, that domain performs that function in the native state.

Human serum contains four subclasses of IgG: IgG1, IgG2, IgG3 and IgG4. Initial studies of subclass specificity concluded that only the human IgG1, IgG2 and IgG3 subclasses could bind to C1 as monomers (35) and activate C1 as aggregates (36). It was not clear from these studies why the IgG4 subclass was unable to bind to C1 and activate complement through the classical pathway. In 1975

Isenman et al. (37) reported that the Fc region of IgG4 was as active as the Fc region of IgG1 in binding to C1. Thus native IgG4 has a potential C1-binding site in the $C_{\gamma}2$ domain . These authors also confirmed the earlier work by Schur and Christian (38) that showed intact disulfide bonds between the heavy chains are important in the interaction between IgG and C1. For example, non-covalently reassembled IgG1 was unable to bind to C1 because the C1-binding site was sterically hindered by the flexible Fab regions. They postulated that the C1-binding site in the native IgG4 molecule is similarly hindered by the Fab regions through increased flexibility in the hinge region. Recently, Schumaker et al. (39) have observed that all four subclasses of native IgG bind to C1q with the following relative affinities: IgG3 > IgG1 > IgG2 > IgG4. It appears that all human immunoglobulin subclasses have the ability to bind to C1 under the appropriate conditions. The C1-binding properties of a particular immunoglobulin subclass evidently is limited by the quaternary structure of the molecules in that subclass.

While all IgG subclasses posess a C1-binding region, only two of the IgG subclasses, IgG1 and IgG3, activate C1 efficiently. The mechanism by which IgG activates C1 is not yet clear. Some investigators believe that C1 activation is dependent upon an antigen-induced conformational change in the Fc region (40-42). Other workers ascribe to the hypothesis that C1 activation is dependent upon Fc aggregation (43,44). These latter studies demonstrated that certain immunoglobulin aggregates that have undergone a conformational change in their Fc regions are unable to activate C1 (43), and that C1 activation can be detected with small IgG aggregates, such as dimers and trimers (44). It is clear that aggregation of Fc regions is required for C1 activation; if subtle conformational are necessary, they have yet to be shown.

Beta-2 microglobulin, a serum protein of approximately the same length as an immunoglobulin domain, shows moderate sequence homology to several immunoglobulin domains (45). Isenman et al. (46) demonstrated that beta-2 microglobulin can bind to C1q in both the native and denatured states and concluded that a small specific linear sequence forms the C1q-binding site of beta-2 microglobulin. Thus the native conformation of beta-2 (and probably the $C_{\gamma}2$ domain) is not necessary for C1q binding. These results suggest that it should be possible to isolate small fragments of $C_{\gamma}2$ or to synthesize small segments of the $C_{\gamma}2$ domain that interact with C1.

An important chemical characteristic of the C1q-binding site of IgG was elucidated through the affinity chromatography studies of Sledge and Bing (47). These workers studied the ability of IgM, $(Fc)_5\mu$, and IgG to inhibit the binding of ^{125}I-labeled C1q to an IgM-agarose affinity support. The development of this solid-phase system allowed them to study inhibitors of the IgG-C1 interaction. At high concentrations, aromatic and aliphatic diamines bound to C1q and inhibited its binding to the IgM-agarose resin. In addition they showed that the more hydrophobic diamines were more potent inhibitors, 2,5-diaminotoluene being the most potent inhibitor studied. These results suggested that there is both an ionic interaction and a hydrophobic interaction between IgG and C1q.

Each of the characterized immunoglobulin fragments that activate or inhibit complement fixation by binding to C1q contain a tryptophan residue. Each immunoglobulin domain in Fc contains two invariant tryptophan residues that exist either in a buried state or in a state exposed to solvent. Recent solvent perturbation studies (48) performed on Fc and isolated domains showed that two of the eight tryptophan residues in the Fc region are exposed to solvent and that each of the the two $C_{\gamma}2$ domains contains one exposed tryptophan residue. Using 2-hydroxy-5-nitrobenzyl bromide as described by Horton and Koshland (49), Allan and Isliker (50) specifically modified tryptophan residues in

IgG, Fc, and fragments of Fc and found that modification of tryptophan-277 in IgG inhibited complement activation. However, IgG and peptide fragments of IgG modified at tryptophan-277 were still able to bind to C1q (51). These studies are consistent with the concept that binding of monomeric IgG to C1q is not equivalent to activation and that other molecular events must be involved in the activation of C1 by immune complexes.

The $C_{\gamma}2$ domain of all IgG subclasses contain an oligosaccharide moiety (Fig. 3). This carbohydrate chain has never been clearly implicated in the IgG-C1 interaction. Several lines of evidence suggest that the carbohydrate is not an integral part of the C1q-binding site of IgG. First, Utsumi (30) progressively digested the amino terminus of Fc with papain to produce a fragment that included half of the $C_{\gamma}2$ domain and the entire $C_{\gamma}3$ domain. This fragment contained carbohydrate but would not fix complement. Second, Isenman et al. (46) have observed that beta-2 microglobulin, which bears both structural and sequence homology to the immunoglobulin constant-region domains (45), is capable of binding to C1q even though it lacks carbohydrate. Third, Hurst et al. (52) have demonstrated that a small tryptic fragment from the $C_{\mu}4$ domain of an IgM protein also binds to C1q but is devoid of carbohydrate. Fourth, X-ray crystallographic studies by Deisenhofer et al.

(53) on the Fc region of pooled IgG revealed that the carbohydrate residues are located internally between the two C_y2 domains and lie very close to the surface of these domains. Thus these carbohydrate chains are probably inaccessible to C1q.

The X-ray crystallographic studies performed by Deisenhofer et al. (54) also revealed a marked structural difference between the C_y2 domain and the C_y3 domain. The latter is similar in tertiary structure to the other constant-region domains (C_y1 and C_L). Fig. 4 shows an alpha-carbon connectivity map of the Fc region based on the X-ray data. The lower C_y3 domain appears to be quite compact, while the upper C_y2 domain assumes a more open and available structure. Initial studies by Deisenhofer et al. indicated that tryptophan-277 may be a part of the exposed open loop region of C_y2. Recently, however, Deisenhofer and his colleagues (55) have established that the tryptophan residues in the C_y2 domain are oriented such that tryptophan-277 is deeply buried in the middle of C_y2 while tryptophan-313 is involved in a close interdomain contact with C_y3 and is more exposed to solvent. Following tryptophan-277 there is an exposed region containing three positively charged residues (histidine-285, lysine-288, and lysine-290) that may be responsible for the ionic interaction with C1q.

In summary, early fragmentation studies suggested that the C1q-binding site of IgG resides in the $C_{\gamma}2$ domain. Chemical inhibitor studies suggested that the C1q-binding site involves both an ionic region and a hydrophobic region. Tryptophan modification and solvent perturbation studies implicated a tryptophan residue in the C1q-binding site. X-ray crystallographic data available when the present study was planned revealed that the unique open structure of the $C_{\gamma}2$ domain has an exposed region consisting of a hydrophobic segment containing tryptophan-277 connected to an ionic segment containing three positively charged residues.

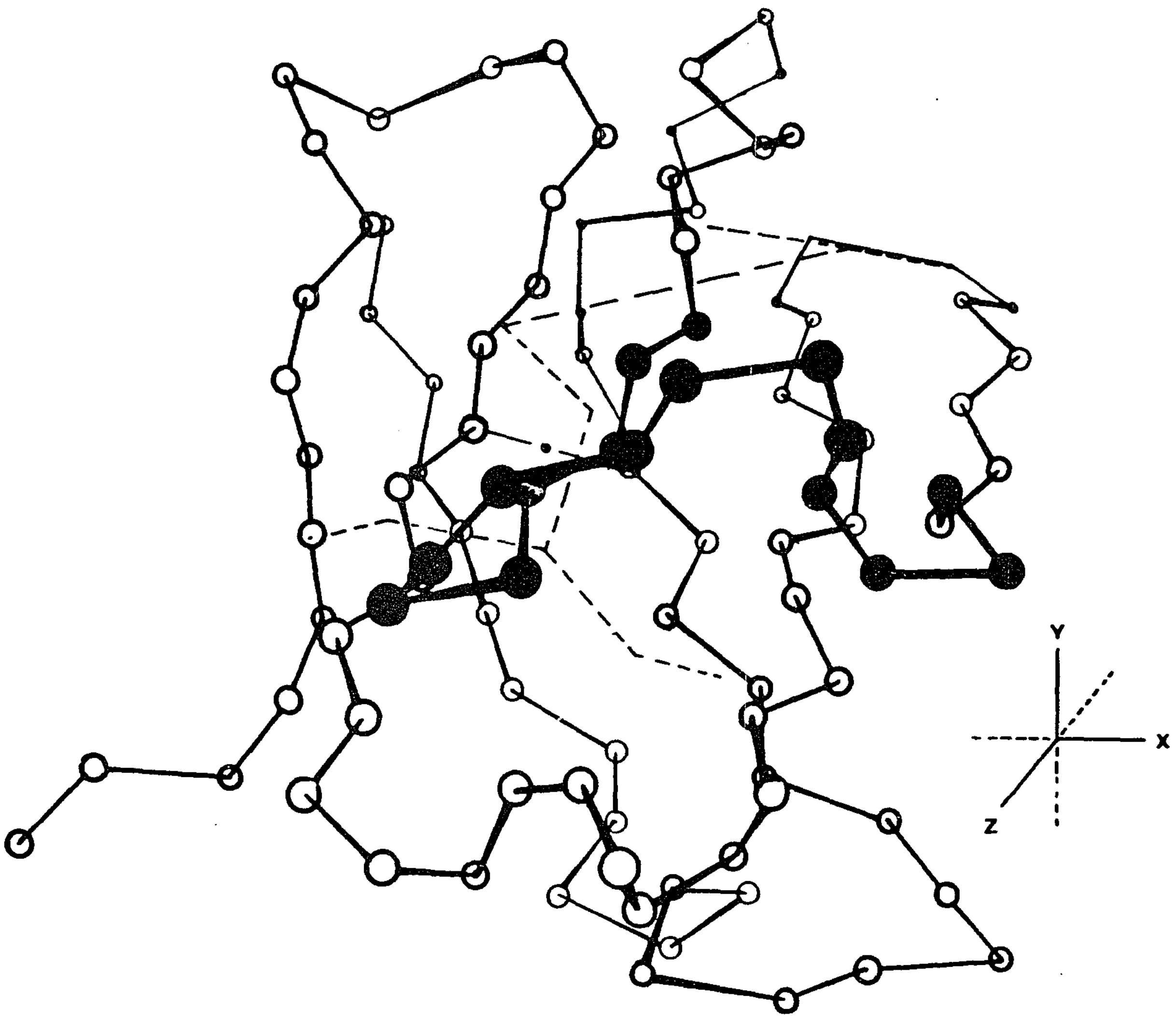

Fig. 3. Computer simulation of the alpha-carbon connectivity map of the $C_\gamma 2$ domain of IgG. The oligosaccharide (---) lies in close contact with the $C_\gamma 2$ domain. The disulfide bridge (-•-) pins two stretches of beta-pleated sheet together. The 16 residues in solid black are residues 275-290. This representation of C_γ is based on the preliminary X-ray crystallographic coordinates of the Fc fragment from pooled human IgG (J. Deisenhofer, personal communication).

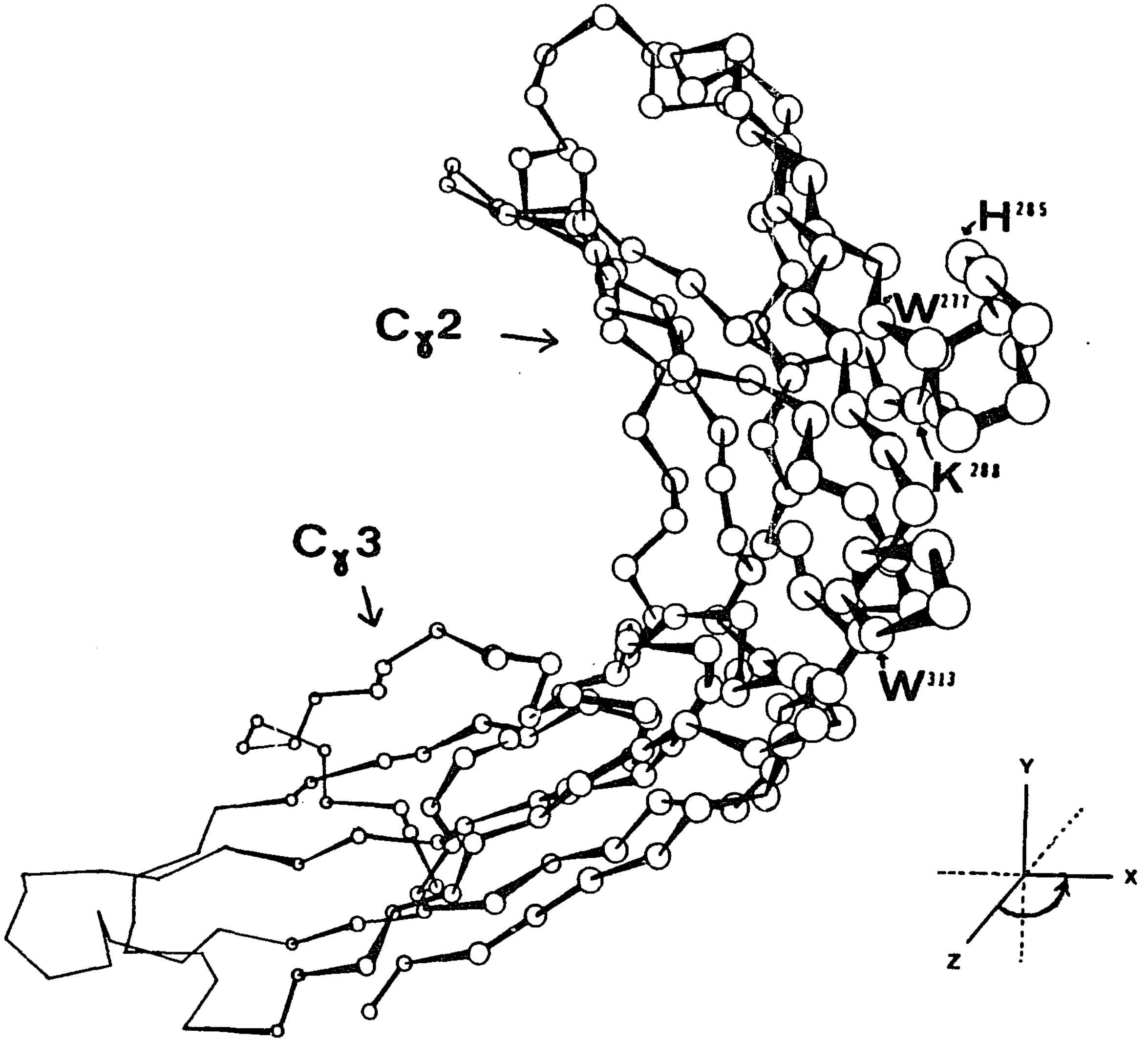

Fig. 4. Computer simulation of the alpha-carbon connectivity map of the Fc region of IgG. The upper C_γ domain is less compact than the lower C_γ domain. The positions of Trp-277, His-285, Lys-288, and Trp-313 are indicated. This representation of Fc is based on the same X-ray coordinates as used for Fig. 3. This perspective was obtained by a 90° rotation of the Fig. 3 perspective of the z-axis into the x-axis.

C. Strategy of Peptide Synthesis

1. Selection of the Synthetic Peptides. In outlining a synthetic strategy, considerable emphasis was placed on four features of the C1q-binding site of IgG defined by previous investigations. First, the synthetic segment was chosen from the $C_{\gamma}2$ domain. Second, the synthetic segment was selected from the structurally unique open-loop region of the $C_{\gamma}2$ domain. Third, the segment was chosen to include the hydrophobic region around the invariant tryptophan residue at position 277. Fourth, the segment was selected to contain an ionic region that resembles a diamine.

The primary structures of the $C_{\gamma}2$ domains of three human myeloma proteins (IgG1, IgG3, and IgG4) are depicted in Fig. 5 (56). The segment containing residues 275-290 shows much homology between the subclasses and satisfies all of the above criteria for the putative C1q-binding site. This peptide segment contains both a hydrophobic region with a tryptophan residue (277) and an ionic region containing two lysine residues (288 and 290) and a histidine residue (285). Examination of the alpha-carbon connectivity map of the $C_{\gamma}2$ domain (Fig. 6) shows that the segment 275-290 comprises most of the structurally unique region of the $C_{\gamma}2$ domain. Thus segments of the 16-residue open-loop region of IgG1 including phenylalanine-275 through lysine-290 were synthesized and tested for binding to C1q.

```
                 240                 250                 260
γ1    L-L-G-G-P-S-V-F-L-F-P-P-K-P-K-D-T-L-M-I-S-R-T-P-E-V-T-C-V-
γ3    __________________________________________________________
γ4    F_________________________________________________________

                             |================================|
                   270       275       280                 290
γ1    V-V-D-V-S-H-E-D-P-Q-V-K-F-N-W-Y-V-D-G-V-Q-V-H-N-A-K-T-K-P-
γ3    __________________Z___Z___K_____________E_________________
γ4    __________Q_______Z___Z_________________E_________________

                     300                 310                 320
γ1    R-E-Q-Q-Y-B-S-T-Y-R-V-V-S-V-L-T-V-L-H-Q-N-W-L-D-G-K-E-Y-K-
γ3    __Z_Z_Z_F_______F_____________________Z_B_____B___________
γ4    ____E___F_____________________________Z_B_________________

                       330                 340
γ1    C-K-V-S-N-K-A-L-P-A-P-I-E-K-T-I-S-K-A-K-G
γ3    ____________________________________T____
γ4    ____________G_____S_S____________________
```

Fig. 5. Primary structure of $C_{\gamma}2$ domains of three human gamma chains (56). The sequences of the marked open-loop region from Phe-275 to Lys-290 are highly conserved.

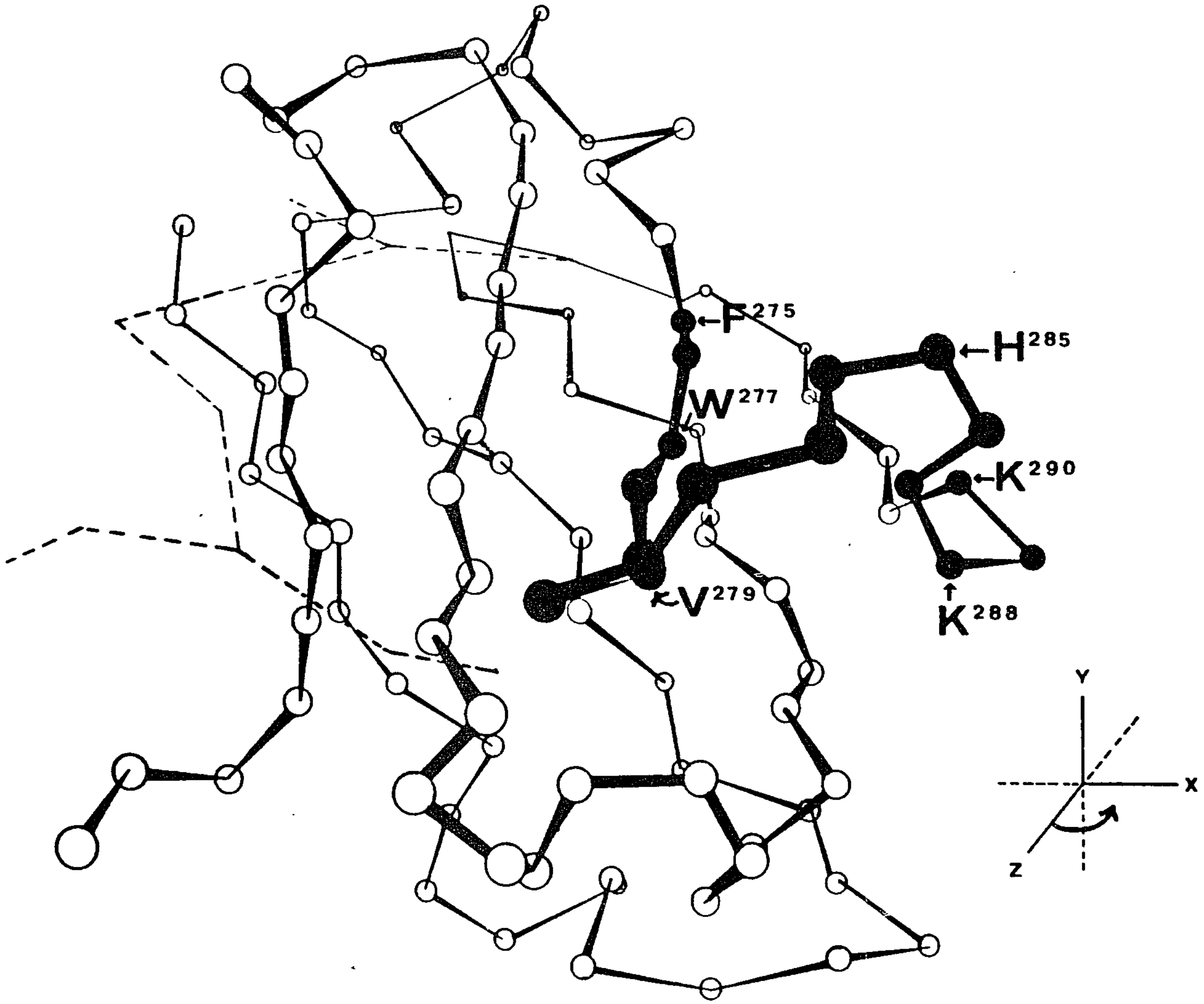

Fig. 6. Computer simulation of the alpha-carbon connectivity map of the $C_\gamma 2$ domain. The oligosaccharide (---) and disulfide bridge (-●-) are indicated . The shaded area represents the open-loop region and the (275-290)-hexadecapeptide. The exact positions of the side chains of the identified residues are not known. This representation of $C_\gamma 2$ is based on the same X-ray coordinates used for Fig. 3 and was obtained by a 60° rotation of the z-axis into the x-axis.

The hexadecapeptide and two segments of this peptide are shown in Fig. 7. The hexadecapeptide exhibits all of the tentative requirements outlined above for the C1q-binding site of IgG. The decapeptide constitutes a very cationic region with a net charge of +3 at physiological pH and lacks the hydrophobic region. The pentapeptide comprises an extremely hydrophobic segment containing three aromatic residues and lacks the the cationic residues.

Two additional peptides which do not correspond to naturally occuring segments of IgG were synthesized and tested. The hexapeptide A6J (Ac-Glu-Trp-Tyr-Glu-Arg-Gly) was the acetylated form of the peptide previously shown by Johnson and Thames (57) to be an inhibitor of complement fixation. The pentapeptide FR5 (Phe-Gly-Leu-Ala-Arg) containing two hydrophobic residues was used as a nonspecific control.

Number of Residues	Primary Structure															
	275				279		281				285					290
	h		h	h	h	-		h		h	+			+		+
16	Phe-	Asn-	Trp-	Tyr-	Val-	Asp-	Gly-	Val-	Gln-	Val-	His-	Asn-	Ala-	Lys-	Thr-	Lys
								h		h	+			+		+
10							Gly-	Val-	Gln-	Val-	His-	Asn-	Ala-	Lys-	Thr-	Lys
	h		h	h	h											
5	Phe-	Asn-	Trp-	Tyr-	Val											

Fig. 7. Synthetic segments selected from the $C_{\gamma}2$ domain of IgG1 Eu. The side chains of the amino acid residues are designated as hydrophobic (h), cationic (+), or anionic (-). The 16-residue peptide includes both hydrophobic and cationic regions. The 10-residue peptide comprises on the cationic region. The 5-residue peptide contains only the hydrophobic residues.

2. Synthetic Side Reactions. After the segments to be synthesized were selected, the desired peptides were evaluated for possible synthetic problems. Each of the solid-phase synthetic problems discussed below have been described in the recent comprehensive review of solid-phase peptide synthesis by Erickson and Merrifield (10). First, coupling of an unprotected histidine residue results in racemization and the incorporation of both the L and D forms into the growing peptide chain (Fig. 8A) (58). Protection of the imidazolium group of histidine with the strongly electron-withdrawing group, 2,4-dinitrophenyl (Dnp), minimizes the opportunity for racemization (59).

Second, many side reactions are possible during cleavage of peptide from the resin with anhydrous HF. One well-defined sequence-dependent side reaction may occur in this synthetic scheme. Under normal HF conditions (0°C for 30 min), the aspartyl-glycyl sequence (residues 280-281) would undergo an α-toβ- aspartyl rearrangement (Fig. 8B) (60). This rearrangement would result in the formation of a β-aspartyl residue at about 75% of the Asp-Gly positions, which introduces an extra methylene group into the backbone of the peptide. Because of this potential rearrangement, the decapeptide was chosen to end with glycine-281 and omit aspartic acid-280 which avoids the problem. Since this solution was not available for the hexadecapeptide, the rearrangement was circumvented by another means. During the solid-phase synthesis the β-carboxyl group of aspartic acid was protected as the benzyl ester. By changing the HF cleavage conditions to 30 min at -25°C (61) followed by 30 min at 0°C, the benzyl protecting group was removed at -25°C to avoid formation of the undesired aspartimide derivative, which leads to the rearrangement product.

Third, the presence of lysine at the beginning of a growing peptide chain poses the problem of forming branched peptides (Fig. 9A) (62). Branching can occur when the protecting group for the epsilon-amino group of lysine (positions 288 and 290 in this scheme) is removed prematurely during a synthesis. This side reaction can be avoided by using the 3-chlorobenzyloxycarbonyl (3-ClZ) protecting group for the ϵ-amino group of lysine. $\underline{N}^{\epsilon}$-(3-Chlorobenzyloxycarbonyl)-L-lysine was not commercially available and was synthesized by the method of Erickson and Merrifield (62).

Fourth, when glycine is the first amino acid coupled to a resin, as was the case for peptide A6J, a side reaction can occur that results in the loss of up to 70% of the growing peptide chains (63). Addition of the third amino acid to the dipeptide-resin catalyzes the intramolecular aminolysis of the ester bond to the resin forming the free cyclic dipeptide (diketopiperazine, Fig. 9B). This carboxylic acid-catalyzed intramolecular aminolysis can be avoided by adding the carbodiimide to the peptide-resin before adding the protected amino acid to be coupled.

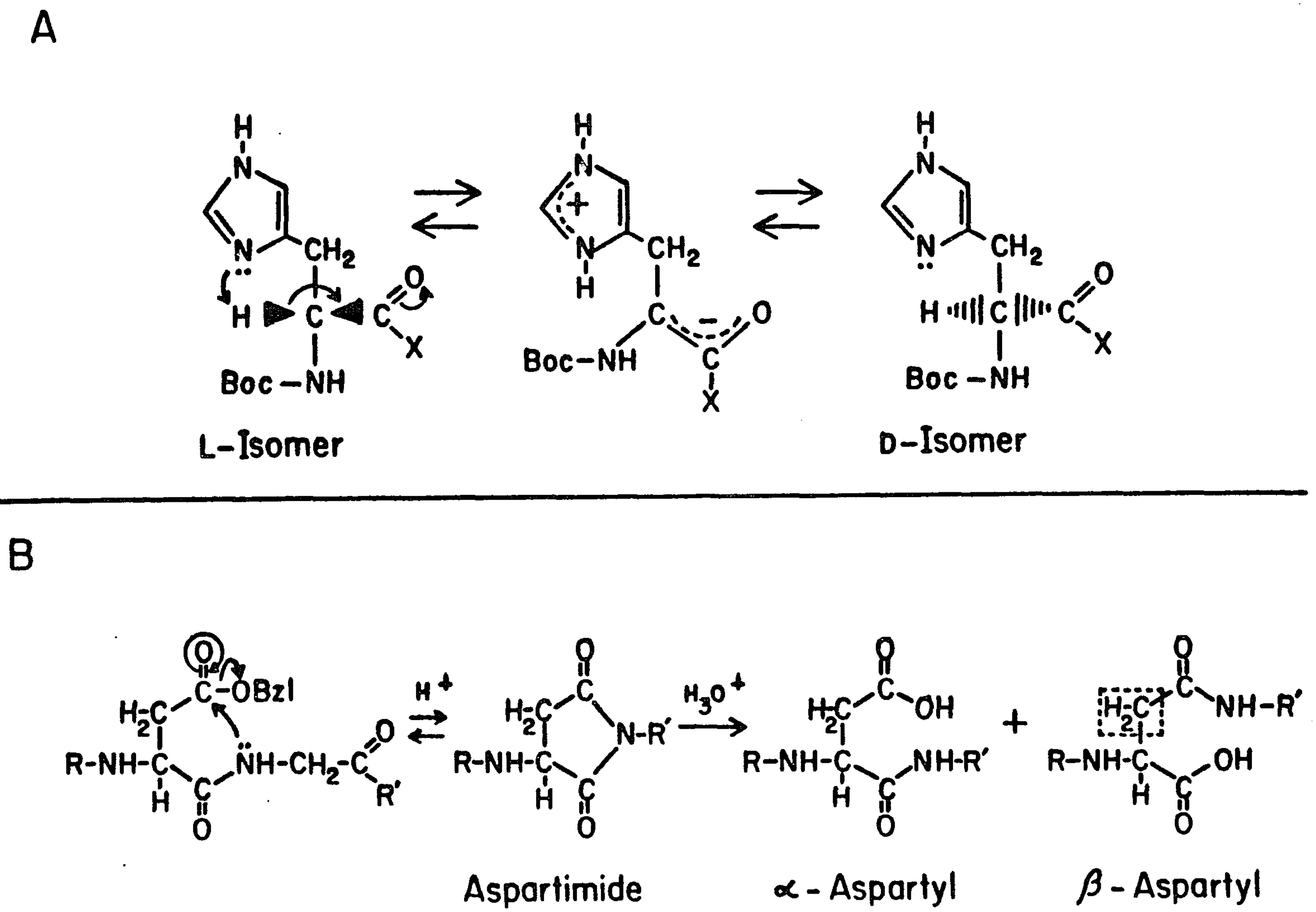

Fig. 8. Boc-Histidine racemization and β-aspartyl formation. (A) The basic imidazole group abstracts the alpha proton giving the planar zwitterion shown. Reprotonation of the alpha carbon yields both the D or the L isomers. (B) Acid catalyzed nucleophilic attack on the carbonyl carbon by the amide nitrogen generates the intermediate aspartimide. Hydrolysis of the aspartimide yields both the natural α-aspartyl residue and a β-aspartyl residue with an extra methylene group in the peptide backbone.

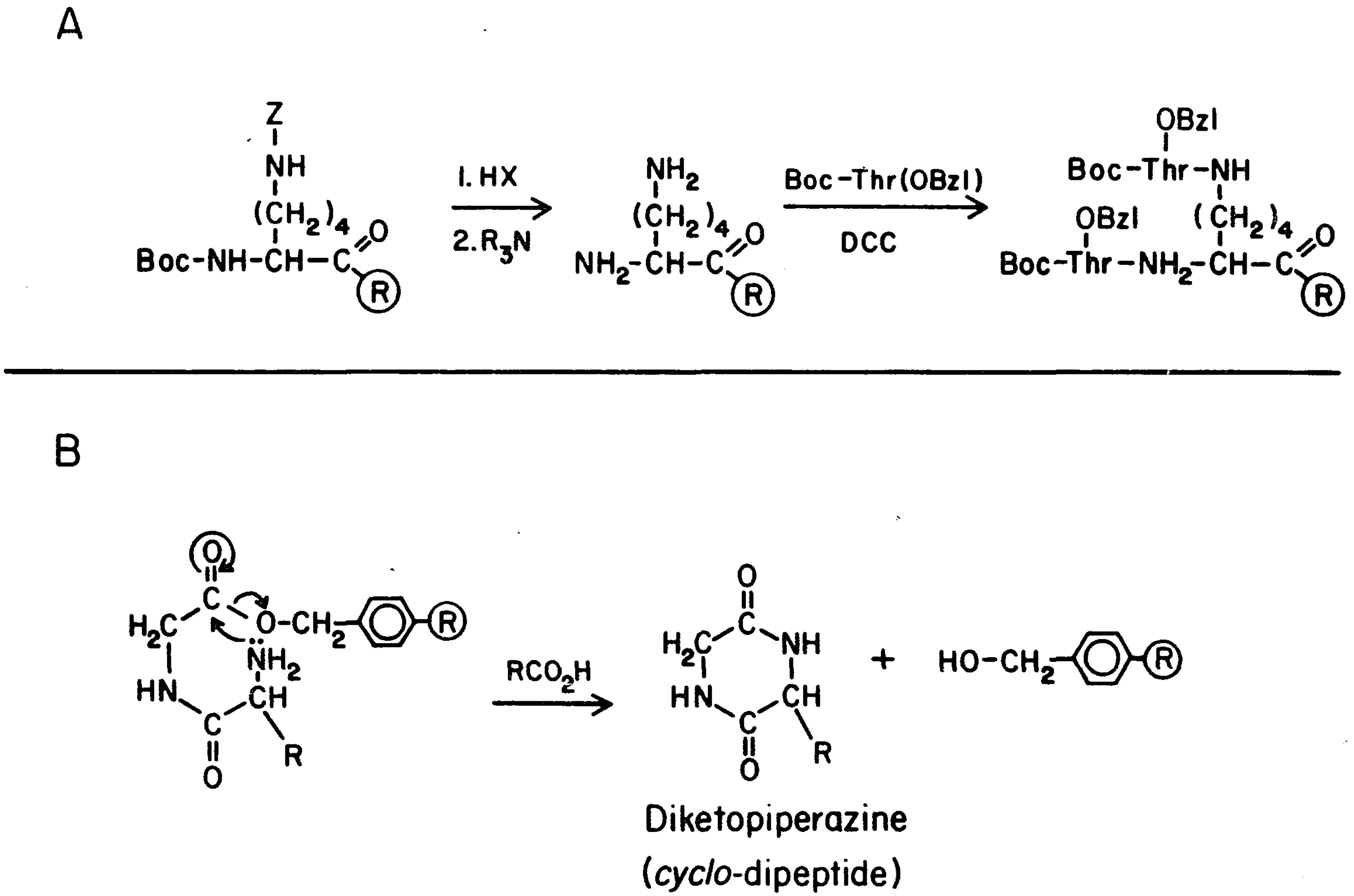

Fig. 9. Branched peptide formation and diketopiperazine formation. (A) Partial removal or the weakly acid-labile benzyloxycarbonyl (Z) group during the normal removal of the N^{α}-tert-butyloxycarbonyl (Boc) group allows not only the desired coupling of the next amino acid to the α-amino group but also the undesired coupling to the ε-amino group. (B) The intramolecular aminolysis is catalyzed by the bidentate carboxylic acid group, which acts as both a base and an acid in this reaction.

MATERIALS AND METHODS

A. Amino Acids

The commercially available protected amino acids were purchased from Bachem Inc. (Torrence, CA), Beckman Instruments Inc. (Palo Alto, CA) or Chemical Dynamics Corp. (South Plainfield, NJ). All amino acids were protected at the α-amino position with the *tert*-butyloxycarbonyl (Boc) group except for arginine, which was protected with the *tert*-amyloxycarbonyl (Aoc) group. For trifunctional amino acids the following side-chain protecting groups were used: Asp(OBzl), Thr(Bzl), Glu(OBzl), Tyr(2,6-Cl_2 Bzl), His(Dnp), Lys(3-ClZ), Arg(Tos), and Trp(For).

Radiolabeled [^{3}H]acetic anhydride (400 mCi/mmol) was purchased from New England Nuclear (Boston, MA). Radiolabeled L-[2,3-^{3}H]alanine (30 - 50 Ci/nmol) was purchased from Amersham (Arlington Heights, IL). The α-amino position was protected with the Boc group as described below in the preparation of Boc-Lys(3-ClZ).

N$^\epsilon$-(*3*-*Chlorobenzyloxycarbonyl*)-*L*-*lysine* was prepared by the method of Erickson and Merrifield (62) as shown in Fig. 10. Briefly, a solution of 3-chlorobenzyl alcohol (49.8 g, 0.351 mol) in 1.25 M phosgene in benzene (309 g) was stored at room temperature for 94 h. The resulting 3-chlorobenzyl chloroformate was slowly added to the blue copper salt of L-lysine at 0°C. The copper salt of Lys(3-ClZ) was produced in 78% yield. Chelation of the copper using EDTA in 0.33 N aqueous HCl and recrystallization of the resulting Lys(3-ClZ) from 70% ethanol in water yielded a white solid with a decomposition range of 218-220°C. It was homogeneous by thin-layer chromatography (TLC) in 17:2:1 (v/v/v) chloroform-methanol-acetic acid ($\underline{R}_f$ 0.06) and 5:5:1:3 (v/v/v/v) 1-butanol-pyridine-acetic acid-water ($\underline{R}_f$ 0.77). Elemental analysis for $C_{14}H_{19}ClN_2O_4$ gave:

Calculated (%): C 53.41, H 6.09, Cl 11.28, N 8.90
Observed (%): C 53.51, H 6.07, Cl 10.96, N 8.93

$\underline{N}^{\alpha}$-tert-Butyloxycarbonyl-$\underline{N}^{\epsilon}$-(3-chlorobenzyloxycarbonyl)-L-lysine was prepared by a modification of the procedure of Schnabel (64). Lys-(3-ClZ) (19.3 mmol) was dissolved in 2:1 (v/v) dioxane-water (150 ml) and 1.8 molar equivalents of MgO and 4.5 molar equivalents of Boc-azide were added. The reaction mixture was incubated at 50°C for 72 h. The reaction was stopped by adding 5 molar equivalents of hydrazine hydrate. After acidification and extraction into ethyl acetate, the solvent was evaporated to afford Boc-Lys(3-ClZ) as a colorless oil. It was homogeneous by TLC in 17:2:1 (v/v/v) chloroform-methanol-acetic acid ($\underline{R}_f$ 0.74) and 5:5:1:3 (v/v/v/v) 1-butanol-pyridine-acetic acid-water ($\underline{R}_f$ 0.85). Elemental analysis for $C_{19}H_{27}ClN_2O_6$ gave:

Calculated (%): C 54.99, H 6.56, Cl 8.56, N 6.75
Observed (%): C 55.03, H 6.82, Cl 8.40, N 6.57

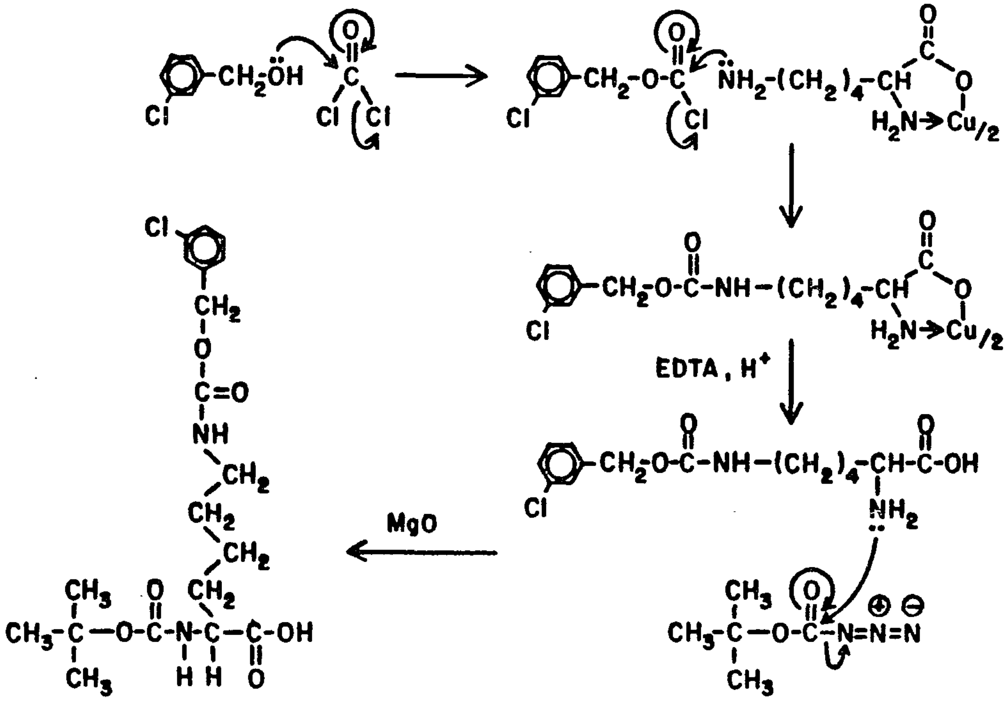

Boc-Lys(3-ClZ)

Fig. 10. Synthesis of N^{α}-*tert*-butyloxycarbonyl-N^{ϵ}-(3-chlorobenzyloxycarbonyl)-L-lysine. 3-Chlorobenzyl alcohol was reacted with phosgene to form 3-chlorobenzyl chloroformate, which was reacted with the copper salt of L-lysine to yield the copper salt of Lys(3-ClZ). The copper was chelated with EDTA in acid and the free α-amino group was protected using Boc-azide to give Boc-Lys(3-ClZ).

B. Resin Preparation

Chloromethylated copoly(styrene-1% divinylbenzene) beads (0.7 meq Cl/g, 200-400 mesh; Bio-Rad Laboratories, Richmond, CA) were used for all syntheses. The first amino acid was esterified to the resin by the method of Gisin (65). The cesium salt of the Boc-amino acid in 1.8 - 2.0 molar excess over the chloromethyl groups was dissolved in N-methyl-2-pyrrolidinone (NMP). The resin was swelled in a minimal amount of NMP, the cesium salt of the Boc-amino acid was added, and the slurry was stirred at 50°C for four to six days. The loading of Boc-amino acid per gram of resin was assessed by the picrate monitoring method described below. The following loading values were obtained: Boc-Lys(3-ClZ)-resin was 0.477 mmol/g, Boc-Val-resin was 0.600 mmol/g, and Boc-Gly-resin was 0.608 mmol/g.

C. Picrate Monitoring

Several methods have been described to monitor coupling reactions during solid-phase synthesis (10). A modification of the picrate monitoring method described by Gisin (66) was used in this study (Fig. 11). The free α-amino group was first neutralized with 5% N,N-diisopropylethylamine (DIEA) in dichloromethane. The neutralized α-amino group was reacted with 0.05 M picric acid in dichloromethane and the excess picric acid was removed by thorough washing of the resin with dichloromethane. The number of free amino groups that had bound picric acid was determined spectrophotometrically at 361 nm ($\varepsilon_{361} = 1.51 \times 10^4\ M^{-1}cm^{-1}$) as the amount of picric acid that could be displaced from the picrate-peptide-resin by 5% DIEA in dichloromethane. All peptide-resins were monitored by this method before use. The coupling reactions were also monitored by the picrate method during synthesis of A5F and A6J.

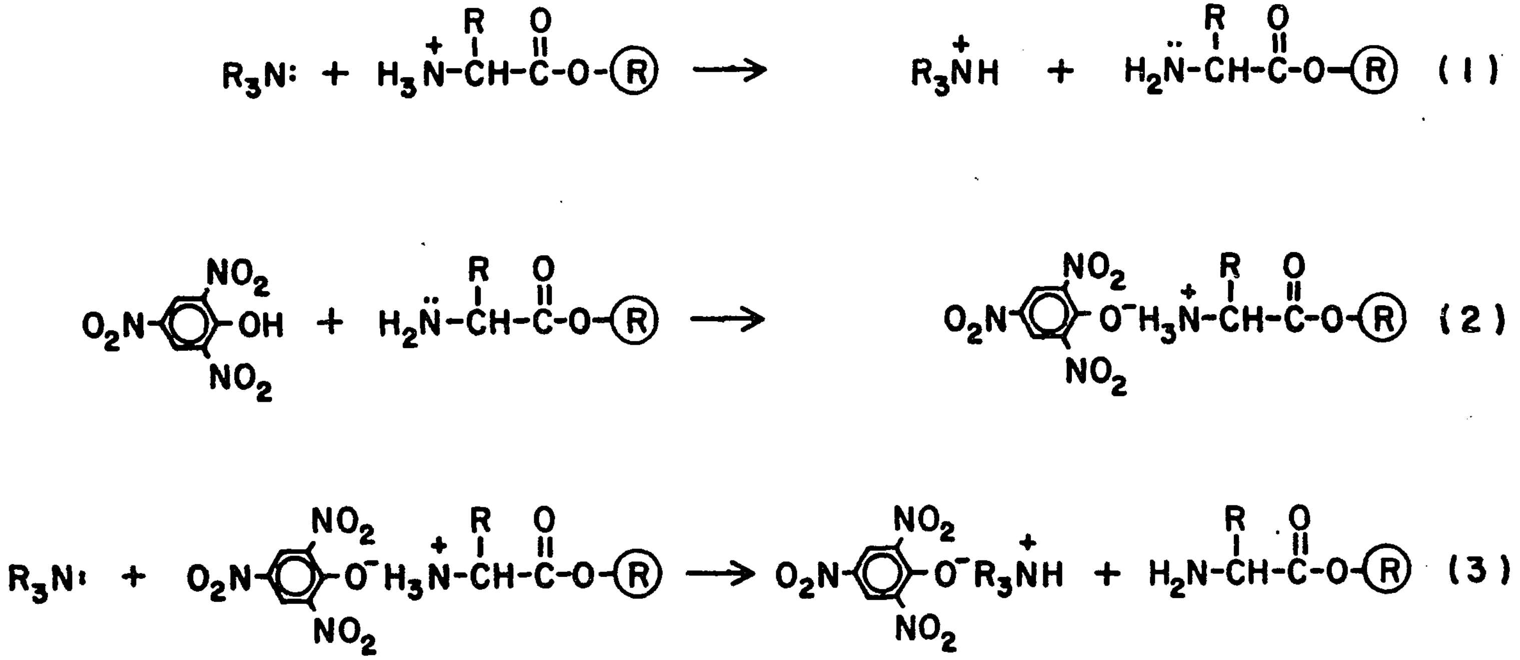

Fig. 11. Picrate monitoring of free amino groups. (1) The amino groups of the peptide-resin are neutralized by a tertiary amine. (2) Picric acid is added to form a resin-bound ammonium picrate salt. (3) A tertiary amine is added to neutralize the amino groups and displace the picric acid from the resin as the soluble ammonium picrate salt.

D. Solid-Phase Synthetic Protocol

A new era in peptide synthesis began with the introduction of solid-phase peptide synthesis by Merrifield (67). A general scheme for solid-phase peptide synthesis is shown in Fig. 12 (68). The solid-phase method provides a simple and rapid means for the assembly of synthetic peptides. Soluble by-products and excess reagents are removed from the growing peptide chain by simply washing the insoluble solid support. This procedure avoids any further purification of the peptide intermediates. One major drawback to the solid-phase method results from the accumulation throughout the synthesis of peptide by-products that remain bound to the resin and complicate the final purification. Thus homogeneity of the final product depends on the efficiency of the assembly process and the resolving power of the purification methods.

All peptides were synthesized by the solid-phase method using a Schwarz/Mann automated peptide synthesizer. The synthetic peptides are shown in Fig. 13. Peptide FR5 was a gift of Dr. Cecille Unson, The Rockefeller University. A detailed protocol for one synthetic cycle is given in Table I. The Boc-amino acid-resin was first deprotected with 50% trifluoroacetic acid (TFA) in dichloromethane for 30 min and then thoroughly washed (Step A). The free α-amino groups were neutralized with 5% DIEA in dichloromethane and the resin was washed again (Step B). Then 2 - 3 molar equivalents of the next amino acid in dichloromethane and an equimolar amount of N,N'-dicyclohexylcarbodiimide (DCC) in dichloromethane were added to the resin, the reaction mixture was shaken at room temperature for 30 min and the resin was thoroughly washed again (Step C). Finally, neutralization step B and coupling step C were repeated. After both coupling steps with the same amino acid had been performed, the next synthetic cycle was started. Alternatively, in the syntheses of peptides A5F and A6J, the peptide-resin was monitored with picric acid for unreacted amino groups after the second coupling reaction. If the monitoring value was unacceptable (< 93% coupled) then a third coupling cycle was performed using equimolar amounts of Boc-amino acid, 1-hydroxybenzotriazole (HOBt), and DCC.

When coupling the third amino acid to the glycine-resin, the DCC was added before adding the Boc-amino acid to minimize diketopiperazine formation (see Synthetic Side Reactions). Asparagine and glutamine were coupled either with DCC alone or with DCC and HOBt. In the synthesis of A6J, Boc-Trp was used instead of Boc-Trp(For). During the deprotection steps following coupling of the tryptophan, 1% indole (w/v) was added to the 50% TFA solution. Acetylation of peptides A5F and A6J was performed on the resin at room temperature for 24 h using a limiting amount of radiolabeled acetic anhydride in pyridine. Peptide A5F was further acetylated for 3 h using an excess of a 1:2 (v/v) solution of nonradiolabeled acetic anhydride and pyridine. For peptide A6J three molar equivalents of DCC were added to the acetylation reaction, which was incubated at room temperature for an additional 120 h. Only four percent of the available α-amino groups were acetylated, and the resulting peptide A6J had a very high specific activity (75,500 cpm/nmol).

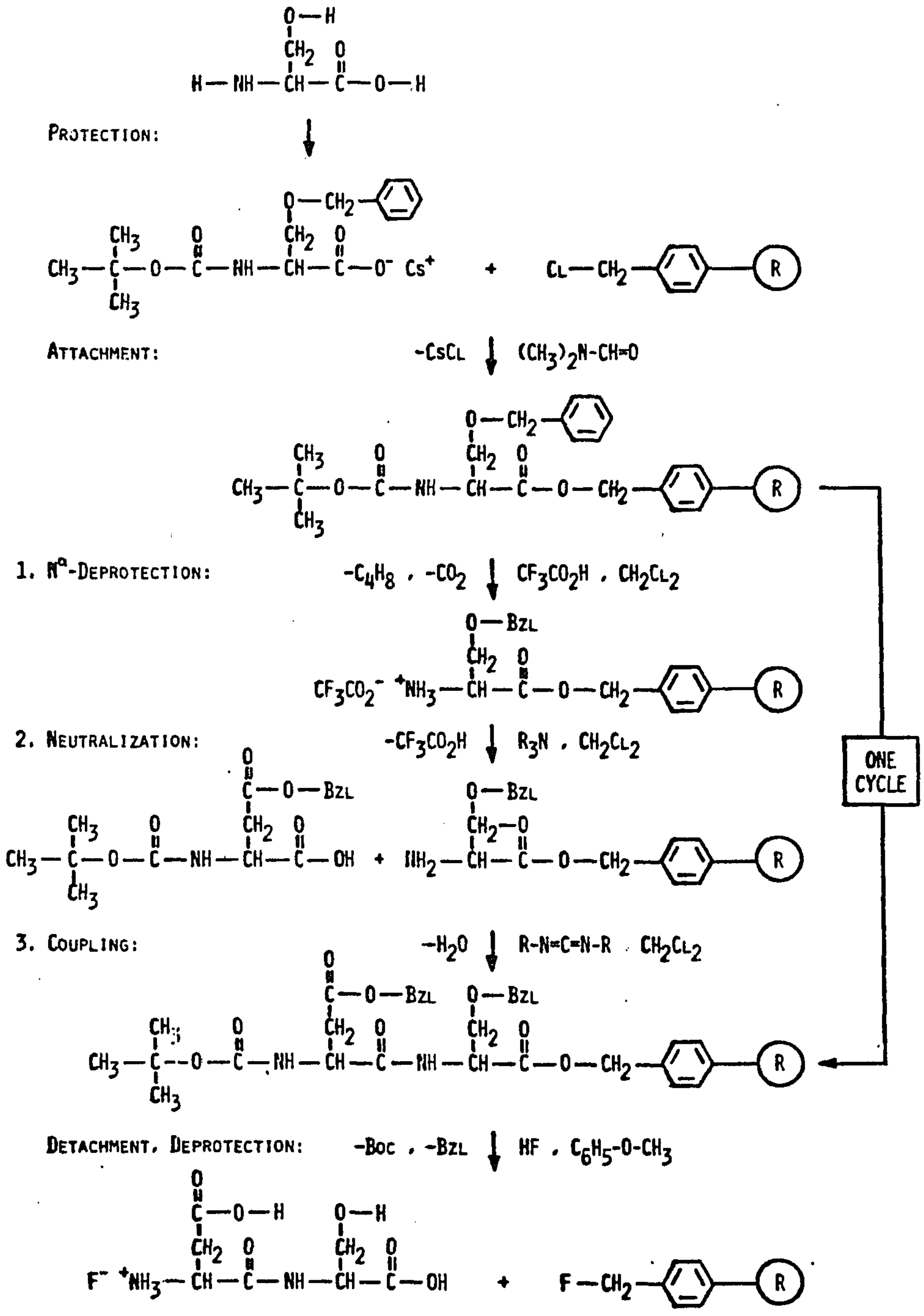

Fig. 12. General scheme for solid-phase peptide synthesis. The protected first amino acid is attached as the cesium salt to the chloromethylated resin. One synthetic cycle consists of Nα-deprotection, neutralization, and coupling. This cycle is repeated until all of the residues have been coupled in the desired sequence. Peptide is cleaved from the resin with anhydrous HF and is purified to homogeneity.

Peptide	Primary Structure
	275 279 281 285 290
16F	Phe-Asn-$\overset{\text{For}}{\text{Trp}}$-Tyr-Val-Asp-Gly-Val-Gln-Val-His-Asn-Ala-Lys-Thr-Lys
16	Phe-Asn-Trp-Tyr-Val-Asp-Gly-Val-Gln-Val-His-Asn-Ala-Lys-Thr-Lys
10	Gly-Val-Gln-Val-His-Asn-Ala-Lys-Thr-Lys
A5F	Ac-Phe-Asn-$\overset{\text{For}}{\text{Trp}}$-Tyr-Val
A5	Ac-Phe-Asn-Trp-Tyr-Val
A6J	Ac-Glu-Trp-Tyr-Glu-Arg-Gly
FR5	Phe-Gly-Leu-Ala-Arg

Fig. 13. Peptides synthesized from the C_γ domain of IgG1. Peptide 16F and 16 contain both the hydrophobic and cationic segments. Peptide 10 comprises only the cationic segment and peptides A5F and A5 include only the hydrophobic segment. Both peptides 16F and A5F are formylated at the indole nitrogen of the tryptophan residue. Peptide A6J is the acetylated form the most active peptide of Johnson and Thames (57). Peptide FR5 served as a control.

Table I

Detailed protocol for one solid-phase synthetic cycle

Step	Reagent or Solvent	Time
		min
A. Deprotection	dichloromethane	0.5
	50% trifluoroacetic acid	2.0
	50% trifluoroacetic acid	30.0
	dichloromethane 5 times	0.5
	isopropanol 2 times	0.5
	dichloromethane 5 times	0.5
B. Neutralization	N,N-diisopropylethylamine 3 times	2.0
	dichloromethane 5 times	0.5
C. Coupling	Boc-amino acid	2.0
	N,N'-dicyclohexylcarbodiimide	30.0
	dichloromethane 5 times	0.5
	isopropanol 2 times	0.5
	dichloromethane 2 times	0.5
	isopropanol 2 times	0.5
	dichloromethane 5 times	0.5
D. Repeat Step B		
E. Repeat Step C		

E. Cleavage

All peptides were cleaved from the resin using 9:1 (v/v) anhydrous HF in anisole (69). Prior to cleavage with HF, the Dnp protecting group on histidine was removed by treatment overnight at room temperature with 1000 molar equivalents of thiophenol in DMF (20). Peptides A5, A6J, and 10 were treated with HF for 1 h at 0°C. Peptide 16 was treated with HF for 30 min at -25°C and for 30 min at 0°C to minimize formation of β-aspartyl residues (see Synthetic Side Reactions). After treatment with HF, the resins were washed with diethyl ether to remove organic by-products formed during HF cleavage. The peptides were then eluted from the resin with either 10% aqueous acetic acid, glacial acetic acid, or mixtures of aqueous acetic acid and methanol, depending upon the solubility of the synthetic peptide.

F. Purification

Pilot studies were performed to establish the most efficient protocol for purifying each synthetic peptide to homogeneity. The following techniques were investigated in the pilot studies: gel-filtration chromatography on Bio-Gel P-2 or Sephadex G-10, G-15, or G-25; ion-exchange chromatography on SP-Sephadex, Biorex-70, or Technicon-P resins; adsorption chromatography using silica gel in columns or on thin-layer plates; and reverse-phase chromatography using using columns of spherical totally porous microparticulate silica bonded with octadecyl or alkylphenyl groups.

The synthetic peptides were eventually purified using the procedures described below. Peptide 16F was first chromatographed over Bio-Gel P-2 and peptide 10 was first chromatographed over superfine Sephadex G-25 . All peptides were subsequently purified using a modular high-pressure liquid chromatography system consisting of two Model 6000A pumps, a Model 660 solvent programmer, and a U6K manual sample injector (Waters Assoc., Milford, MA) and were monitored using a Model 770 variable wavelength UV detector (Schoeffel Instruments Corp., Westwood, NJ). The major mode for purification was reverse-phase chromatography using a column containing µBondapak C18 (3.9 mm x 30 cm, Waters), µBondapak phenyl (3.9 mm x 30 cm, Waters), or Nucleosil C18 (10 mm x 25 cm; Rainin Instruments Co. Inc., Brighton, MA). The mobile phases consisted of varying proportions of methanol and aqueous acetic acid. Chromatographic runs were monitored by UV absorbance, TLC, and liquid scintillation counting (LSC) of the radioactive peptides.

G. Characterization

The synthetic peptides were characterized and tested for homogeneity by several different methods. Homogeneity of each synthetic peptide was shown in three different solvent systems using thin-layer chromatography. The $\underline{R}_f$ values, relative migration of the peptide to the solvent front, for the synthtic peptides ranged between 0.2 and 0.8 on Woelm silica gel (250µ thick; Analtech, Newark, DE). Peptides were visualized on the thin-layer plates (1) by spraying with ninhydrin and heating and (2) by exposure to a Cl_2 atmosphere followed by spraying with o-tolidine (70). Thin-layer electrophoresis (TLE) was performed on the peptides soluble in aqueous systems using 25:1:225 (v/v/v) pyridine-acetic acid-water at pH 6.5 for 30 min (2000 V, about 27 ma) on hard-layer silica plates (Analtech). Arginine, glutamic acid and alanine were used as standards for each TLE experiment. The electrophoretic mobiliities of the peptides were expressed as the relative distance migrated towards Arg (R_{Arg}) or Glu (R_{Glu}) from Ala.

The ultraviolet spectrum (200 - 400 nm) was recorded for all peptides containing Trp or Trp(For) (71) using a Cary Model 14 spectrophotometer. For reference, spectra of Boc-Trp and Boc-Trp(For) are shown in Fig. 14. The nuclear magnetic resonance (NMR) spectrum of peptide A5F was measured in dimethylsulfoxide-$\underline{d}_6$ and in D_2O using a Varian HR-220 spectrometer at 220 MHz. Reverse-phase HPLC in methanol-aqueous acetic acid was also used to test the homogeneity of synthetic peptides. A peptide was considered to be homogeneous if it eluted as one sharp peak with a k' value between 1.5 and 12, where $k' = (V_P-V_0)/V_0$, V_P is the volume of the peptide peak, and V_0 is the breakthrough volume as measured by an unretained solute.

Amino acid compositions were determined by automatic amino acid analysis using a Durrum Model D-500 HPLC analyzer, a Beckman Model 121 two-column analyzer, or a modified Beckman Model MS single-column analyzer equipped with Durrum D-6 resin. Synthetic peptides were hydrolyzed in preparation for amino acid analysis by the following methods: 6 N HCl containing 0.3% (w/v) phenol for 24 h and 48 h at 110°C (72), 4 N NaOH containing thiodiglycol for 24 h and 48 h at 110°C (73,74), 10 μM aminopeptidase M (1 μg per nmol of peptide; Boehringer Mannheim Biochemicals, Indianapolis, IN) in 0.1 M ammonium carbonate (pH 7.5) for 20 h at room temperature (75), or 10 μM carboxypeptidase Y (1 μg per nmol of peptide; Carlsberg Laboratory, Copenhagen, Denmark) in 0.1 M ammonium acetate (pH 5.4) for 20 h at room temperature (75).

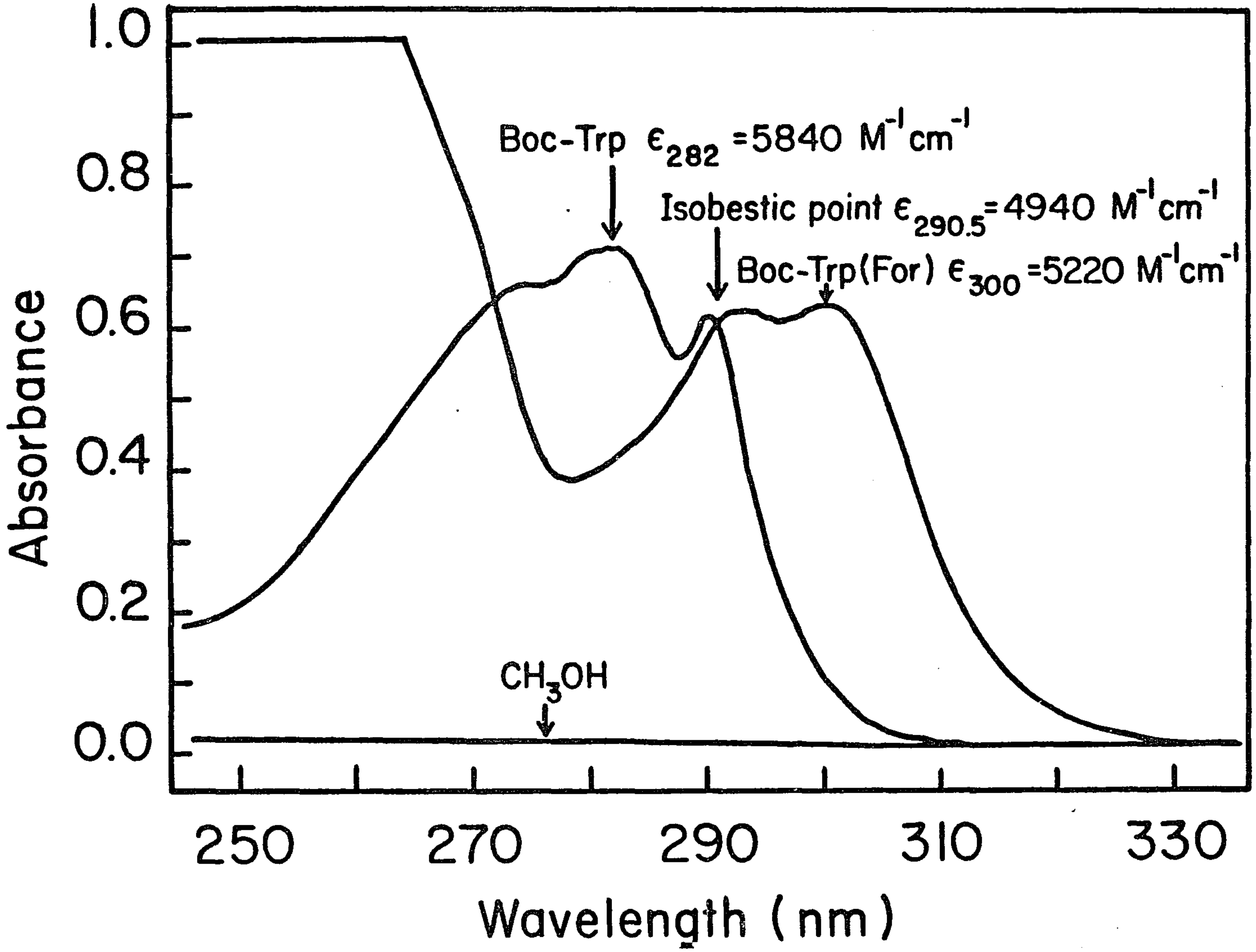

Fig. 14. Ultraviolet absorption spectra of Boc-Trp and Boc-Trp(For). Spectra were taken in methanol versus a methanol reference. The baseline spectrum of methanol versus methanol is shown. The observed absorption maxima and molar absorptivities (ε) were 274 nm (5430 $M^{-1}cm^{-1}$), 282 nm (5840 $M^{-1}cm^{-1}$) and 290 nm (5060 $M^{-1}cm^{-1}$) for Boc-Trp and 292 nm (5100 $M^{-1}cm^{-1}$) and 300 nm (5220 $M^{-1}cm^{-1}$) for Boc-Trp(For). The isobestic point occurred at 290.5 nm with an ε of 4940 $M^{-1}cm^{-1}$. The ultraviolet absorbance of Trp(For)-containing peptides was monitored at 290 nm during HPLC purification and characterization.

H. C1 Inhibition Assay

The C1 inhibition assay used in this study has been described by Borsos and Rapp (76) and modified by Augener et al. (35). Hyslop et al. (40) added an important wash step which separates the indicator red cell system from unbound C1 and inhibitor. This assay measures the ability of a compound to inhibit activation of the classical complement pathway through binding to C1.

Three IgG protein standards were used in the C1 inhibition assay. The IgG1 myeloma protein Pen, which was chromatographed twice on Sephadex DEAE A-50 and once on Sephadex G-200, was found by analytical ultracentrifugation at a concentration of 4.5×10^{-6} M to consist of heterogeneous IgG aggregates with an average $s_{20,w}$ value of 12.5 Svedberg units (77). The IgG1 myeloma protein Bah was purified by Pevikon block electrophoresis and used as the monomeric IgG standard. Protein fragment Fc was prepared by papain digestion of the slowly migrating portion of the FII fraction obtained from Pevikon block electrophoresis of pooled human serum (28). The Bah and Fc proteins were gifts from Dr. Robert Winchester, The Rockefeller University.

Each peptide and protein was assayed at a series of concentrations produced by successive twofold dilution. Since each peptide contained a known specific activity of radiolabel, its dilution was monitored by liquid scintillation counting. The amount of peptide in the highest (H) and lowest (L) solutions were calculated by determining the radioactivity of these dilutions in duplicate. The average dilution factor (DF) was calculated as DF = $(A_H/A_L)^{1/n}$, where A_H and A_L were the average radioactivity in cpm for dilutions H and L, respectively, and n was the number of twofold dilutions used to prepare L from H. The mean and standard deviation of the population of dilution factors was 2.01 ± 0.11.

All complement components were purchased from Cordis Laboratories (Miami, FL). The EAC4 cells were sheep erythrocytes coated with IgG and human C4. Only human complement components were used in this study. The buffer used in this C1 inhibition assay was a sucrose-gelatin-veronal buffer (SGVB) (78), containing 1 mM $MgCl_2$, 0.15 mM $CaCl_2$, 0.06 M NaCl, 0.17 M sucrose, 0.1% (w/v) gelatin, and 5 mM sodium-5,5 diethyl barbiturate at pH 7.3-7.4. This low ionic strength buffer (μ = 0.065) increases the association of C1 with IgG and immune complexes (76). C-EDTA solution containing complement components C3-C9 was prepared by diluting one part of normal human serum with 49 parts of a dilution buffer consisting of 4.5 mM sodium-5,5 diethyl barbiturate, 0.135 M NaCl, 0.1% (w/v) gelatin, 0.01 M EDTA at pH 7.3-7.4. For each assay a sufficient amount of C1 was used to lyse 61 ±8% of 8.5 ±1.1 x 10^6 erythrocytes. A C1 titration was performed before each assay to insure that only about 61% of 8.5 x 10^6 cells would be lysed. The amount of C1 used in each assay was approximately 25 femtomoles or approximately 500 C1 molecules per erythrocyte.

The assay procedure used in this study is shown in Fig. 15. All assays were performed in triplicate. SGVB buffer, IgG, or peptide (0.10 ml) was incubated with C1 (0.10 ml) for 10 min at 30°C. The C1 that was not complexed with IgG or peptide was available to react with activated erythrocytes, EAC4. This free C1 was measured in the following test system. A solution (1.0 ml) containing 8.5 x 10^6 EAC4 cells was added, and the mixture was incubated at 30°C for 10 min. The resulting $EAC\overline{14}$ cells and remaining EAC4 cells were washed once with SGVB at 4°C. Then C2 (10 CH_{50} units in 0.10 ml) was added and the mixture incubated at 30°C for 10 min. The temperature was raised to 37°C and the reaction mixture was incubated with the C-EDTA solution (1.0 ml) for 1 h. After the unlysed erythrocytes were pelleted by centrifugation, the amount of lysis was determined spectrophotometrically using a Zeiss Model PM QII spectrophotometer by measuring the absorbance at 412 nm of the hemoglobin released into the supernatant. Complete lysis of 6.7 x 10^6 erythrocytes in 1 ml gave an absorbance of 0.660 at 412 nm.

Three controls were run with each experiment. (1) The amount of complement-mediated hemolysis (H_1) was measured from a buffer control lacking peptide or IgG but containing C1, EAC4, C2, and C-EDTA. (2) The amount of background hemolysis (H_2) was determined from a control lacking peptide, IgG and Cl but including EAC4, C2, and C-EDTA. (3) The maximum possible hemolysis (H_3) was measured after hypotonically lysing the washed EAC4 cells with distilled water. The observed background lysis was subtracted from all other values. The complement color value, which is the absorbance at 412 nm of the dilute C-EDTA solution, was added to the absorbance value for the maximal possible lysis to give the absorbance corresponding to 100% lysis because C-EDTA was not added to this control.

The amount (Z) of free C1 capable of initiating hemolysis (76) is defined for control 1 as

$$Z_1 = -\ln (1 - [(H_1 - H_2)/(H_3 - H_2)])$$

Z_1 represents the total amount of complement lysis found in the first control. The percentage of free C1 remaining after complexation with IgG or peptide was calculated as $100 \times Z_{exp}/Z_1$.

The percentage of C1 remaining was plotted against the $\log_{10}$ of the concentration of the IgG or peptide inhibitor.

The peptide concentration at which 50% of the initial C1 was inhibited from initiating hemolysis (I_{50}) was a convenient measure of the ability of the peptides to bind to C1 and inhibit the classical complement pathway.

$$\text{Inhibitor} + \text{C1} \xrightleftharpoons{30^\circ\text{C}, 10\text{ min}} \text{Inhibitor-C1} \qquad (1)$$

$$\text{EAC4} + \text{C1} \xrightarrow[\text{2) wash cells}]{\text{1) } 30^\circ\text{C}, 10\text{ min}} \text{EAC}\overline{14} \qquad (2)$$

$$\text{EAC}\overline{14} + \text{C2} \xrightarrow{30^\circ\text{C}, 10\text{ min}} \text{EAC}\overline{142} \qquad (3)$$

$$\text{EAC}\overline{142} + \text{C3-C9} \xrightarrow{37^\circ\text{C}, 1\text{ h}} \text{Hemolysis } (A_{412}) \qquad (4)$$

Fig. 15. Inhibition of C1-mediated hemolysis. (1) Free inhibitor and C1 establish an equilibrium with the inhibitor-C1 complex. (2) Uncomplexed C1 reacts with sheep erythrocytes (E) bearing antibody (A) and and human C4 to form $\text{EAC}\overline{14}$, which are washed to remove the free C1 and inhibitor not bound to the cells. (3) C2 is added to form the classical C3 convertase. (4) Incubation of $\text{EAC}\overline{142}$ with the remaining complement proteins C3 through C9 produces hemolysis, which is measured spectrophotometrically at 412 nm as the amount of hemoglobin released into the supernatant.

I. Equilibrium Dialysis

Either functionally pure C1 (Cordis) or Clq was used for the equilibrium dialysis experiments. The C1q was prepared from outdated human plasma (New York City Blood Center) using the modification by Knobel et al. (79) of the method of Agnello et al. (80). Outdated plasma was recalcified by adding $CaCl_2$ to a final concentration of 0.1 M and incubating at 37°C for 45 min. Recalcified plasma was dialyzed at 4°C overnight against a buffer consisting of 25 mM sodium diethyl barbiturate and 10 mM EDTA at pH 8.6. After 40 mg of calf thymus DNA (Worthington Biochemical Corporation, Freehold, NJ) were added to 1.4 l. of recalcified plasma, the mixture was stirred at room temperature for 1 h and kept at 4°C for 48 h. The mixture was centrifuged at 1000 x g for 30 min to yield a white precipitate, which was washed four times with 25 mM sodium diethyl barbiturate buffer at pH 8.6. The precipitate was resuspended in a solution containing 50 mM KPO_4, 3 mM $MgCl_2$, 50 mM NaCl and adjusted to pH 6.9 with 1 N HCl. After 4 mg of DNase I (Worthington) were added to 32 ml of the suspension, it was incubated at room temperature for 3 h. The suspension was dialyzed against the suspending buffer for 48 h and centrifuged at 100,000 x g for 30 min. The supernatant was divided into two aliquots. One aliquot was dialyzed against 10 mM sodium acetate at pH 4.9 and chromatographed over a CM-52 resin (Whatman Inc., Clifton, NJ) prepared in dialysis buffer. C1q was eluted with a NaCl gradient from starting buffer to starting buffer containing 1 M NaCl (5 - 29 mS).

Either Visking cellulosic membranes (Visking Corp., Chicago, IL) or Spectrapore 2 dialysis membranes ($\underline{M}_r$ cutoff of 12,000 - 14,000; Spectrum Medical Industries Inc., Los Angeles, CA) were used for the dialysis experiments. The Visking membranes were prepared by thorough washing with distilled water and phosphate buffered saline (PBS; 0.05 M KPO_4 and 0.15 M NaCl at pH 7.4). The Spectrapore 2 membranes were prepared by a modification of the method of McPhie (81). Membranes were heated to 60°C for 15 min in 1:1 (v/v) ethanol-water and washed three times with distilled water. Then they were then heated to 60°C for 15 min in 10 mM Na_4-EDTA and washed three times with distilled water. Finally they were heated to 60°C for 15 min in distilled water and washed three times with PBS containing 0.3 mM NaN_3 (PBSA).

The method of membrane dialysis (82) has recently been reviewed. All dialysis experiments were performed at room temperature in PBS or PBSA. Dialysis membranes were mounted between two 120-µl dialysis chambers. A 0.78 µM solution of C1q (9.4 µM in binding sites assuming 12 sites per molecule (39)) in PBS (50 - 100 µl) was added to one chamber and radiolabeled peptide in PBS (50 - 100 µl) was added to the other. In parallel with each experiment, a PBS solution of the largest peptide being tested was dialyzed against PBS. At 24-h intervals, aliquots were removed from each chamber of this test system and their radioactivities were measured. When the test system had reached equilibrium, aliquots from the experimental chambers were analyzed for the distribution of peptide radioactivity. Each experimental point was measured in triplicate.

RESULTS

A. Purification and Characterization of Synthetic Peptides

Before assembling the synthetic peptides by the solid-phase method, a detailed synthetic scheme was designed. While the actual assembly process using the solid-phase method requires relatively little time, most of the synthetic by-products remain attached to the resin until they are cleaved with HF. If assembly is efficient and few side reactions occur, the yield of the desired peptide is high and purification is straightforward. When the coupling reactions are inefficient or when a significant number of side reactions occur, the yield may be low and purification may be complicated and tedious, requiring the use of several techniques. In the present study, both efficient and inefficient syntheses were observed. The following sections describe the purification and characterization of synthetic peptides from four solid-phase syntheses.

1. $\underline{N^i}$-Formyl-IgG1 Eu γ-chain-(275-290)-hexadecapeptide (16F).

The crude synthetic mixture obtained after HF cleavage of the hexadecapeptide (16F) contained many different peptides as shown by reverse-phase HPLC (Fig. 16). This mixture was gel filtered on Bio-Gel P-2 to provide five pools (PI - PV) based on TLC analysis of the fractions

(Fig. 17). Reverse-phase HPLC analysis (Fig. 18) showed that pools PII and PIII both contained two of the major UV-active peaks found in crude 16F. In addition, these pools contained most of the synthetic product and had amino acid compositions in reasonable agreement with the expected composition of 16F (Fig. 17). Pool PII from Fig. 17 was further purified by reverse-phase HPLC using a µBondapak phenyl support to give two major UV-active pools (fractions 7-8, 9-11) based on TLC analysis of the fractions (Fig. 19). The amino acid compositions of these pools were very similar and in good agreement with the expected composition for 16F. Rechromatography of pool 7-8 from Fig. 19 on two µBondapak C18 columns produced two fractions (29 and 30) that contained a single peptide by TLC analysis (Fig. 20). In a similar fashion, pools PII and PIII were chromatographed semipreparatively on a Nucleosil C18 column to obtain a larger amount of the peptide corresponding to fractions 29 and 30 of Fig. 20. This peptide was homogeneous by HPLC, TLC, and TLE. It showed a single peak ($k' = 4.1$) on reverse-phase HPLC and one spot in four different TLC systems (Fig. 21). In addition, it exhibited on spot ($R_{Glu} = 0.05$) on thin-layer electrophoresis at pH 6.5. This peptide was assigned the structure Phe-Asn-Trp(For)-Tyr-Val-Asp-Gly-Val-Gln-Val-His-Asn-Ala-Lys-Thr-Lys (16F) based on the stepwise method of synthesis, its amino acid composition (Fig. 21), and its UV spectral maximum at 300 nm (Fig. 22) characteristic of the N^{i}-formyltryptophan residue. The specific activity of the hexadecapeptide calculated from the amino acid analysis was 170 cpm/nmol.

2. *IgG1 Eu γ-chain-(275-290)-hexadecapeptide* (*16*). The formyl protecting group was removed from 70% of the tryptophan residues of 16F by treatment at room temperature for 77 h with 0.01 M aqueous ammonium carbonate adjusted to pH 9.0 with ammonium hydroxide (83). Peptide 16 (k' = 2.5) was separated from the starting peptide 16F (k' = 5.9) on a μBondapak C18 column isocratically using 35% methanol in 1% aqueous acetic acid at 3 ml/min.

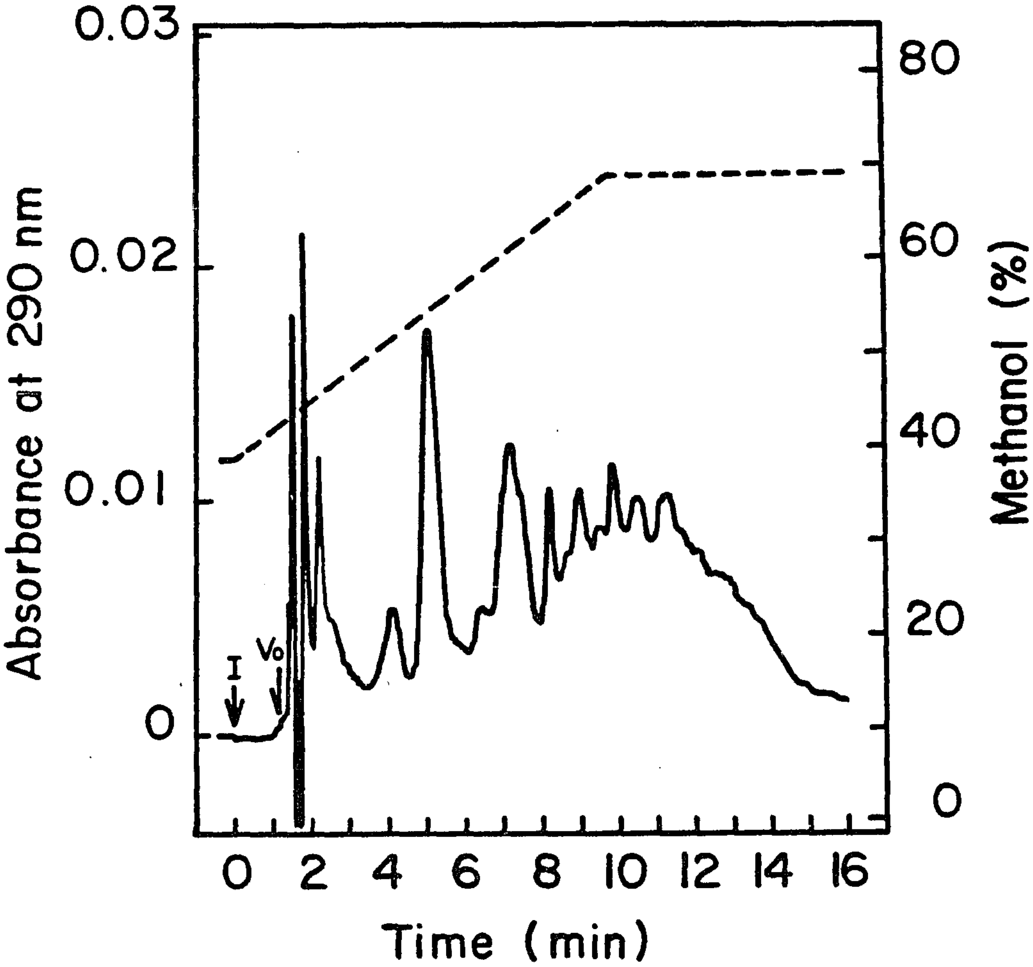

Fig. 16. Analytical reverse-phase HPLC of the crude synthetic mixture of peptide 16F. The peptides were eluted from a μBondapak C18 column for 10 min with a linear gradient of 40 to 70% methanol in 1% aqueous acetic acid at 2 ml/min and were monitored at 290 nm.

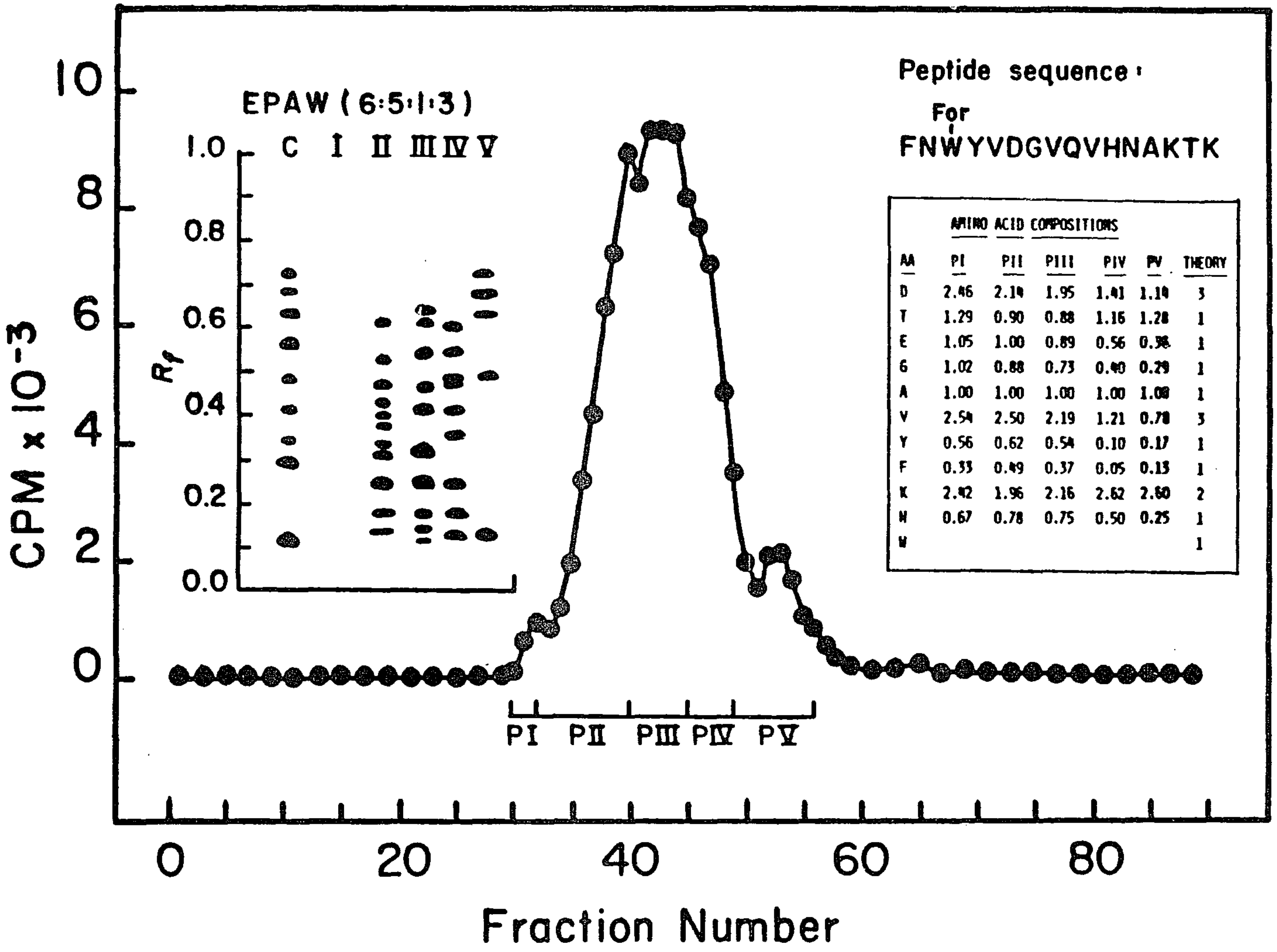

AMINO ACID COMPOSITIONS

AA	PI	PII	PIII	PIV	PV	THEORY
D	2.46	2.14	1.95	1.41	1.14	3
T	1.29	0.90	0.88	1.16	1.28	1
E	1.05	1.00	0.89	0.56	0.98	1
G	1.02	0.88	0.73	0.40	0.29	1
A	1.00	1.00	1.00	1.00	1.08	1
V	2.54	2.50	2.19	1.21	0.78	3
Y	0.56	0.62	0.54	0.10	0.17	1
F	0.33	0.49	0.37	0.05	0.13	1
K	2.42	1.96	2.16	2.62	2.60	2
H	0.67	0.78	0.75	0.50	0.25	1
W						1

Fig. 17. Gel-filtration chromatography of crude synthetic peptide 16F. Peptides were eluted from a Bio-Gel P-2 column (2.5 cm x 200 cm) with 20% aqueous acetic acid at 20 ml/h. The column fractions (10 ml) were monitored for radioactivity and divided into five pools (PI - PV). The left insert shows the TLC patterns of crude 16F (C) and each pool after separation with 6:5:1:3 (v/v/v/v) Ethyl acetate-Pyridine-Acetic acid-Water. The right insert shows the amino acid compositions of each pool after acid hydrolysis.

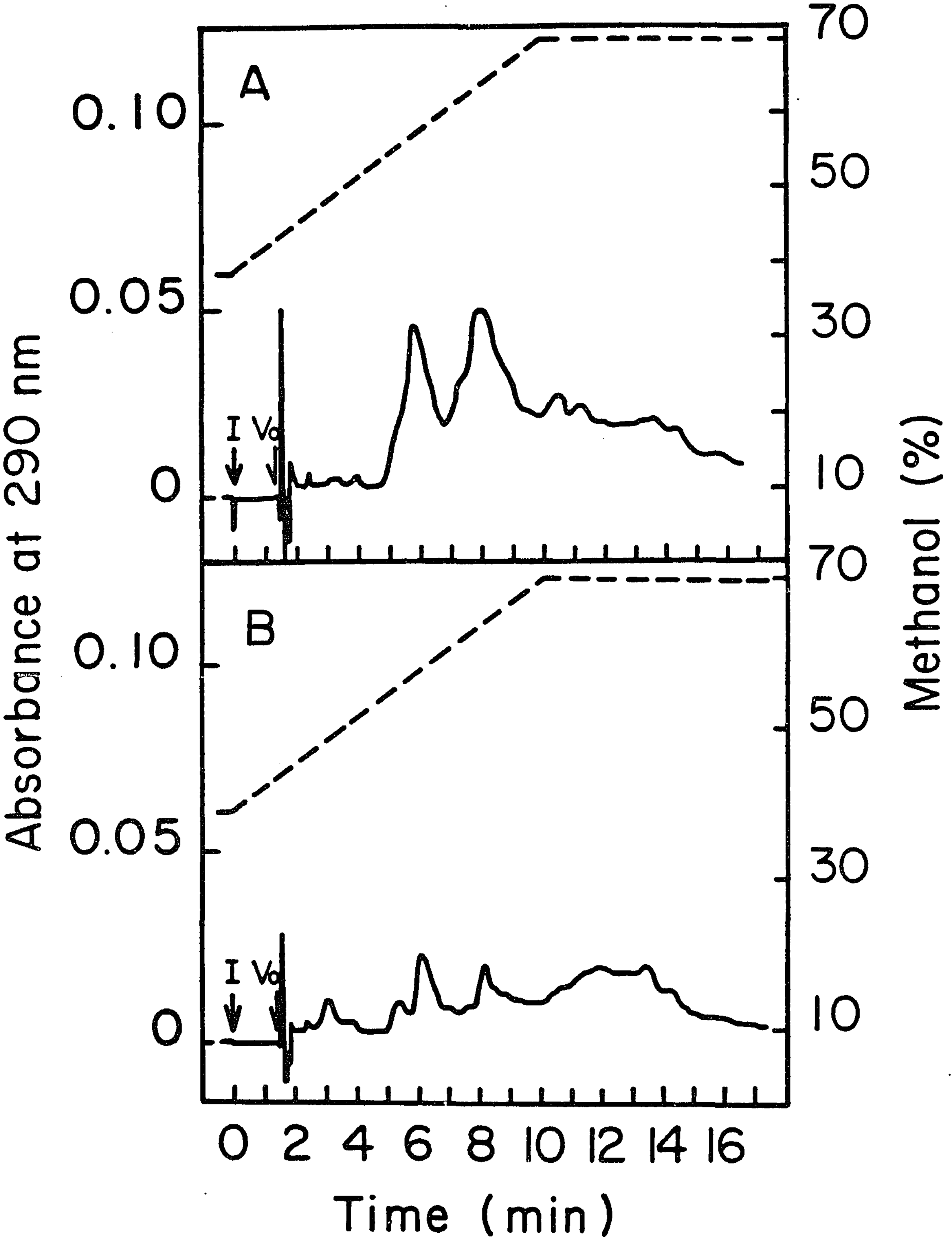

Fig. 18. Analytical reverse-phase HPLC of peptide 16F pools PII (A) and PIII (B) from Fig. 17. Peptides were eluted from a μBondapak phenyl column for 10 min with a linear gradient of 40 to 70% methanol in 1% aqueous acetic acid at 2 ml/min and were monitored at 290 nm.

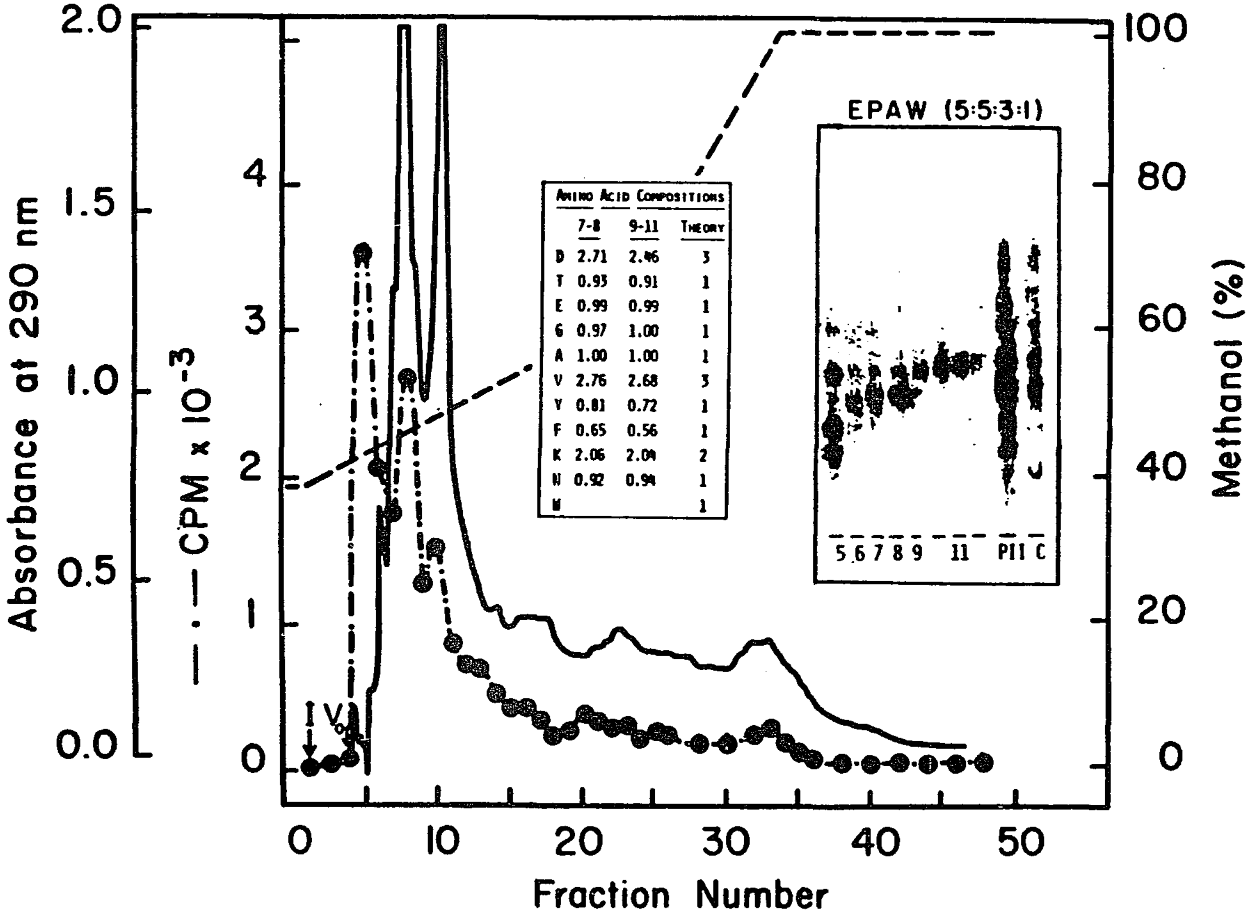

AMINO ACID COMPOSITIONS

	7-8	9-11	THEORY
D	2.71	2.46	3
T	0.93	0.91	1
E	0.99	0.99	1
G	0.97	1.00	1
A	1.00	1.00	1
V	2.76	2.68	3
Y	0.81	0.72	1
F	0.65	0.56	1
K	2.06	2.04	2
N	0.92	0.94	1
M			1

Fig. 19. Semipreparative reverse-phase HPLC of peptide 16F pool PII from Fig. 17. Peptides were eluted from a μBondapak phenyl column for 10 min with a linear gradient of 40 to 70% methanol in 1% aqueous acetic acid at 2 ml/min and were monitored at 290 nm and for radioactivity. The right insert shows the TLC patterns for fractions 5 through 12, PII, and crude 16F (C) after separation with 5:5:1:3 (v/v/v/v) Ethyl acetate-Pyridine-Acetic acid-Water. The left insert shows the amino acid compositions after acid hydrolysis of two pools consisting of fractions 7-8 and fractions 9-11.

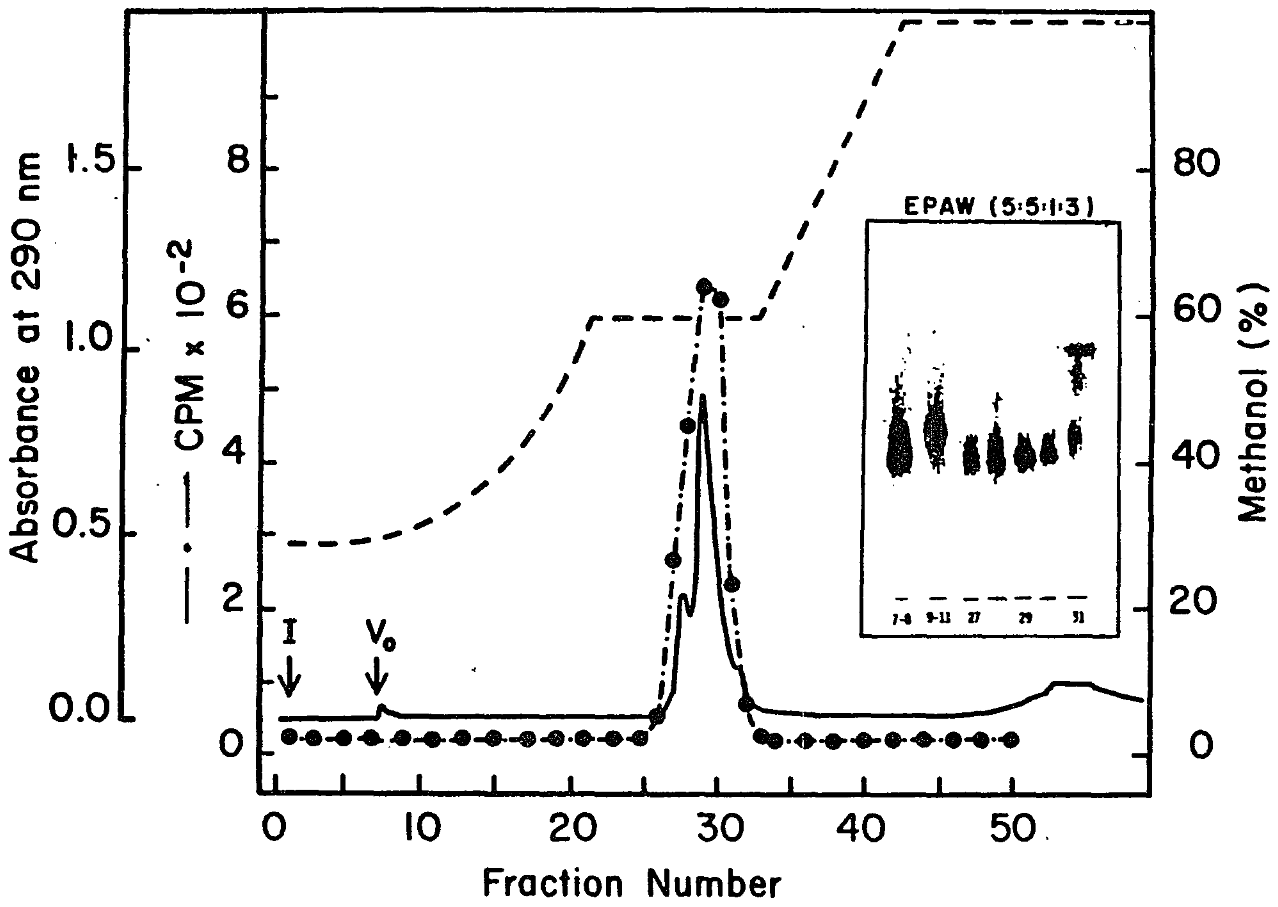

Fig. 20. Semipreparative reverse-phase HPLC of peptide 16F pool 7-8 from Fig. 19. Peptides were eluted from two μBondapak C18 columns for 10 min with a#8 concave gradient from 30 to 60% methanol in 1% aqueous acetic acid at 2 ml/min followed by 60% methanol in 1% acetic acid. The eluate was monitored at 290 nm and for radioactivity. The insert shows the TLC patterns of 16F pools 7-8 and 9-11 from Fig. 19 and fractions 27 through 31 after separation with 5:5:1:3 (v/v/v/v) Ethyl acetate-Pyridine-Acetic acid-Water.

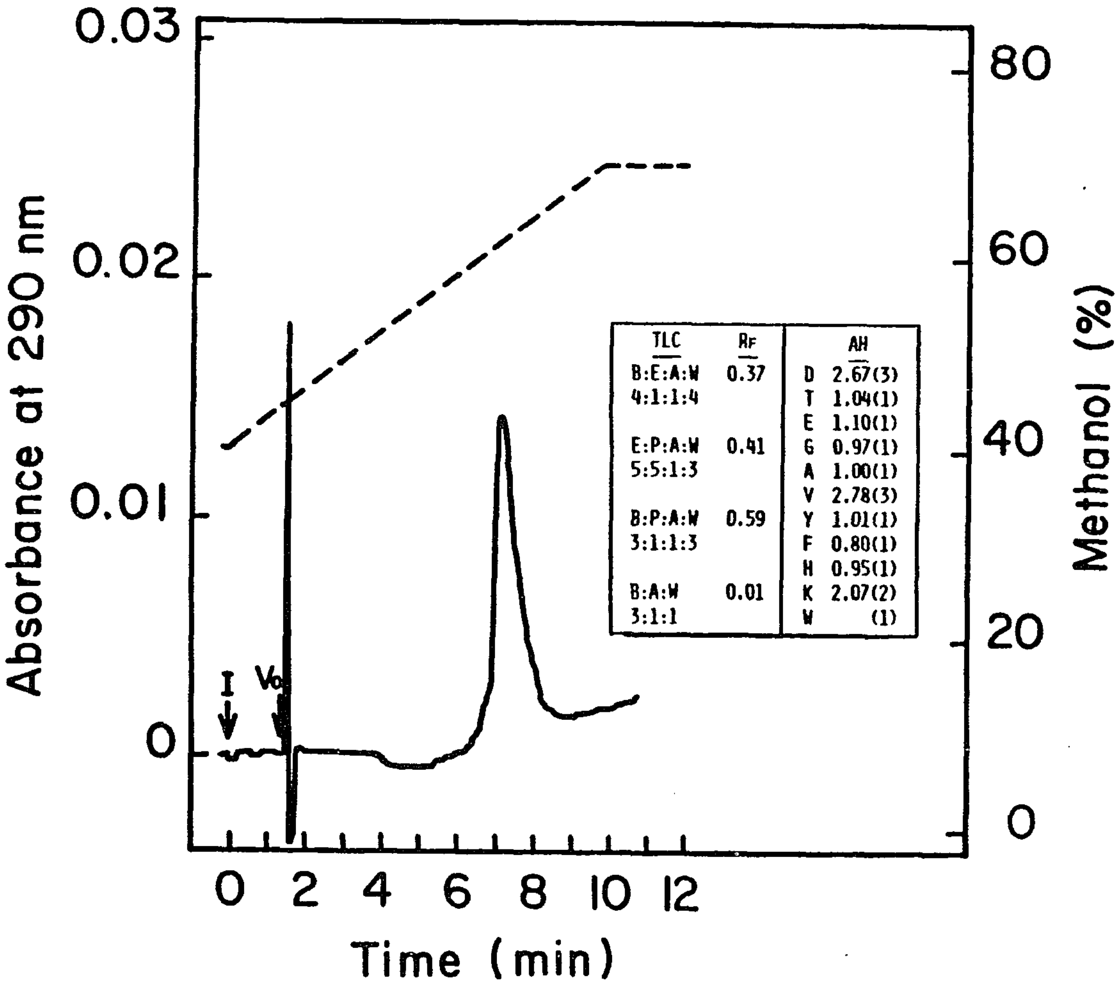

TLC	RF
B:E:A:W 4:1:1:4	0.37
E:P:A:W 5:5:1:3	0.41
B:P:A:W 3:1:1:3	0.59
B:A:W 3:1:1	0.01

AH	
D	2.67(3)
T	1.04(1)
E	1.10(1)
G	0.97(1)
A	1.00(1)
V	2.78(3)
Y	1.01(1)
F	0.80(1)
H	0.95(1)
K	2.07(2)
W	(1)

Fig. 21. Analytical reverse-phase HPLC of homogeneous peptide 16F prepared from pools PII and PIII of Fig. 17 by HPLC on a Nucleosil C18 column. Peptide 16F was eluted from a μBondapak phenyl column for 10 min with a linear gradient from 40 to 70% methanol in 1% aqueous acetic acid at 2 ml/min and monitored at 290 nm (k' = 4.1). TLC analysis of 16F (insert) showed a single spot by both ninhydrin and Cl/tolidine in four different solvent systems (B, 1-butanol; E, ethyl acetate; P, pyridine; A, acetic acid; and W, water). Amino acid composition after acid hydrolysis was in good agreement with theoretical values (insert).

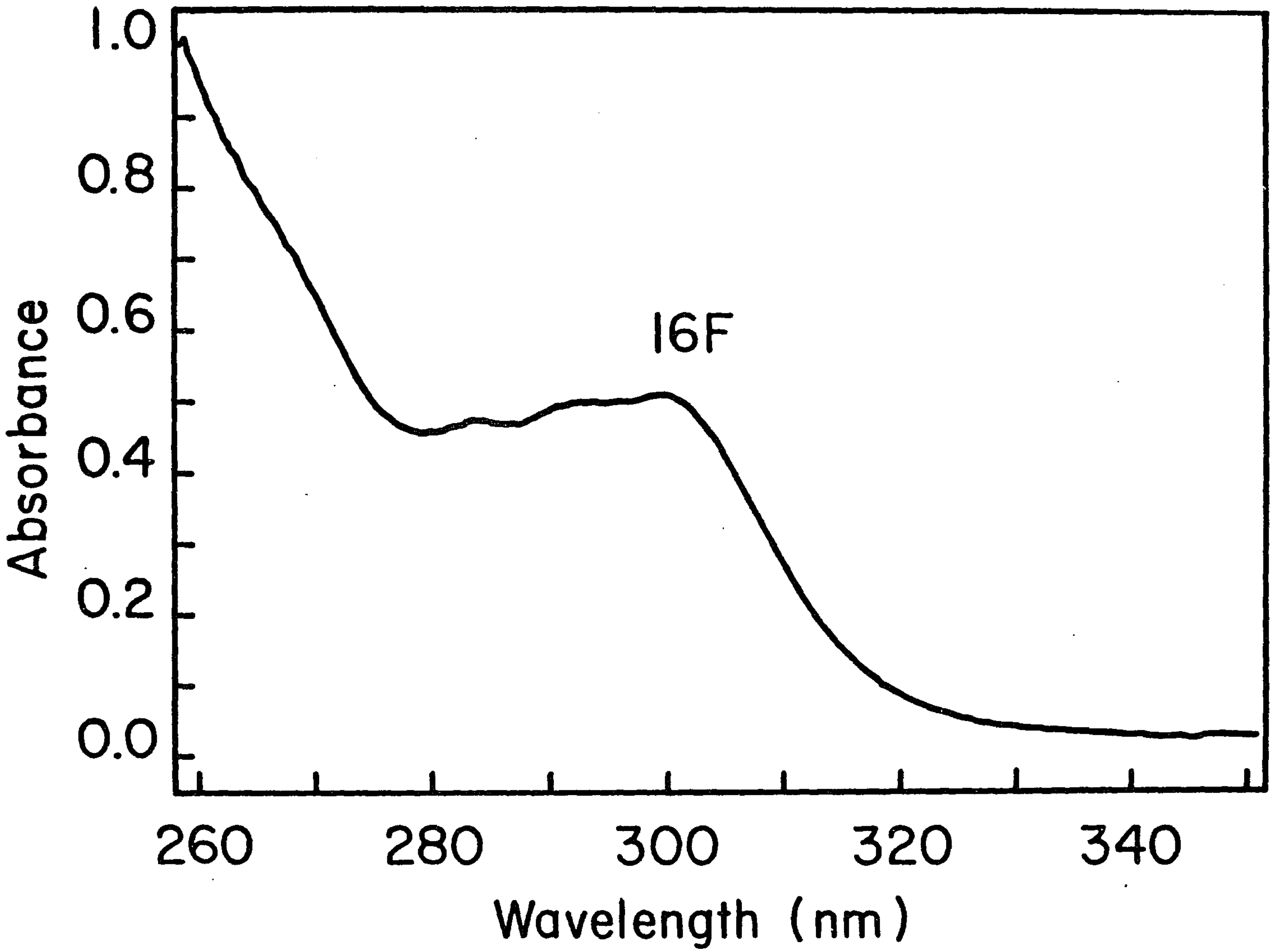

Fig. 22. Ultraviolet spectrum of peptide 16F. Pure peptide from Fig. 21 was examined in 1:4 (v/v) methanol-1% aqueous acetic acid versus methanol. The absorption maximum at 300 nm indicates the presence of a Trp(For) residue.

3. IgG1 Eu γ-chain-(281-290)-decapeptide (10). The crude decapeptide was chromatographed on superfine Sephadex G-25, and the fractions collected were divided into four pools (PI - PIV) based on TLC analysis (Fig. 23). Thin-layer chromatography and amino acid compositions of the four pools (Fig. 23) indicated that PIII contained most of the desired product. Pool PIII was chromatographed semipreparatively on a μBondapak C18 column (Fig. 24) and the fractions were analyzed by TLC and monitored for radioactivity. Fractions 7 through 9 from Fig. 24 were pooled and further characterized by HPLC, TLC, and TLE. This pool chromatographed as one peak by reverse-phase HPLC ($k' = 2.0$) and showed one spot in five different TLC systems (Fig. 25). Also, it exhibited one spot ($R_{Arg} = 0.59$) on thin-layer electrophoresis. This peptide was assigned the structure Gly-Val-Gln-Val-His-Asn-Ala-Lys-Thr-Lys based on the stepwise method of assembly and the amino acid compositions (Fig. 25). Aminopeptidase M digestion of peptide 10 revealed only asparagine and glutamine residues without a trace of aspartic acid or glutamic acid above the background control containing only enzyme. Both asparagine and glutamine co-elute with threonine under the standard chromatographic conditions for the Durrum D-500 single column analyzer. This decapeptide had a specific activity of 210 cpm/nmol.

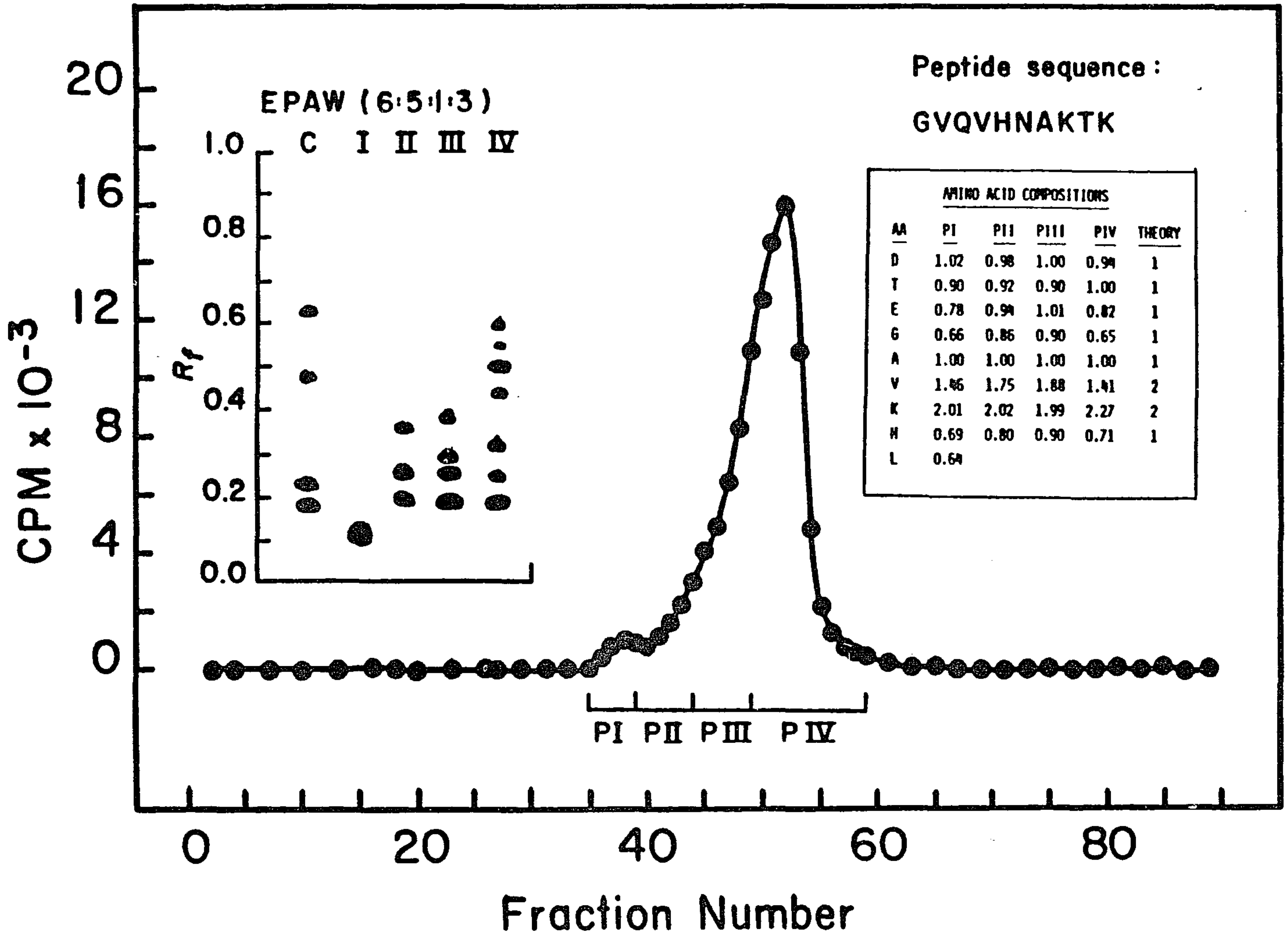

AMINO ACID COMPOSITIONS

AA	PI	PII	PIII	PIV	THEORY
D	1.02	0.98	1.00	0.94	1
T	0.90	0.92	0.90	1.00	1
E	0.78	0.94	1.01	0.82	1
G	0.66	0.86	0.90	0.65	1
A	1.00	1.00	1.00	1.00	1
V	1.46	1.75	1.88	1.41	2
K	2.01	2.02	1.99	2.27	2
H	0.69	0.80	0.90	0.71	1
L	0.64				

Fig. 23. Gel-filtration chromatography of the crude synthetic peptide 10. Peptides were eluted from a superfine Sephadex G-25 column (2.5 cm x 200 cm) in 20% aqueous acetic acid at 20 ml/h. Column fractions (10 ml) were monitored by TLC and for radioactivity and divided into four pools (PI - PIV). The left insert shows the TLC patterns of crude 10 (C) and each pool after separation with 6:5:1:3 (v/v/v/v) Ethyl acetate-Pyridine-Acetic acid-Water. The right insert shows the amino acid compositions of each pool after acid hydrolysis.

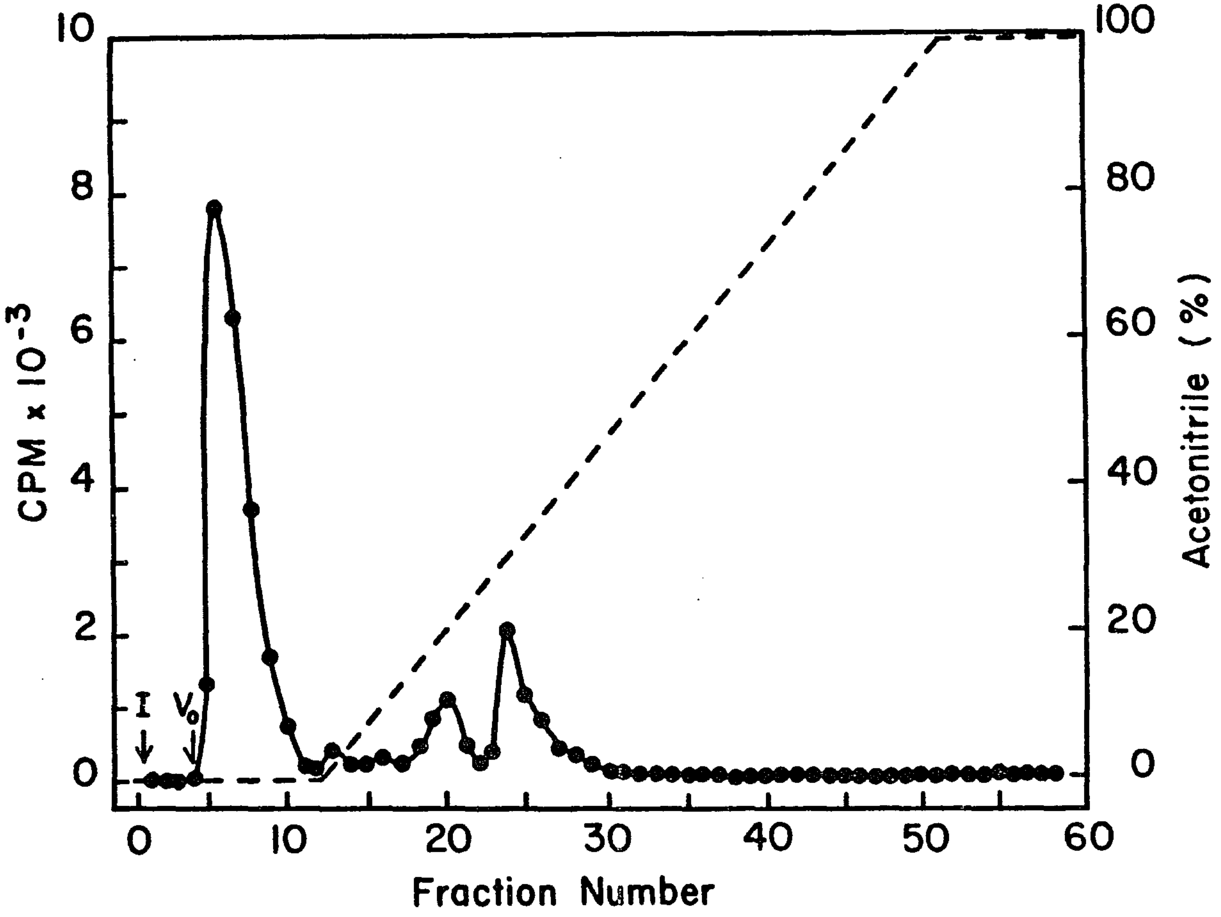

Fig. 24. Semipreparative reverse-phase HPLC of peptide 10 pool PIII from Fig. 23. Peptides were eluted from a μBondapak C18 column with 0.5% aqueous acetic acid for 7 min followed by a linear gradient of 0 to 100% acetonitrile over 20 min. Fractions were monitored for radioactivity and examined by TLC. Fractions 7-9 were pooled based on the TLC results.

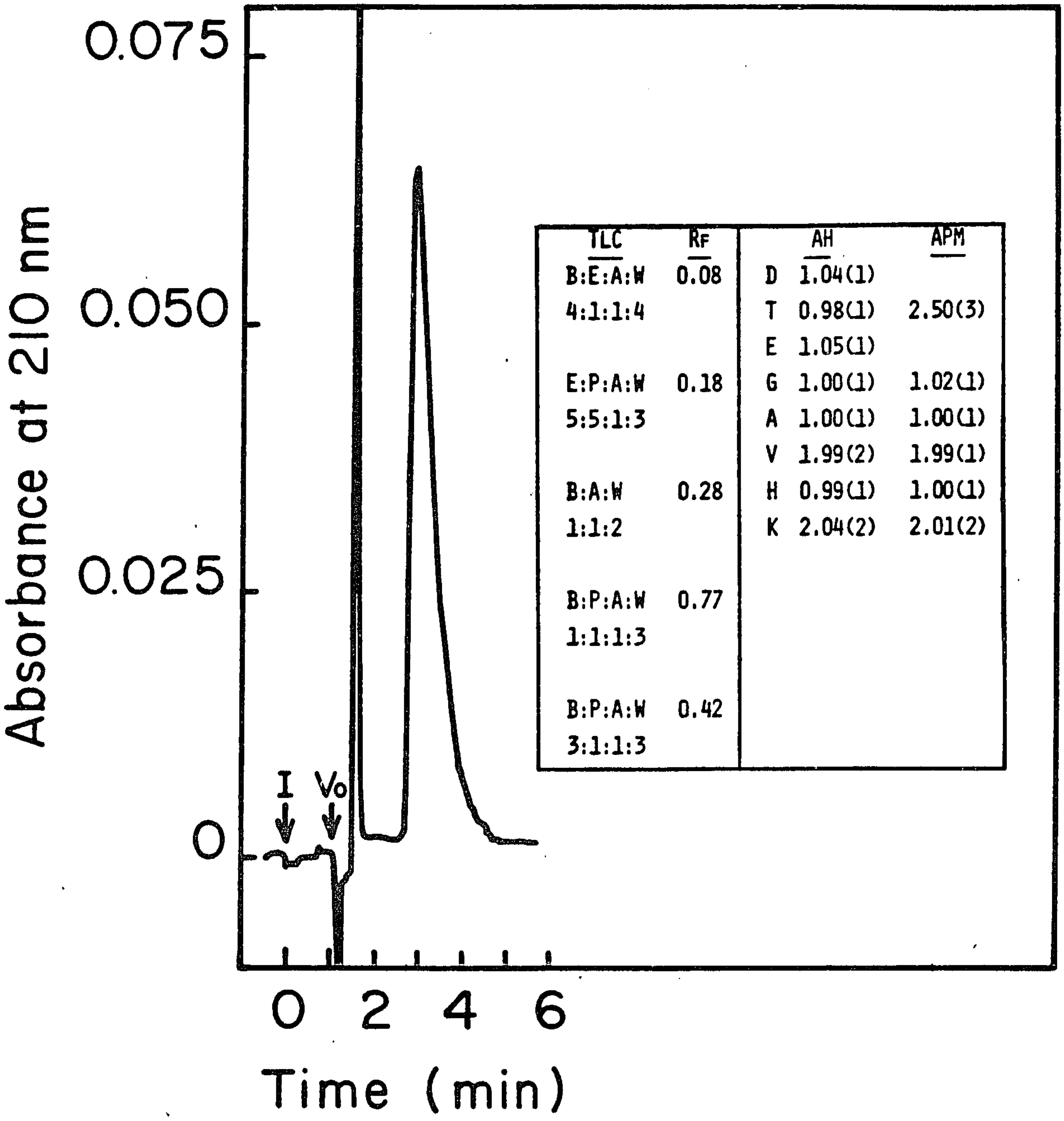

TLC	RF
B:E:A:W 4:1:1:4	0.08
E:P:A:W 5:5:1:3	0.18
B:A:W 1:1:2	0.28
B:P:A:W 1:1:1:3	0.77
B:P:A:W 3:1:1:3	0.42

	AH	APM
D	1.04(1)	
T	0.98(1)	2.50(3)
E	1.05(1)	
G	1.00(1)	1.02(1)
A	1.00(1)	1.00(1)
V	1.99(2)	1.99(1)
H	0.99(1)	1.00(1)
K	2.04(2)	2.01(2)

Fig. 25. Analytical reverse-phase HPLC of the pure peptide 10 pool 7-9 from Fig. 24. Peptide 10 was eluted from a μBondapak C18 column isocratically using 2% methanol in 1% aqueous acetic acid and monitored at 210 nm (k' = 2.0). Peptide 10 was one spot by TLC in five different solvent systems as visualized by ninhydrin and Cl/tolidine (B, 1-butanol; E, ethyl acetate; P, pyridine; A, acetic acid; and W, water). Amino acid composition after acid hydrolysis (AH) agreed well with theoretical values. After aminopeptidase M digestion (APM), amino acid analysis revealed only Asn and Gln, which co-eluted with Thr.

4. <u>N$^{\alpha}$-Acetyl-L-glutamyl-L-tryptophanyl-L-tyrosyl-L-glutamyl-L-arginyl-glycine</u> (<u>A6J</u>). The peptide-resin was radiolabeled at a high specific activity by acetylating 4% of the peptide-resin with tritiated acetic anhydride. This resulted in peptide A6J comprising only 4% of the total synthetic products. Analytical reverse-phase HPLC of the crude synthetic product revealed many UV-active peaks but only one major radioactive peak (Fig. 26). Semipreparative reverse-phase chromatography of crude peptide A6J produced one major radioactive pool, fraction IV (Fig. 27). Rechromatography of fraction IV yielded a pool, fraction 3, that contained peptide A6J in greater than 95% purity (Fig. 28). A6J was purified to homogeneity by rechromatography of fraction 3 through two µBondapak columns linked in series. The resulting peptide A6J eluted as one peak ($k' = 11.7$) on reverse-phase HPLC in an isocratic system (Fig. 29A) and as one single peak ($k' = 8.1$) by gradient elution (Fig. 29B). A6J also appeared as one spot in four different TLC systems and had an amino acid composition consistent with the theoretical values (Fig. 29). The presence of the tryptophan was shown by ultraviolet spectroscopy (Fig. 30). Peptide A6J was assigned the structure Ac-Glu-Trp-Tyr-Glu-Arg-Gly based on the stepwise method of synthesis, its amino acid composition, and its ultraviolet spectrum. The specific activity of peptide A6J was 75,500 cpm/nmol.

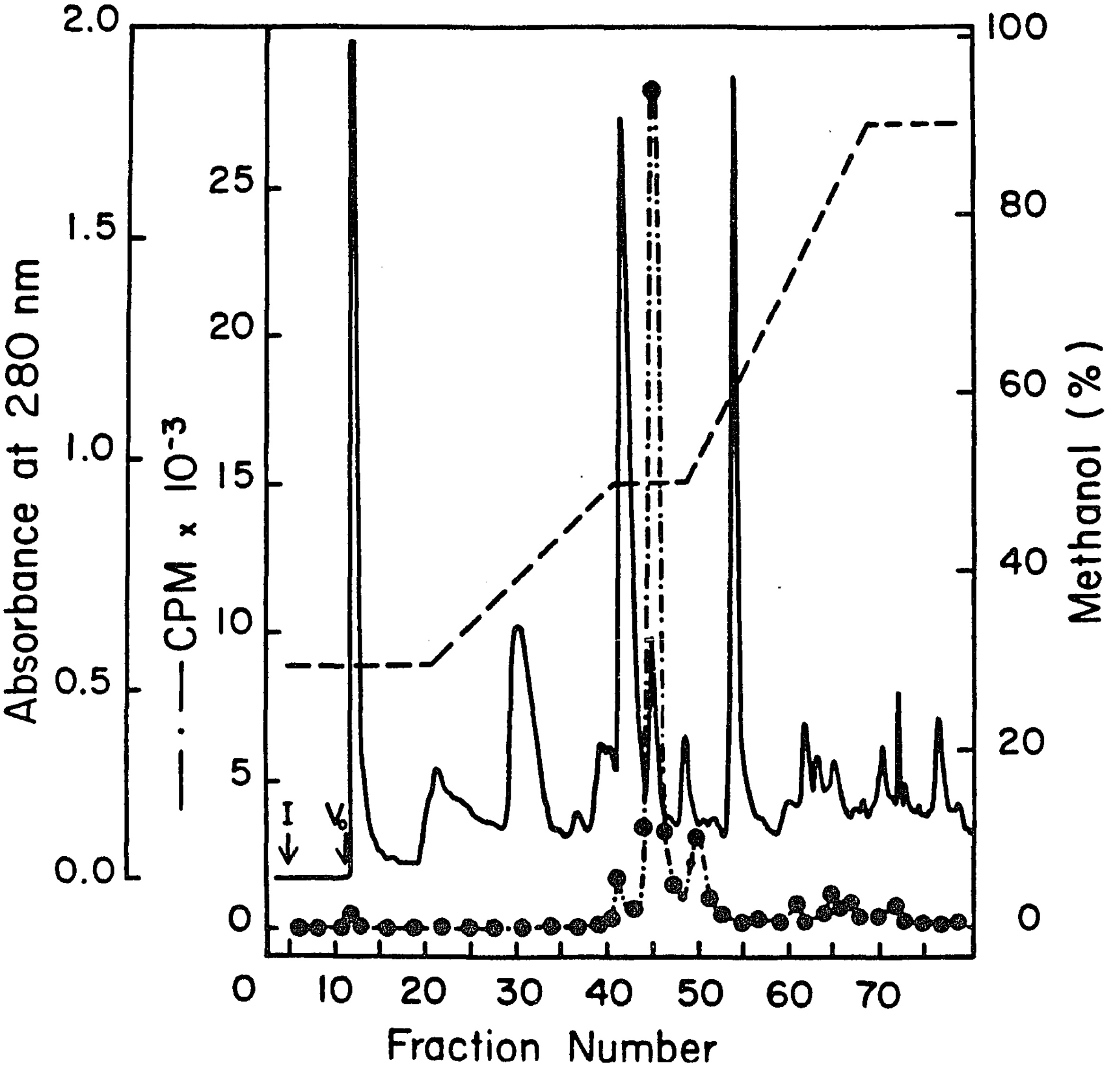

Fig. 26. Analytical reverse-phase HPLC of the crude synthetic mixture of peptide A6J. Peptides were eluted from a Nucleosil C18 column with two linear gradients from 30 to 50% methanol and 50 to 90% methanol in 1% aqueous acetic acid at 5 ml/min. The eluate was monitored at 280 nm and for radioactivity.

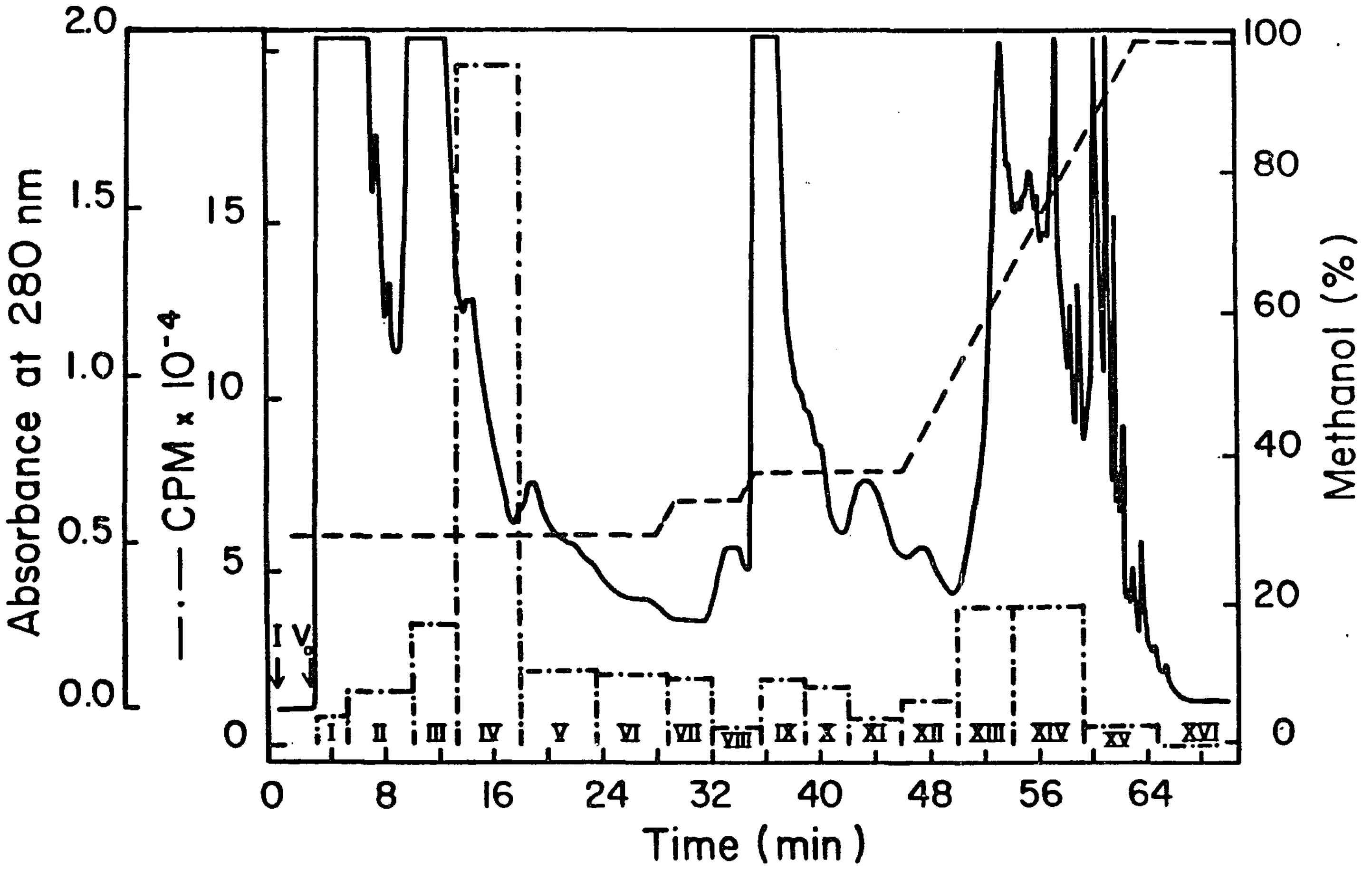

Fig. 27. Semipreparative reverse-phase HPLC of crude peptide A6J. The major radiolabeled product was eluted isocratically from a Nucleosil C18 column using 30% methanol in 1% aqueous acetic acid at 5 ml/min. The eluate was monitored at 280 nm and the 16 designated fractions were examined for radioactivity, which showed that the major radiolabeled peptide was in fraction IV.

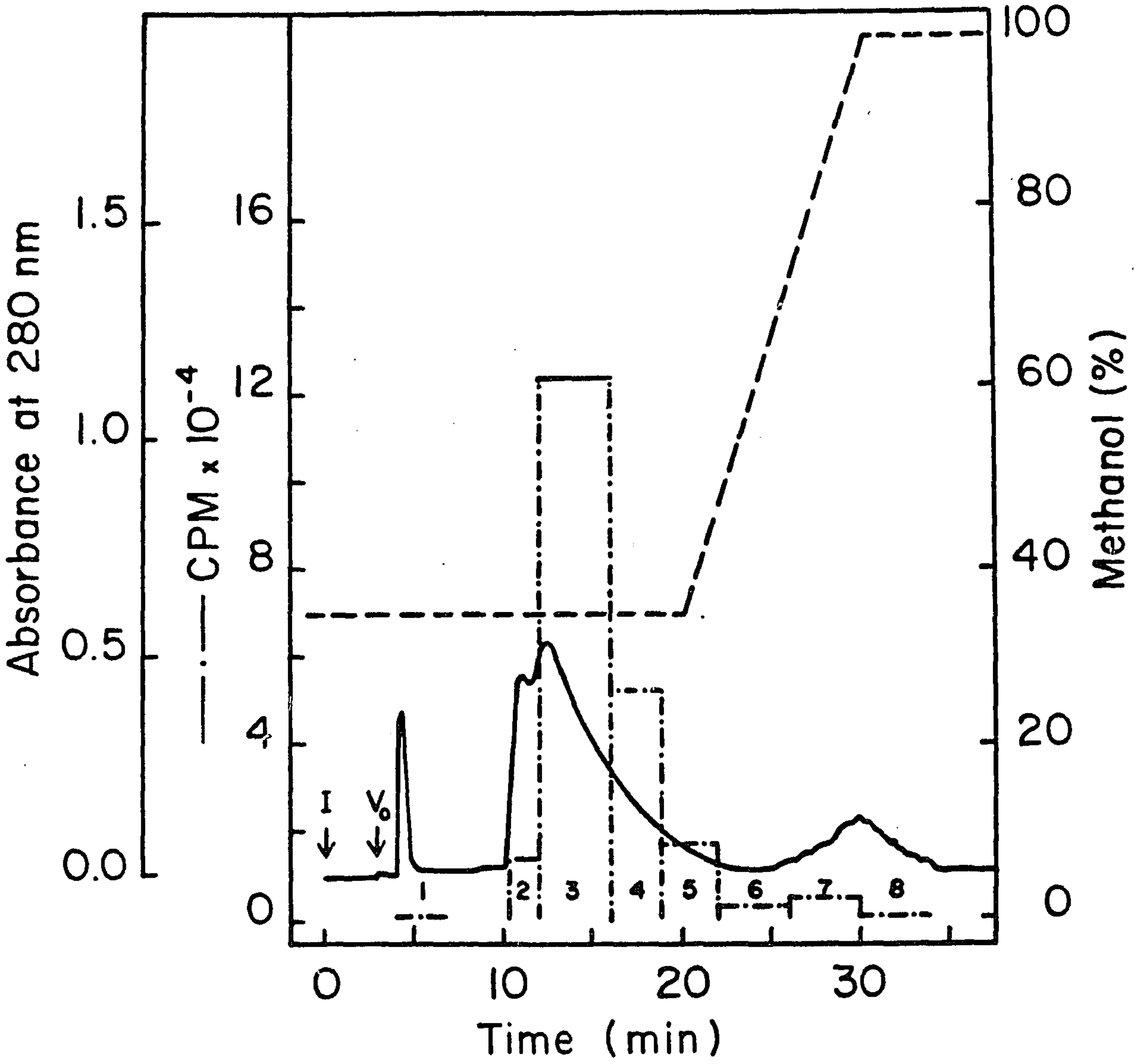

Fig. 28. Semipreparative reverse-phase HPLC of peptide A6J fraction IV from Fig. 27. Radiolabeled peptides were eluted isocratically from a Nucleosil C18 column using 35% methanol in 1% acetic acid at 5 ml/min. The eluate was monitored at 280 nm and for radioactivity. The major radiolabeled peptide from fraction 3 was purified to homogeneity using two μBondapak C18 columns in series.

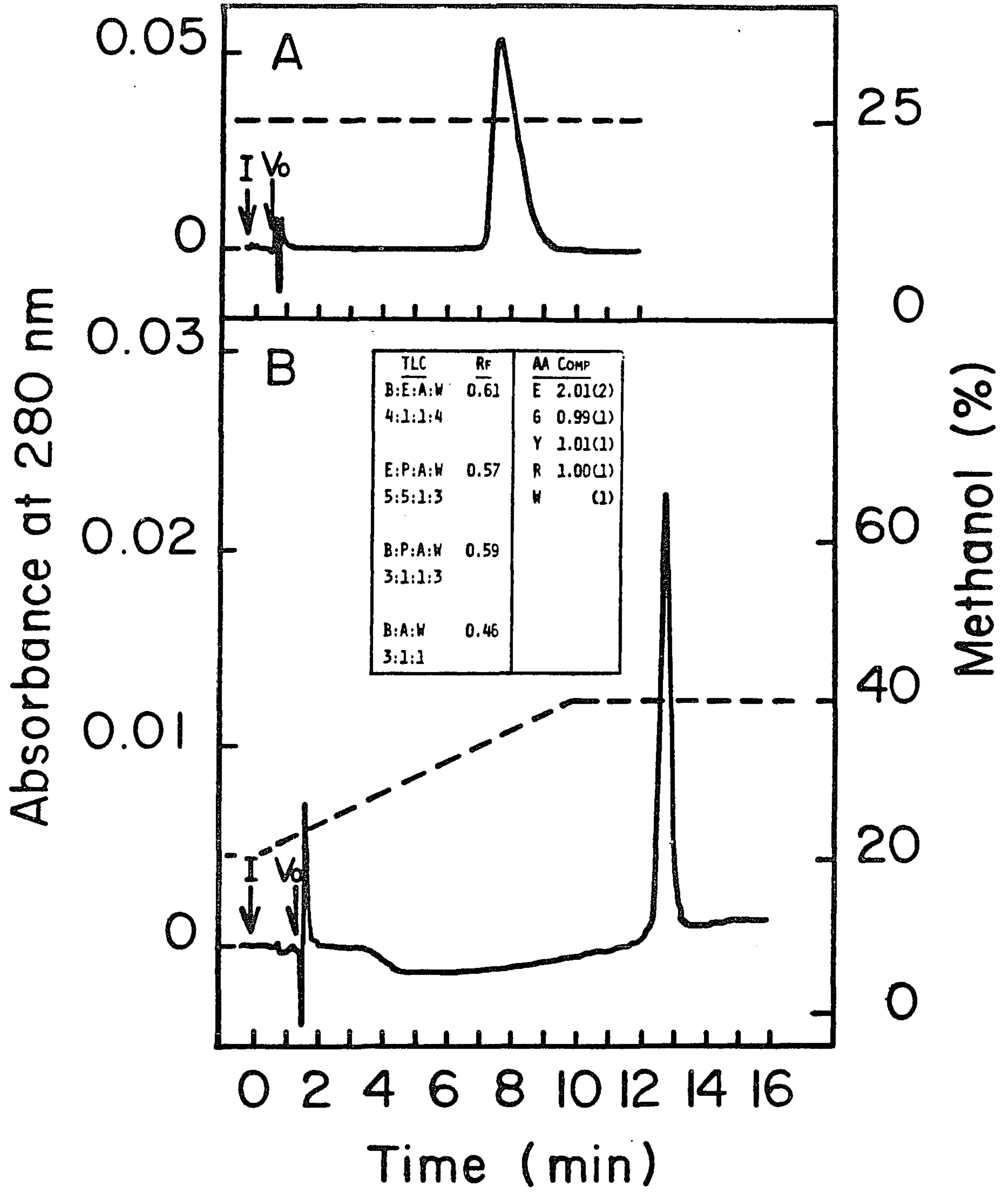

TLC	RF	AA COMP
B:E:A:W	0.61	E 2.01(2)
4:1:1:4		6 0.99(1)
		Y 1.01(1)
E:P:A:W	0.57	R 1.00(1)
5:5:1:3		W (1)
B:P:A:W	0.59	
3:1:1:3		
B:A:W	0.46	
3:1:1		

Fig. 29. Analytical reverse-phase HPLC of homogeneous peptide A6J. (A) Peptide A6J was eluted isocraically as a single peak (k' = 11.7) from a μBondapak C18 column using 25% methanol in 1% aqueous acetic acid at 5 ml/min. (B) Peptide A6J was eluted as a single peak (k' = 8.1) from a μBondapak C18 column with a linear gradient of 20 to 40% methanol in 1% aqueous acetic acid at 2 ml/min. Aromatic peptides were detected by monitoring at 280 nm. The insert shows that the amino acid composition was in good agreement with the theoretical values and that A6J was one spot by TLC in four solvent systems (B, 1-butanol; E, ethyl acetate; P, pyridine; A, acetic acid; and W, water) as visualized by Cl/tolidine.

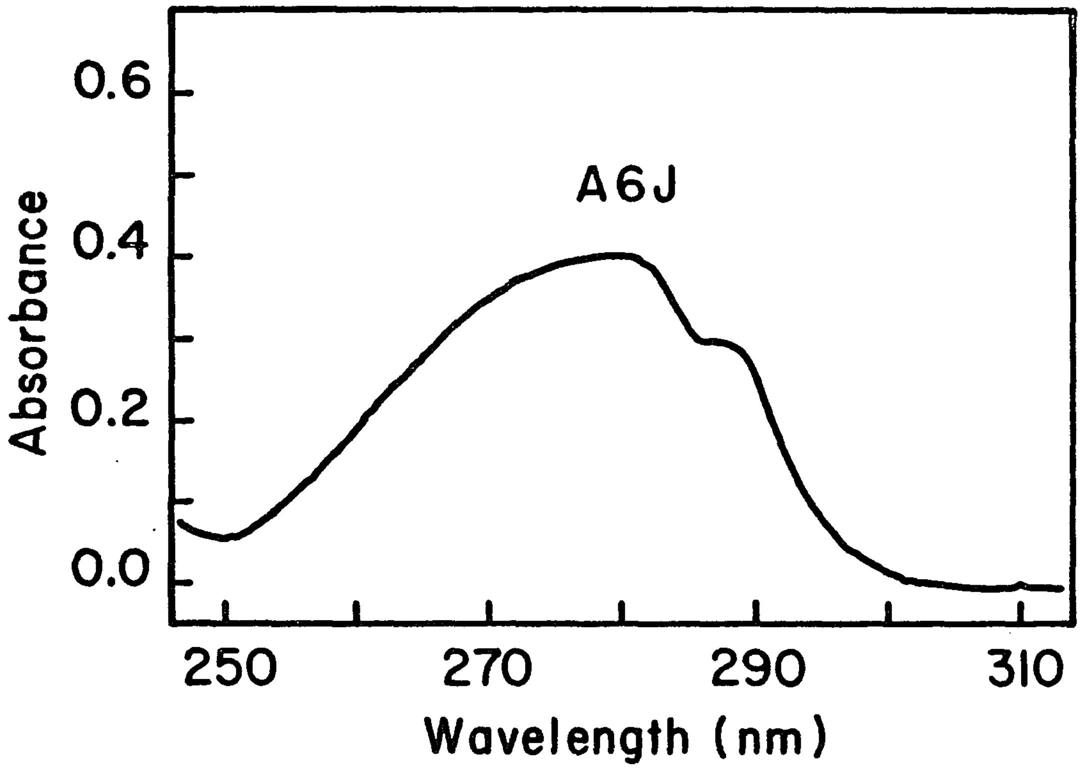

Fig. 30. Ultraviolet spectrum of peptide A6J. Pure peptide from Fig. 29 was examined in 1:3 (v/v) methanol-1% aqueous acetic acid versus methanol. The absorption maximum at 280 nm indicates the presence of a tryptophan residue.

5. *N$^{\alpha}$-Acetyl-IgG1 Eu γ-chain-(275-279)-pentapeptide* (*A5*) and *N$^{\alpha}$-Acetyl-N^{i}-Formyl-IgG1 Eu γ-chain-(275-279)-pentapeptide* (*A5F*). The portion of the crude synthetic pentapeptide that dissolved in 10% aqueous acetic acid contained many components. Semipreparative reverse-phase chromatography of this crude mixture provided peptides A5 and A5F (Fig. 31). Both peptides chromatographed as single peaks by HPLC and single spots by TLC in three different solvent systems (Fig. 32 and 33). The amino acid composition of peptide A5 after acid hydrolysis was satisfactory. The tyrosine and valine values after base hydrolysis were low because of incomplete hydrolysis of the Tyr-Val dipeptide (Fig. 32). From the stepwise method of assembly, the amino acid compositions, and the absorption maximum at 280 nm (Fig. 34), peptide A5 was assigned the structure Ac-Phe-Asn-Trp-Tyr-Val. The amino acid compositions for peptide A5F were generally in good agreement with theoretical values (Fig. 33). The low value for aspartic acid obtained after acid hydrolysis was a consistent finding. Peptide A5F was assigned the structure Ac-Phe-Asn-Trp(For)-Tyr-Val based on the stepwise method of synthesis and the UV spectral maximum at 300 nm (Fig. 34). The specific activity of both pentapeptides was 2040 cpm/nmol.

After storing the synthetic pentapeptide mixture at 4°C, a white amorphous solid formed that contained most of the radioactivity and was mostly peptide A5F. When the solid was redissolved in 1:1 (v/v) methanol-1% aqueous acetic acid and chromatographed on a μBondapak phenyl column, one major peak (78%) and four minor peaks (3-6%) were observed (Fig. 35). The single peptide present in the major peak was identical to the previously isolated peptide A5F and was 80% converted into peptide A5 through deformylation of the tryptophan residue by treatment for 49 h at room temperature with 1:1 (v/v) aqueous 0.01 M ammonium carbonate-methanol adjusted to pH 9.0 with ammonium hydroxide.

The 220 MHz nuclear magnetic resonance (NMR) spectrum of peptide A5F in dimethylsulfoxide-$\underline{d}_6$ is shown as the upper spectrum in Fig. 36. The solution was diluted with D_2O and the protons were allowed to exchange with deuterons. The NMR spectrum was recorded periodically. After two months, 10.4 protons had exchanged (Table II). This result is consistent with the exchange of the phenolic proton of tyrosine, five main-chain amide protons, both side-chain protons of asparagine, and the carboxyl proton of valine. After exchanging with D_2O, 15 protons remained in the aromatic region as expected. The extra 1.4 exchangeable protons are ascribed to trace amounts of acetic acid in the sample.

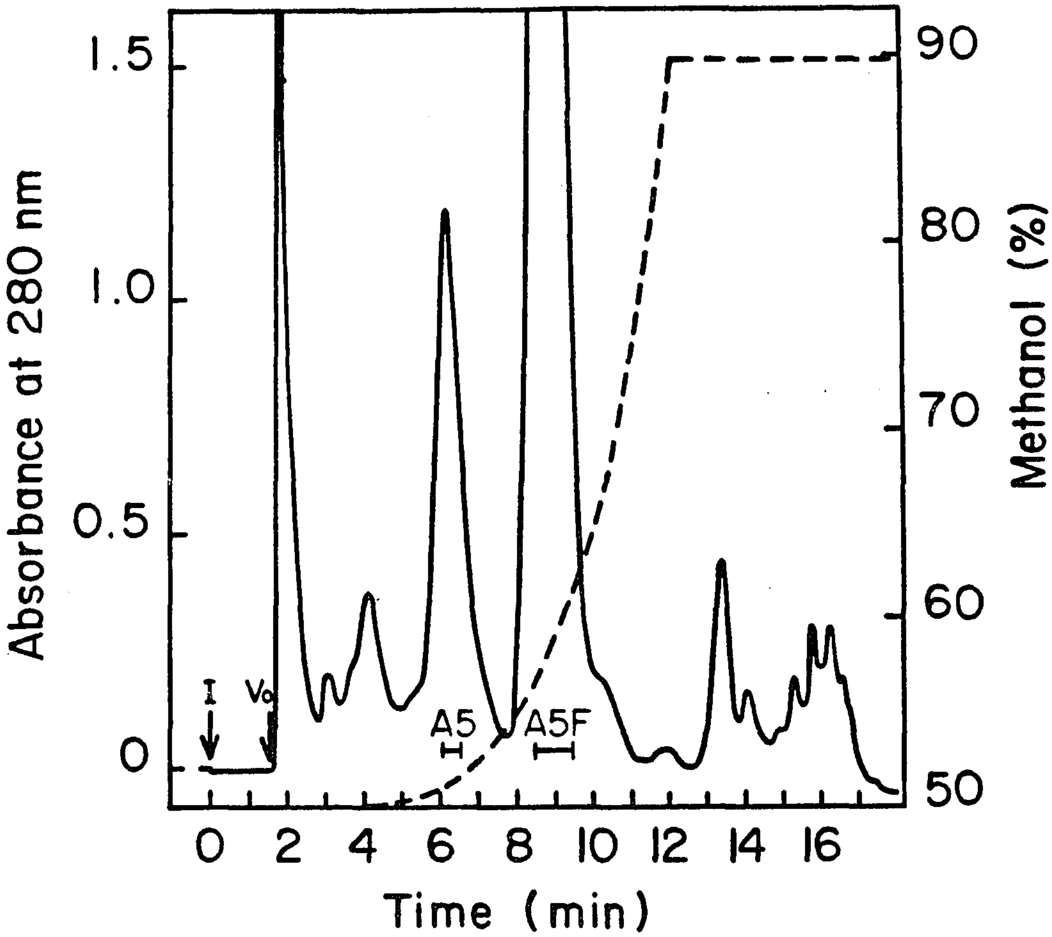

Fig. 31. Semipreparative reverse-phase HPLC of the crude peptide A5F that was soluble in 10% acetic acid. Peptides were eluted from a µBondapak phenyl column with a # 10 concave gradient from 50 to 90% methanol in 5% aqueous acetic acid at 2 ml/min. The eluate was monitored at 280 nm and the major products were pooled as A5 and A5F.

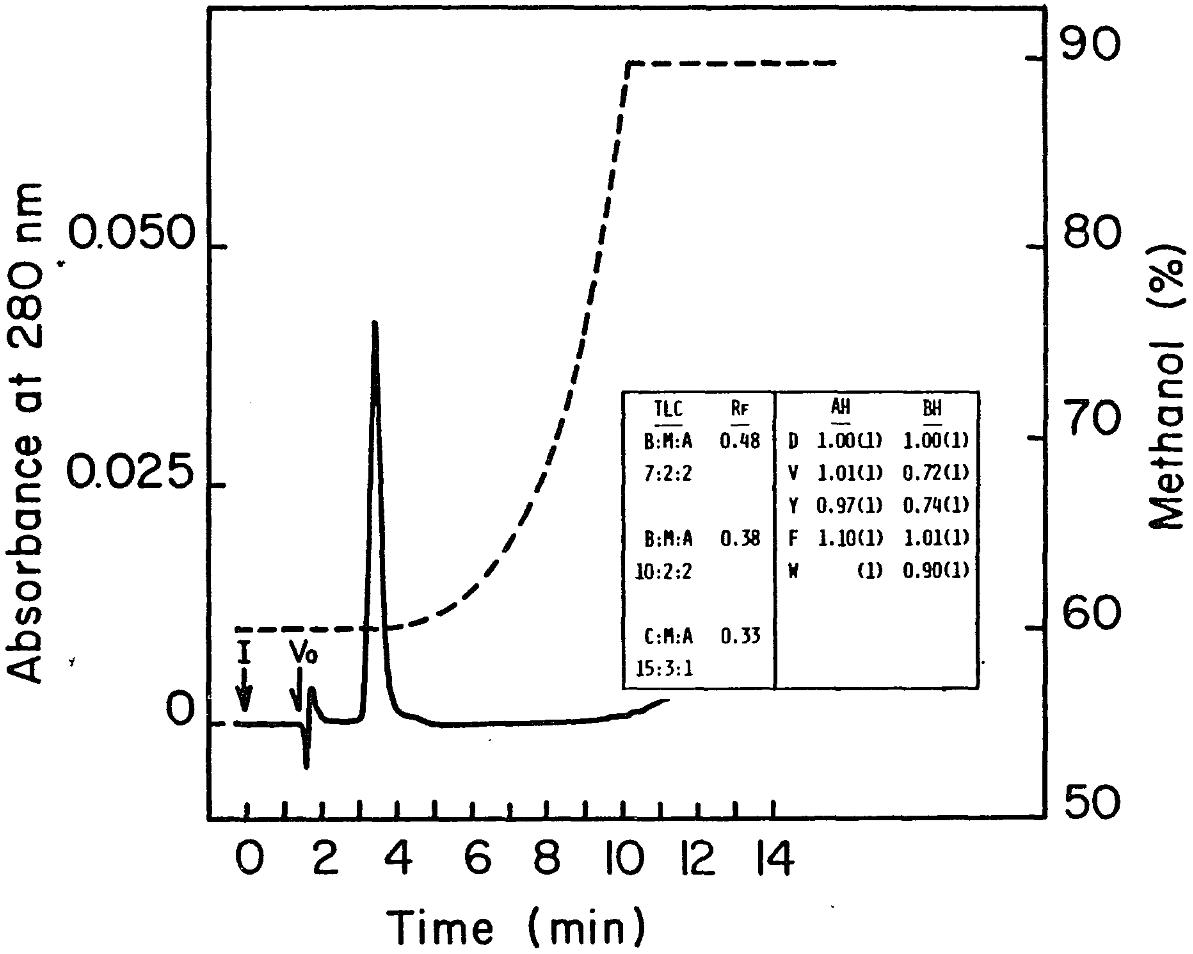

TLC	RF
B:M:A 7:2:2	0.48
B:M:A 10:2:2	0.38
C:M:A 15:3:1	0.33

	AH	BH
D	1.00(1)	1.00(1)
V	1.01(1)	0.72(1)
Y	0.97(1)	0.74(1)
F	1.10(1)	1.01(1)
W	(1)	0.90(1)

Fig. 32. Analytical reverse-phase HPLC of peptide A5 from Fig. 31. Peptide A5 was eluted as a single peak (k' = 1.5) from a μBondapak phenyl column using a 10 min # 10 concave gradient from 60 to 90% methanol in 5% aqueous acetic acid at 2 ml/min. The eluate was monitored at 280 nm. The insert shows that A5 was a single spot by TLC in three solvent systems (B, benzene; A, acetic acid; M, methanol; and C, chloroform) as visualized by Cl/tolidine and that amino acid compositions after acid hydrolysis (AH) and base hydrolysis (BH) were in good agreement with the theoretical values.

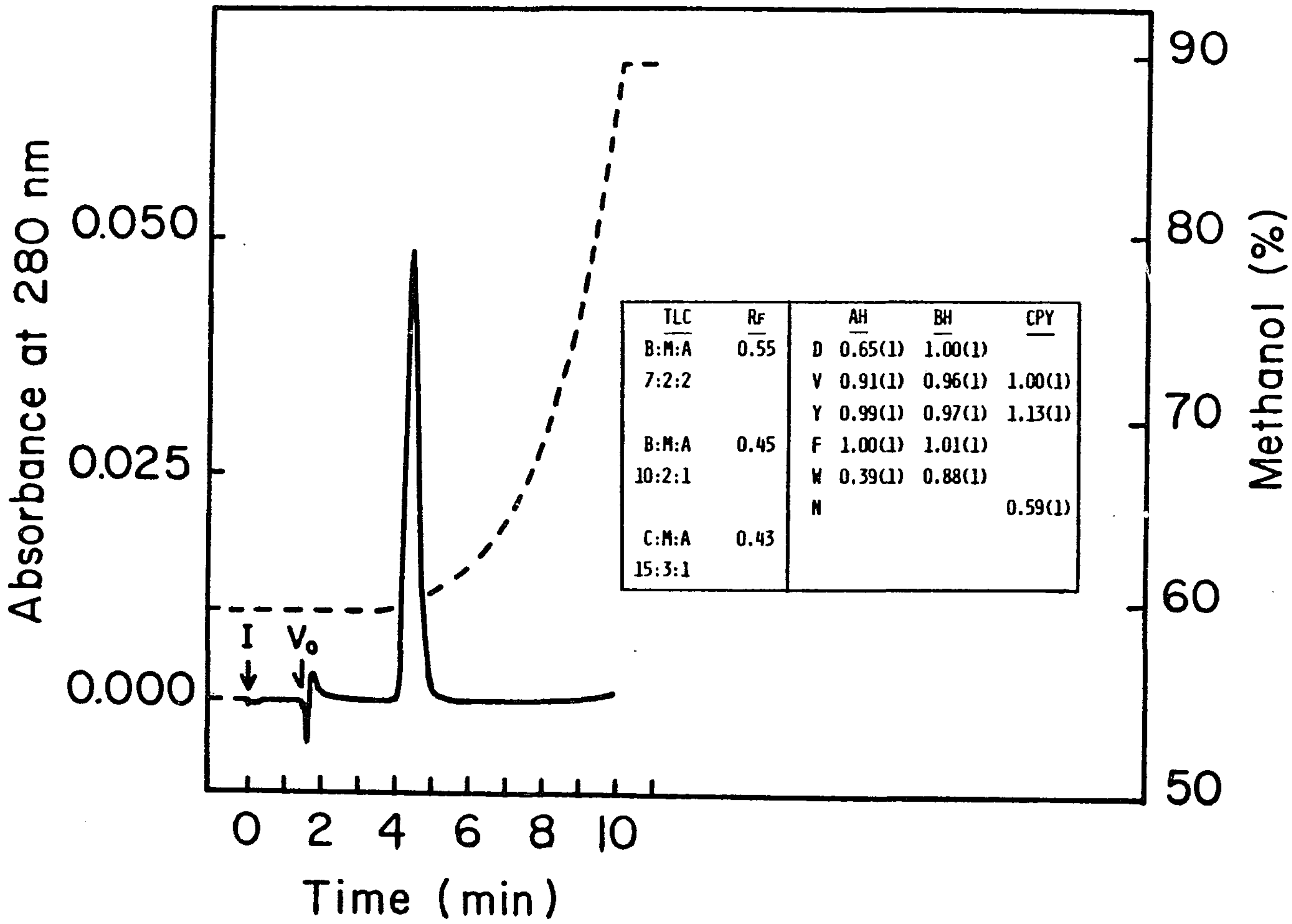

TLC	R_F
B:M:A 7:2:2	0.55
B:M:A 10:2:1	0.45
C:M:A 15:3:1	0.43

	AH	BH	CPY
D	0.65(1)	1.00(1)	
V	0.91(1)	0.96(1)	1.00(1)
Y	0.99(1)	0.97(1)	1.13(1)
F	1.00(1)	1.01(1)	
W	0.39(1)	0.88(1)	
N			0.59(1)

Fig. 33. Analytical reverse-phase HPLC of peptide A5F from Fig. 31. A5F eluted as one peak (k' = 2.2) from a μBondapak phenyl column using a 10 min # 10 concave gradient from 60 to 90% methanol in 5% aqueous acetic acid at 2 ml/min. The eluate was monitored at 280 nm. The insert shows that A5F was a single spot by TLC in three solvent systems (B, benzene; A, acetic acid; M, methanol; and C, chloroform) as visualized by Cl/tolidine and that amino acid compositions after acid hydrolysis (AH), base hydrolysis (BH), and carboxypeptidase Y digestion (CPY) were in good agreement with the theoretical values.

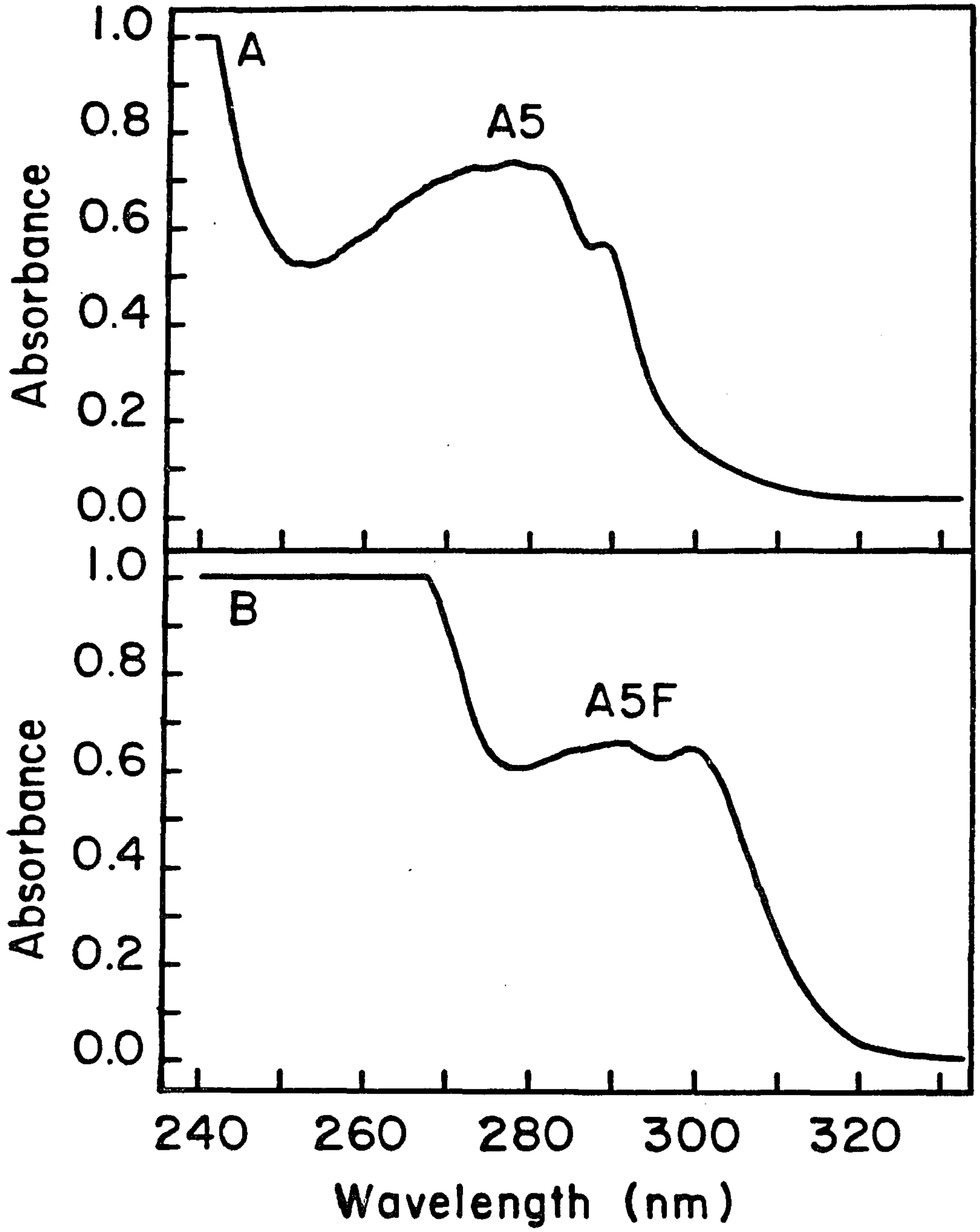

Fig. 34. Ultraviolet absorption spectra of peptides A5 and A5F. Pure peptides from Fig. 32 and 33 were examined in 1:1 (v/v) methanol-1% aqueous acetic acid versus methanol. (A) The absorption maxima at 280 and 290 nm for peptide A5 indicate the presence of an unformylated tryptophan residue. (B) The absorption maxima at 290 and 300 nm for peptide A5F indicate the presence of an $\underline{N}^{\alpha}$-formyltryptophan residue.

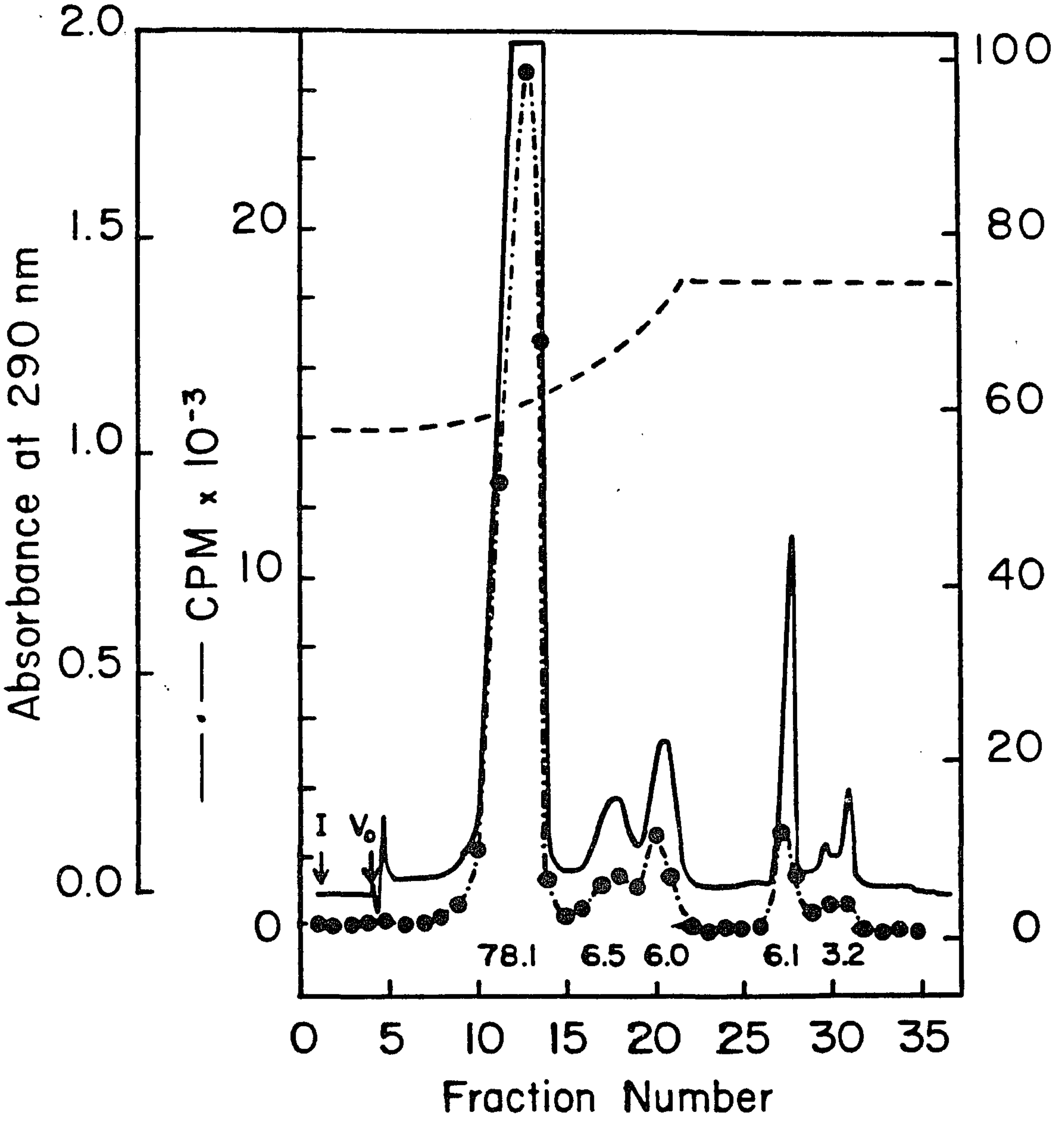

Fig. 35. Semipreparative reverse-phase HPLC of the crude peptide A5F that was soluble in 1:1 (v/v) methanol-1% aqueous acetic acid. Peptides were eluted from a μBondapak phenyl column with a 10 min # 8 concave gradient from 60 to 75% methanol in 1% aqueous acetic acid at 2 ml/min. The eluate was monitored at 290 nm and for radioactivity. The number under each peak corresponds to the percentage of the total radioactivity eluted in that peak.

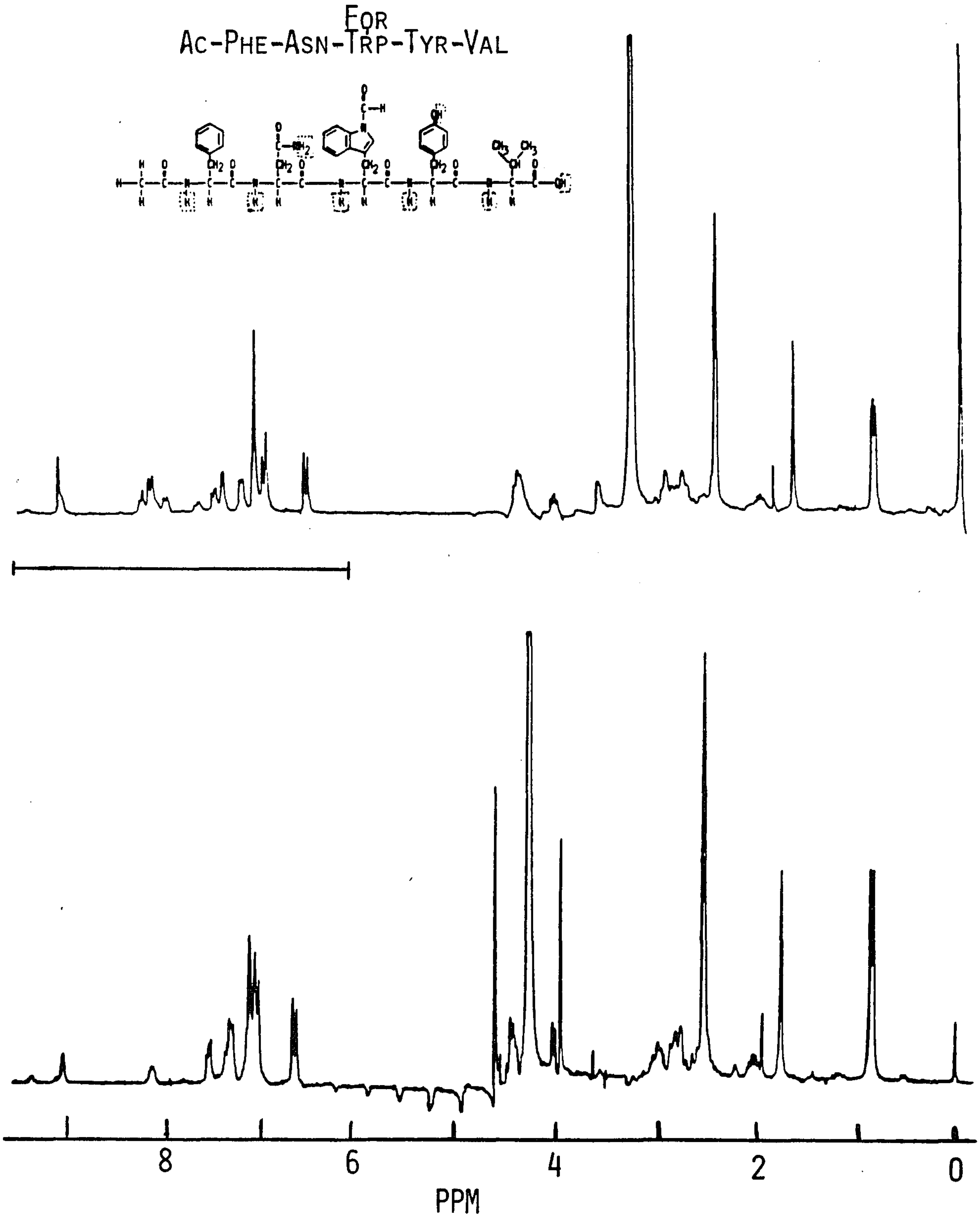

Fig. 36. NMR spectra at 220 MHz of peptide A5F. Peptide was examined (A) in dimethylsulfoxide-d_6 and (B) two months after adding D_2O to (A). As shown in Table II 10.4 protons were exchanged from the region indicated. Protons available for exchange are in dashed boxes in the inset structural formula.

Table II

Exchange of peptide A5F protons for deuterons

Before D_2O Added		60 Days After D_2O Added	
Chemical Shifts	Number of Protons*	Chemical Shifts	Number of Protons*
ppm		ppm	
8.70 - 9.74	1.95	9.29 - 9.84	0.26
7.94 - 8.70	5.06	8.60 - 9.26	0.64
7.67 - 7.94	1.26	7.98 - 8.60	0.69
7.41 - 7.67	3.48	7.70 - 7.98	0.35
7.25 - 7.41	2.27	7.51 - 7.70	1.30
7.12 - 7.25	5.43	7.28 - 7.51	2.96
6.83 - 7.12	4.01	6.78 - 7.28	7.16
6.54 - 6.83	2.36	6.55 - 6.78	2.00
Total:	25.8	Total:**	15.4

---

*All values were normalized to the valine methyl multiplet at 0.9 ppm, which was taken as 6 protons. The solvent was dimethylsulfoxide-$\underline{d}_6$ with or without 10% D_2O.

**The 15 protons remaining correspond to the 14 aromatic protons of Phe, Tyr, and Trp and the N^1-formyl proton.

B. Bioassay of the Synthetic Peptides

1. C1 Inhibition Assay. Seven synthetic peptides were compared with three protein controls, aggregated IgG, monomeric IgG and the IgG fragment Fc, for their ability to inhibit the classical complement pathway by binding to C1. Aggregated IgG was the most active species tested, producing 50% inhibition of C1-mediated hemolysis (I_{50}) at a concentration of 2.5×10^{-8} M. It was approximately 3000 times more active than monomeric IgG ($I_{50} = 7.4 \times 10^{-5}$ M) and 2000 times more active than Fc ($I_{50} = 4.7 \times 10^{-5}$ M) (Fig. 37).

The cationic decapeptide 10 ($I_{50} = 1.8 \times 10^{-4}$ M) was 41% as active as monomeric IgG (Fig. 37) . The formylated hexadecapeptide 16F ($I_{50} = 1.5 \times 10^{-4}$ M), which contained both the hydrophobic region and the cationic region, was only as active as the decapeptide (Fig. 38). When the formyl protecting group was removed, the resulting hexadecapeptide 16 showed no inhibition at the highest concentrations tested (Fig. 38). Insufficient material was available to examine the effect of higher concentrations of peptide 16.

Peptide A6J ($I_{50} = 1.4 \times 10^{-4}$ M), the N^{α}-acetylated form of the most active peptide described by Johnson and Thames (57), was only as active as peptides 10 and 16F but was four times more active than their unacetylated hexapeptide (84). The unrelated hydrophobic pentapeptide, FR5 (Phe-Gly-Leu-Ala-Arg), served as a negative control. It showed no dose-dependent hemolysis at a concentration higher than the I_{50} of peptides 16F, 10, and A6J (Fig. 37).

In contrast, pentapeptide A5F ($I_{50} = 2.7 \times 10^{-6}$ M) was the most active peptide assayed. On a molar basis pentapeptide A5F was 27 times more active than monomeric IgG at inhibiting C1-mediated hemolysis. A representative dose-response curve for peptide A5F is shown in Fig 39. This curve was reproduced in 5 separate experiments. Peptide A5, which was identical to peptide A5F except for the absence of the N^{i}-formyl group, showed no inhibition at a saturating concentration (1.6×10^{-5} M). Since peptide A5 was inactive at a concentration ten times higher than the highest concentration at which peptide A5F was inactive, the unformylated peptide A5 is at least ten times less active than formylated peptide A5F.

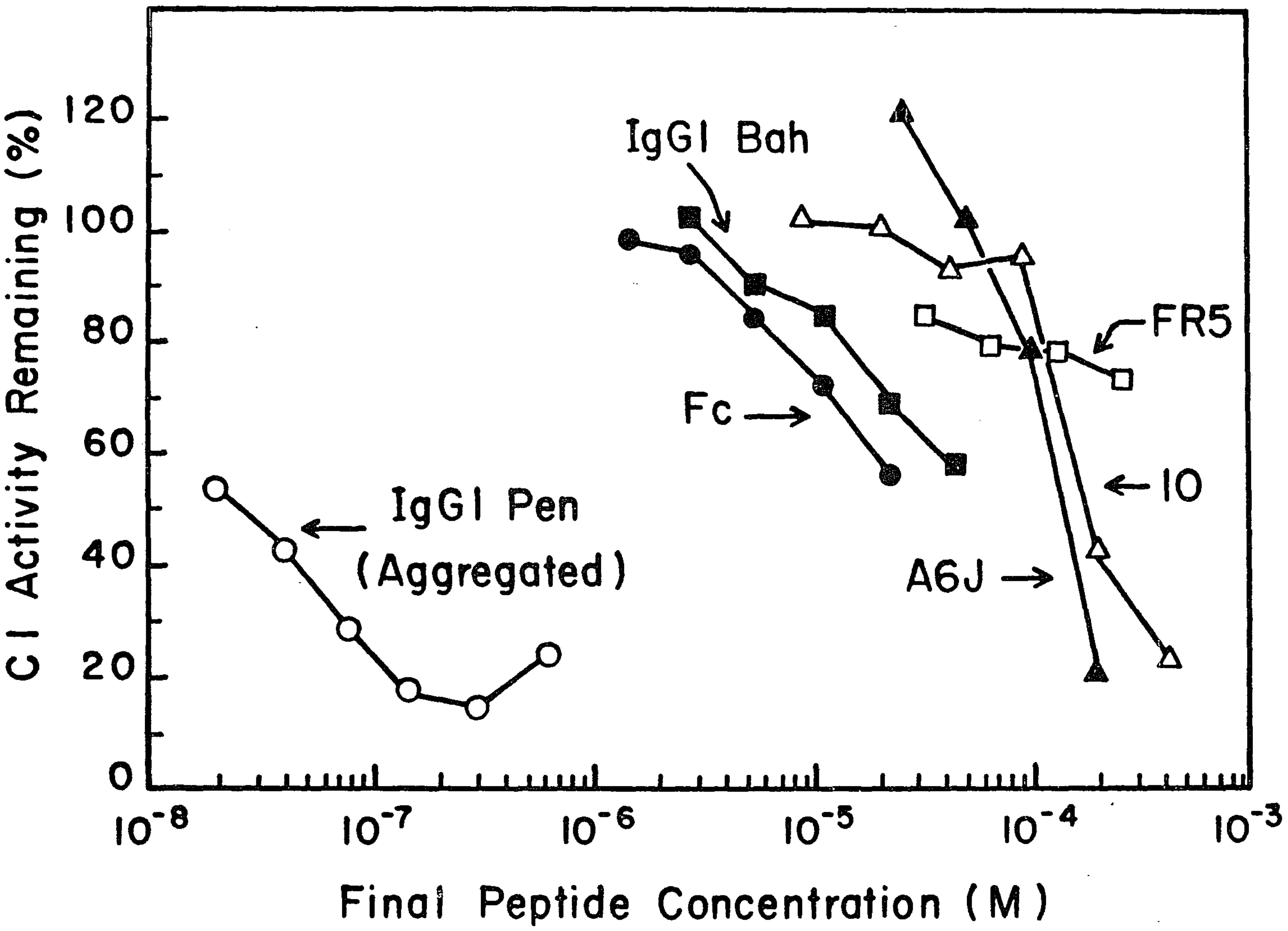

Fig. 37. Inhibition of C1-mediated hemolysis by synthetic peptides 10, A6J, and FR5. Dose-response curves are shown for peptides 10 (△–△), A6J (▲–▲), FR5 (□–□) and protein standards IgG1 (■–■), Fc (●–●), aggregated IgG1 (○–○). The percentage of C1-mediated hemolytic activity remaining is plotted versus the molar concentration of synthetic peptide or protein standard in the initial reaction mixture.

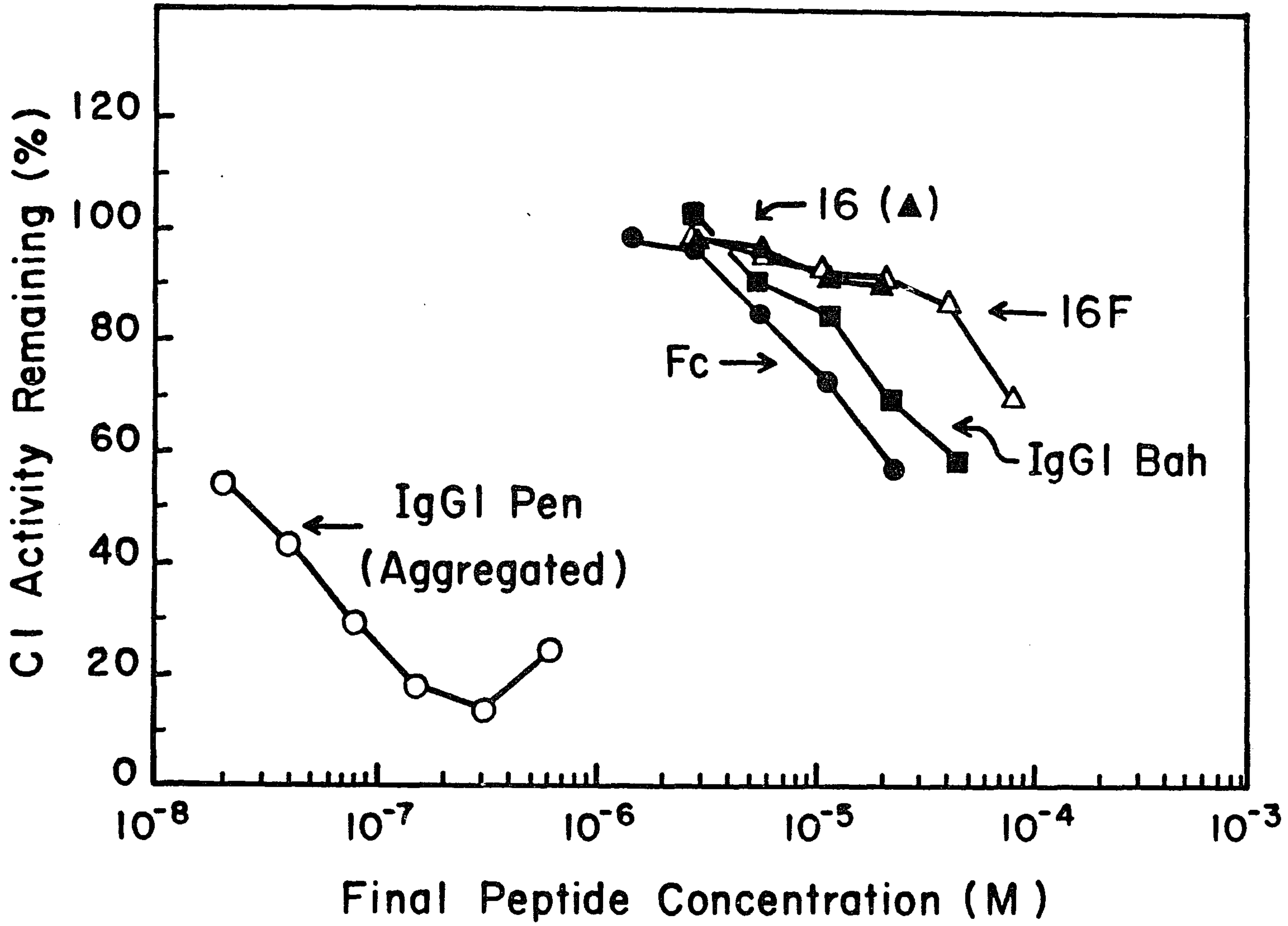

Fig. 38. Inhibition of C1-mediated hemolysis by the synthetic IgG1 hexadecapeptides 16 and 16F. Dose-response curves are shown for peptides 16 (▲—▲), 16F (△-△) and protein standards IgG1 (■—■), Fc (●—●), aggregated IgG1 (○—○). The percentage of C1-mediated hemolytic activity remaining is plotted versus the molar concentration of synthetic peptide or protein standard in the initial reaction mixture.

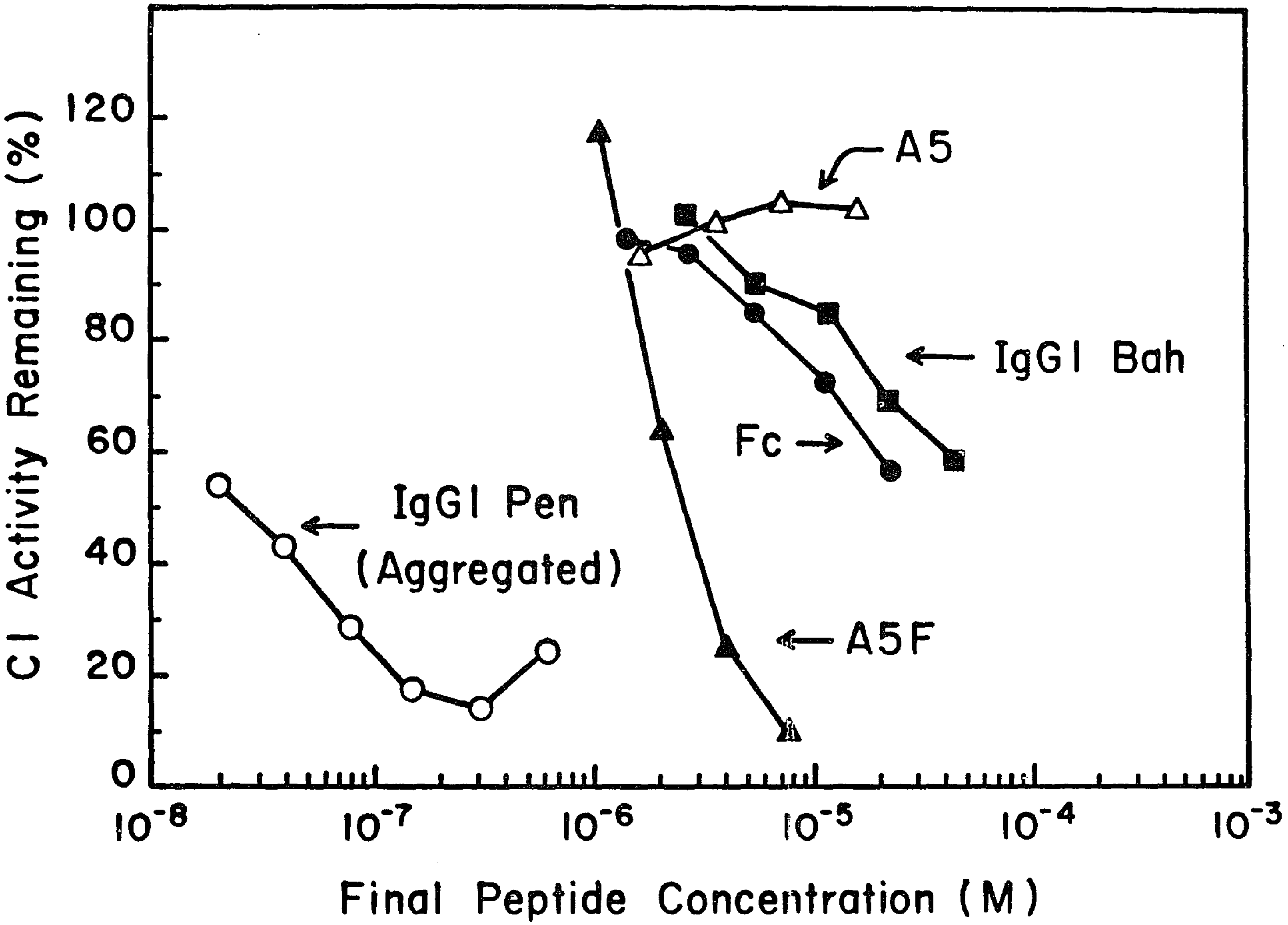

Fig. 39. Inhibition of C1-mediated hemolysis by the synthetic IgG1 pentapeptides A5 and A5F. Dose-response curves are shown for peptides A5 (△—△), A5F (▲—▲) and protein standards IgG1 (○—○), Fc (●—●), aggregated IgG1 (■—■). The percentage of C1-mediated hemolytic activity remaining is plotted versus the molar concentration of synthetic peptide or protein standard in the initial reaction mixture.

2. Equilibrium Dialysis The synthetic peptides 16F, 10, A5, A5F and A6J were examined by equilibrium dialysis for their ability to bind to IgG. No detectable binding was observed under conditions where positive binding would have been detected if any peptide bound with an association constant (K_{ass}) of greater than 1 x 10^4 $l.mol^{-1}$. Positive binding was defined as binding of 5% of the peptide to the protein.

Human C1q was precipitated from outdated plasma with calf thymus DNA and the precipitate was digested with DNase I and chromatographed on carboxymethyl-cellulose (Fig. 40). Fractions 22-25 showed the presence of greater than 95% C1q by polyacrylamide gel electrophoresis and the absence of IgG by immunodiffusion. When peptides 16F, 10, A5, A5F, and A6J were dialyzed against this C1q preparation, no binding was observed. If 5% of the peptide had bound to C1q, binding would have been detected corresponding to an association constant of 1 x 10^4 $l.mol^{-1}$.

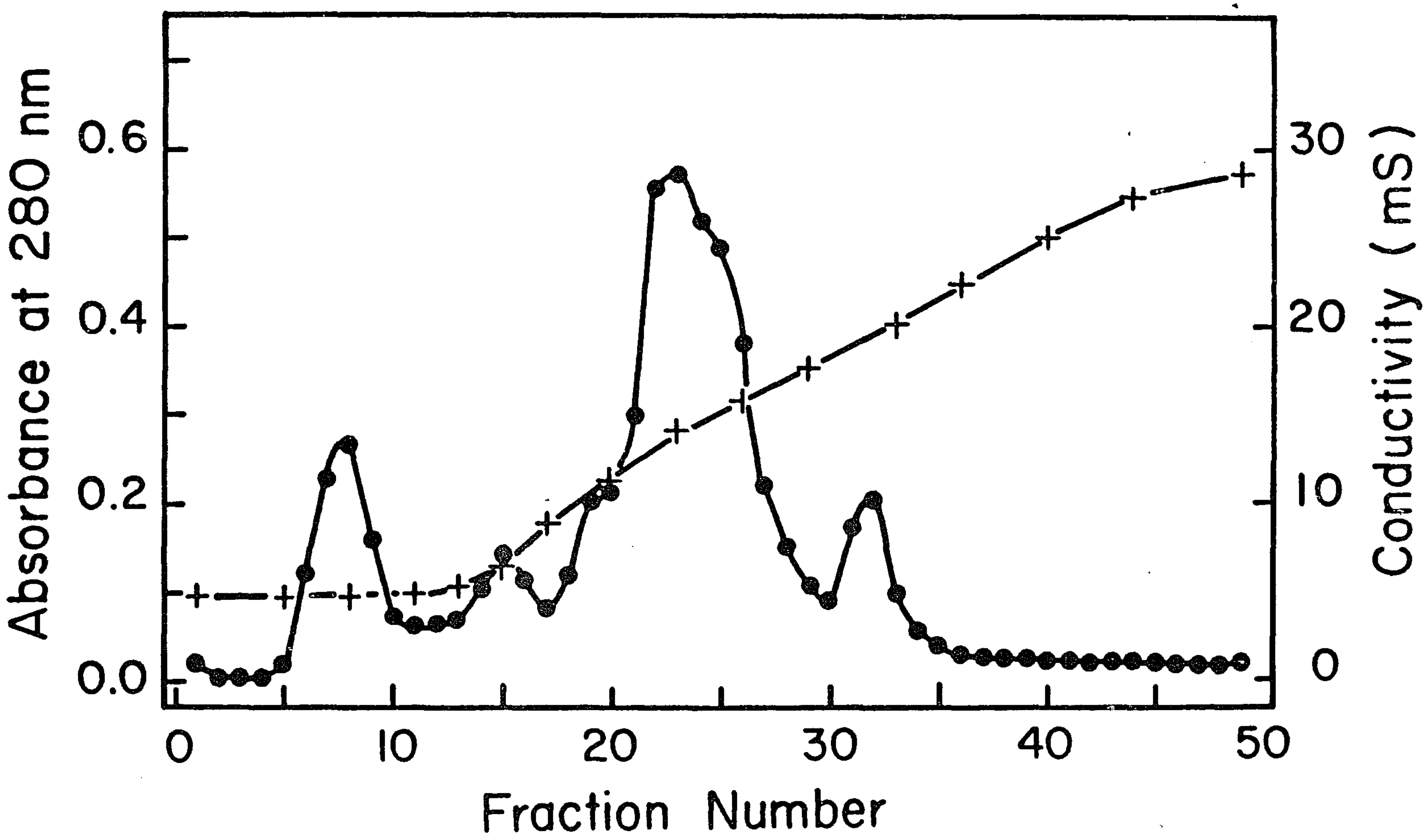

Fig. 40. CM-52 column chromatography of DNA-precipitated C1q. DNA-precipitated proteins from human plasma were treated with DNA'se I and chromatographed on a CM-52 column (1.5 x 30 cm). The C1q was eluted with a linear gradient from 10 mM sodium acetate to 10 mM sodium acetate containing 1 M NaCl (5-29 mS). Fractions 22 through 24 contained at least 95% C1q by polyacrylamide gel electrophoresis and no IgG by immunodiffusion.

DISCUSSION

A. Selection

Enzyme and chemical degradation studies (31-33) of native IgG during the past two decades have suggested that the C1-binding site of IgG resides in the C_y2 domain. Chemical characterization of the C1-binding site has led to several suggestions concerning the nature of the IgG residues involved in binding IgG to C1. Sledge and Bing (47) observed that aromatic and aliphatic diamines bind to C1q and inhibit its interaction with IgG. They found that hydrophobic diamines were more potent inhibitors of the IgG-C1 interaction. Allan and Isliker (50,51) showed that IgG with modified tryptophan residues was incapable of activating C1. Isenman et al. (48) demonstrated that one of the two tryptophan residues in the C_y2 domain was exposed to solvents and available to bind to C1q. Finally, Deisenhofer et al. (54) observed that the X-ray crystallographic structure of C_y2 was unique when compared with the other IgG constant region domains. The structurally unique portion of the C_y2 domain contained both a cationic region with two lysine residues and a histidine residue and a hydrophobic region with a buried tryptophan residue.

The present study was undertaken as an attempt to define the structural requirements for the C1-binding site of IgG. Solid-phase peptide synthesis was used to assemble small synthetic segments and structural analogues of the $C_{\gamma}2$ domain of IgG. Selection of the synthetic segments was chosen based on the previously described chemical characteristics of the C1-binding site of IgG. After designing a synthetic strategy, the following peptides were synthesized: (1) a hexadecapeptide (16F) including both the cationic and hydrophobic regions of the structurally unique portion of $C_{\gamma}2$ (γ-chain residues 275-290), (2) a decapeptide (10) containing only the cationic region (γ-chain residues 281-290), (3) an acetylated pentapeptide (A5) comprising the hydrophobic region (γ-chain residues 275-279), and (4) the acetylated form (A6J) of a synthetic hexapeptide shown by Johnson and Thames (57) to inhibit complement fixation.

B. Assembly

In studying the sequences of the synthetic peptide segments, several potential side reactions were noted and strategies were adopted to circumvent them. Racemization of the histidine residue during the coupling step was avoided by using a strongly electron-withdrawing group (Dnp) to reduce the basicity of the imidazole ring (59). Formation of beta-aspartyl residues was minimized by either avoiding the aspartyl-glycyl sequence, as for peptide 10, or by altering the HF cleavage conditions, as for peptide 16F (61). Branched peptides formed through the epsilon-amino group of lysine were avoided by using a more acid-stable protecting group (3-chlorobenzyloxycarbonyl) for lysine (62). Diketopiperazine formation in the synthesis of A6J was minimized by adding DCC to the peptide-resin before adding the Boc-amino acid during the coupling of the third amino acid (63). While dehydration of asparagine and glutamine residues during the coupling reaction can be a serious problem resulting in β-cyanoalanine and γ-cyano-α-aminobutyric acid, respectively (85,86), during HF cleavage the cyano derivatives revert to the original amide residues (87). Also, infrared spectroscopy of crude peptide 16F showed that less than 4% of any cyano derivative formed during synthesis was present after treatment with HF.

C. Purification

Many different methods of purification were tried on the crude synthetic peptides with varying degrees of success. Gel-filtration chromatography on Bio-Rad and Sephadex gels afforded little resolution of the synthetic mixtures (Fig. 17 and 23). Also, the hydrophobic peptide A5F adsorbed avidly to both polystyrene and carbohydrate supports in 20% acetic acid, which precluded using gel-filtration chromatography as a method of purifying this peptide. Analytical gel filtration on the HPLC supports μPoragel E125 in 1% acetic acid and μStyragel 100Å in dichloromethane (Waters) resulted in well resolved peaks.

However, the separations achieved could be attributed to a combination of gel filtration and adsorption, since some peptides eluted after the total column volume. In addition, the analytical columns did not have sufficient capacity for preparative peptide purification.

Ion-exchange chromatography did not prove to be useful for this series of peptides. Elution of the hexadecapeptide containing both the formyl and Dnp protecting groups from Technicon-P resin or the formyl-protected peptide from Bio-Rex 70 resin required high salt concentrations (8.6 M pyridine in 3.6 M formic acid and 50% acetic acid, respectively) and produced little resolution. Also, SP-sephadex chromatography on the decapeptide provided low resolution and low yields.

Silica-gel chromatography using either a partition mode on glass plates or columns or using an adsorption mode by gradient elution on columns gave moderate sample resolution with variable yields. The partition systems involved elution of peptides from dry silica columns using a mixture of ethyl acetate, pyridine, acetic acid, and water. For adsorption chromatography, silica gel was washed with distilled water and a graded series of nonpolar solvents until initial conditions were reached. Elution of the peptides was achieved using sequential gradients of hexanes to isopropanol, isopropanol to methanol, methanol to water, water to 10% aqueous acetic acid, and 10% to 50% aqueous acetic acid. Elution of hydrophilic peptides, such as peptide 10, was difficult even with 50% aqueous acetic acid. One advantage of adsorption chromatography is that milligram quanties of sample can be resolved on relatively small columns (0.9 cm x 50 cm). In general, if the desired product can be eluted from silical gel, adsorption chromatography on this support provides a better starting point for purification of synthetic peptides than gel-filtration chromatography.

Reverse-phase HPLC accounted for all of the purifications of the synthetic peptides used in this study. This mode of chromatography afforded high-resolution separations in a minimal amount of time. As illustrated by peptide A5F, reverse-phase HPLC may be the only method required to obtain rapidly large quantities of homogeneous compounds. For complex separations such as 16F and A6J, rechromatography of carefully pooled samples resolved the desired products to purity. Low-pressure reverse-phase chromatography has been used recently as an initial step for purification of synthetic peptides followed by final purification using high-pressure reverse-phase chromatography. The low-pressure system consisted of a fully porous macroparticular reverse-phase gel in a glass column.

This gel (Porasil B C18, Waters) has a high capacity and is similar to the microparticular C18 gel used for HPLC. The initial low-pressure separation greatly simplified the final HPLC separation by providing separations that involved only two or three peptides rather than eight or more.

D. Characterization

Partially purified preparations of synthetic peptides are useful in certain pilot studies to orient the course of further research. But highly homogeneous preparations are essential when the peptides are to be used in defining biochemical mechanisms. Many criteria can be used to characterize peptides and to measure their homogeneity, including thin-layer chromatography, thin-layer electrophoresis, high-pressure liquid chromatography, amino acid analysis, amino acid sequence analysis and ultraviolet spectroscopy.

The separation acheived by partition thin-layer chromatography on silica-gel is based on differences in the polar group content of different peptides. Conversely, reverse-phase TLC depends upon the differences in nonpolar groups. Peptides should migrate as single spots with $\underline{R}_f$ values between 0.2 and 0.8 in at least three different solvent systems using either separation mode to verify purity. Thin-layer electrophoresis separates peptides with respect to charge. Preferably, electrophoretic mobility in two different pH ranges should be examined as criteria for purity.

In this study, HPLC yielded the best resolution of any system available at the present time. Modified silica-gel supports are available for many modes of separation, including adsorption, ion exchange, reverse phase, and gel filtration. Through these various modes of separation, peptides could be extensively characterized using only HPLC methods. When determining homogeneity by HPLC the sample should be retained on the support for at least 1.5 and preferably 2.0 column volumes (k').

Amino acid analysis is essential in characterizing synthetic peptides. Amino acid compositions obtained after acid hydrolysis can be helpful in detecting deletion peptides. Base hydrolysis is used mainly for the determination of tryptophan residues. Enzymatic digestion of peptides with aminopeptidase M or carboxypeptidase Y is useful in determining the presence of asparagine and glutamine residues.

Amino acid sequence analysis is generally used to confirm the primary structure of synthetic peptides. However, if a stepwise method of assembly is used and the amino acids are added in the desired order, the primary structure is assumed to be correct, providing that the amino acid compositions are correct. Solid-phase sequence analysis can also be a useful tool in monitoring large stepwise syntheses.

Ultraviolet spectroscopy can be used to detect specific chromophores contained within synthetic peptides. One example is the differentiation of peptides containing either tryptophan or $\underline{N}^{i}$-formyltryptophan residues.

While it is not necessary to use all of these methods for characterization and demonstration of homogeneity, it is necessary to provide amino acid compositions and analytical data based on at least two different modes of separation such as, adsorption chromatography on silica gel and reverse-phase chromatography on octadecyl-silica gel.

Several of the above criteria were used to characterize the synthetic peptides in this study. Each peptide was shown to be homogeneous by TLC in at least three different solvent systems with $\underline{R_f}$ values between 0.2 and 0.8 (Table III). Peptides 16F and 10 were homogeneous by TLE at pH 6.5. Each peptide was homogeneous by reverse-phase HPLC with k' values between 1.5 and 11.7. Finally, amino acid analysis results for the homogeneous peptides after acid hydrolysis, base hydrolysis, and/or enzymatic digestion were in good agreement with the theoretical values (Table IV).

Table III

Analytical thin-layer chromatography of purified peptides

Solvent System (by volume)	R_f Values				
	16F	10	A6J	A5	A5F
BuOH:EtOAc:AcOH:H_2O (4:1:1:4)	0.37	0.08	0.61		
EtOAc:Pyr:AcOH:H_2O (5:5:1:3)	0.41	0.18	0.57		
BuOH:AcOH:H_2O (1:1:2)		0.28			
Pyr:AcOH:H_2O (5:1:3)		0.83			
BuOH:Pyr:AcOH:H_2O (1:1:1:3)		0.77			
BuOH:Pyr:AcOH:H_2O (3:1:1:3)	0.59	0.42	0.59		
BuOH:AcOH:H_2O (3:1:1)	0.01		0.46		
C_6H_6:CH_3OH:AcOH (7:2:2)				0.48	0.55
C_6H_6:CH_3OH:AcOH (10:2:1)				0.38	0.45
$CHCl_3$:CH_3OH:AcOH (15:3:1)				0.33	0.43

Table IV

Amino acid compositions of purified synthetic peptides

Amino acids were obtained by acid hydrolysis (AH), base hydrolysis (BH), aminopeptidase M digestion (APM), or carboxypeptidase Y digestion (CPY).

Amino Acid	16F	10		A6J	A5		A5F		
	AH	AH	APM	AH	AH	BH	AH	BH	CPY
Asp	2.67 (3)	1.04 (1)			[1]	[1]	0.65 (1)	[1]	
Asn									0.59 (1)
Thr	1.04 (1)	0.98 (1)	2.50 (3)*						
Glu	1.10 (1)	1.05 (1)		2.01 (2)					
Gly	0.97 (1)	1.00 (1)	1.02 (1)	0.99 (1)					
Ala	[1]	[1]	[1]						
Val	2.78 (3)	1.99 (2)	1.99 (2)		1.01 (1)	0.72 (1)	0.91 (1)	0.96 (1)	[1]
Tyr	1.01†(1)			1.01 (1)	0.97 (1)	0.74 (1)	0.99 (1)	0.97 (1)	1.13 (1)
Phe	0.80 (1)				1.10 (1)	1.01 (1)	[1]	1.01 (1)	
His	0.95 (1)	0.99 (1)	1.00 (1)						
Lys	2.07 (2)	2.04 (2)	2.01 (2)						
Trp	ND (1)			ND (1)	ND (1)	0.90 (1)	0.39 (1)	0.88 (1)	ND (1)
Arg				1.00 (1)					

---

*This value includes Asn, Gln and Thr.

†This value was corrected for destruction (5% per 24 h).

E. C1 Inhibition Assay

The C1 inhibition assay used in this study involves the binding of free C1 to erythrocytes bearing IgG and C4 (EAC4 cells) followed by hemolysis through the subsequent addition of C2 and C3-C9. Compared to a standard complement fixation assay, where inhibition could be obtained at any step from C1 activation to formation of the C5-9 complex, this C1 inhibition assay is relatively specific for C1. The assay was designed to measure the ability of polypeptides, such as IgG and Fc, to inhibit C1-mediated hemolysis. Monomeric IgG and Fc do not cause inhibition by activating and consuming C1, rather they inhibit by binding to C1q and blocking C1 from binding to erythrocyte-bound IgG. However, small molecules with undefined binding specificities could also inhibit hemolysis by binding to C1r or C1s thus preventing C1 activation, through binding to erythrocyte-bound IgG thus inhibiting C1 binding and activation, by binding to erythrocyte-bound C4 thus preventing its activation, and/or by binding to an erythrocyte surface receptor and thereby indirectly inhibiting hemolysis.

Dorrington, Painter and coworkers (33) have used this C1 inhibition assay and shown that intact $C_{\gamma}2$, which bears a carbohydrate chain, inhibits C1-mediated hemolysis. These investigators have also demonstrated that reduced and alkylated beta-2 microglobulin and $C_{\gamma}3$, which lack carbohydrate, inhibit C1-mediated hemolysis (46,33) but reduced and alkylated $C_{y}2$ is devoid of inhibitory activity (33). These results suggest that there is a linear segment responsible for the inhibition of C1-mediated hemolysis by beta-2 and $C_{y}3$. The carbohydrate moiety linked to $C_{y}2$ may induce this reduced and alkylated domain to adopt a different set of conformations than those assumed by beta-2 and $C_{y}3$. This may cause the C1q binding site to become masked, which would decrease inhibition of C1-mediated hemolysis. If the carbohydrate residues were removed from $C_{y}2$, inhibitory activity may return. The presence of the oligosaccharide probably prevented these investigators from producing inhibitory enzymatic fragments of $C_{y}2$.

Kehoe et al. (31) found and active fragment by using latex particles in their complement fixation assay. The peptide conformations induced by the polystyrene beads are probably quite different than those present in solution. One way to avoid the complicating presence of carbohydrate is to synthesize likely peptide segments from the $C_{y}2$ domain.

Pilot studies on synthetic peptides using the C1 inhibition assay indicated that partially purified peptides were able to inhibit the classical complement pathway. Compared to the inhibitory activity of a preparation containing some aggregates of IgG1 Pen ($I_{50} = 2.4 \times 10^{-6}$ M) taken as 100%, peptide 16F exhibited a relative activity of 5.4%, peptide A5F showed 4.2% relative activity, peptide 10 demonstrated 1.0% the activity of the partially aggregated IgG1, and the original hexapeptide of Johnson and Thames (57) was only as active as peptide 10. When peptide 10 containing a His(Dnp) residue (10D) was assayed, approximately 83% of the C1 activity remained using 3.5×10^{-4} M peptide. Also, peptide 16F containing a His(Dnp) residue (16FD) lysed the EAC4 cells in the absence of the other complement proteins.

While these pilot studies provided some indication that the synthetic peptides could inhibit the classical complement pathway, these preliminary findings were difficult to interpret because they were obtained using heterogeneous peptide mixtures. Precise definition of which peptides were inhibitors in the C1 inhibition assay, required assaying homogeneous compounds. Also, it was important to assay both monomeric and aggregated IgG as standards for evaluating the relative activities of the synthetic peptides.

The concentrations of protein standards and peptides at which 50% of the C1-mediated hemolytic activity was inhibited (I_{50}) are shown in Table V. The aggregated IgG standard had an average $s_{20,w}$ value of 12.5, which corresponds to a size range consistent with efficient complement activation (40). As expected from previous studies (33,35), aggregated IgG was much more active than monomeric IgG. Also, monomeric IgG and Fc were equally active in inhibiting the classical complement pathway. On a molar basis, peptides 16F, 10 and A6J were each about half as active as monomeric IgG. However, the peptides only represent one of the two equivalent C1-binding sites found in intact IgG. If each C1-binding site in the $C_{\gamma}2$ domain functions independently, then the I_{50} per C1-binding site of IgG would be 1.5×10^{-4} M. Thus peptides 16F, 10 and A6J would be just as inhibitory as one of the two C1-binding sites of the native IgG molecule.

Peptide A5F was 27 times more active on a molar basis than IgG or 54 times more active than each C1-binding site of IgG. The sparingly soluble peptide A5, however, was totally inactive at the highest concentrations that could be assayed and was at least 10 times less active than A5F. Peptides A5 and A5F differ only by three-atom formyl group (HC=O) attached to the indole nitrogen of tryptophan. Addition of the formyl group decreases the electron density of the indole ring while only slightly increasing the size of the side chain. It is not clear why this modification converts the inactive peptide A5 into the highly active peptide A5F. Although peptide 16F contains a formyl group on the same tryptophan as A5F, it is only as active as the decapeptide, which lacks the tryptophan residue.

One explanation for these results is that peptide A5F is acting as a latent C1q binding site. For example, a large conformational change in Fc would expose a segment similar to A5F, which would be more active than the latent protein. This explanation is unlikely because there is no evidence for large conformational changes in the Fc region on antigen binding. A more likely explanation is that peptides A5F and 16F are acting at two different sites and inhibit the classical complement pathway by different mechanisms. In this case, the cationic segment would be more likely to inhibit by binding to C1q because its inhibitory activity is similar to that of the $C_{\gamma}2$ domain. Thus A5F is probably acting at another site, such as C1s.

In examining the slopes of the dose-response curves, inhibitory peptides show a full range of activity over a much narrower range than the standard proteins. This may reflect the involvement of a cooperative phenomenon such as aggregation or micelle formation.

Table V

C1-Mediated hemolysis: concentrations of protein standards and purified peptides for 50% inhibition

Inhibitor	I_{50}	Relative Molar Activity
	M	
Aggregated IgG	2.5×10^{-8}	3000
Monomeric IgG	7.4×10^{-5}	[1]
Fc	4.7×10^{-5}	1.6
16F*	1.5×10^{-4}	0.5
10	1.8×10^{-4}	0.41
A6J	1.4×10^{-4}	0.53
A5F	2.7×10^{-6}	27

*Extrapolated from the results in Fig. 38.

F. Equilibrium Dialysis

Preliminary equilibrium dialysis experiments were performed to explore the binding of the partially purified peptides 16FD, 10D, and A5F to functionally pure C1. The peptides were dissolved in the C1 inhibition assay buffer (SGVB) and dialyzed against a 2.0 µM solution of C1 in 0.05 M $NaPO_4$, 1.5 M NaCl, 25% dextrose, 5% gelatin, and 1.5 mM $CaCl_2$ at pH 7.5. Control experiments showed no detectable binding of the peptides to gelatin. After reaching equilibrium, the following association constants were calculated for the peptides: (1) 16FD, $K_{ass} = 1.1 \times 10^4$ $l.mol^{-1}$, (2) A5F, $K_{ass} = 1.0 \times 10^4$ $l.mol^{-1}$, and (3) 10D, no detectable binding. While these results were suggestive of the peptides binding to C1, it was necessary to examine homogeneous compounds using salt concentrations that would enable ionic interactions to be measured.

Since the mechanism of inhibition of the classical complement pathway by the synthetic peptides is not clear from the C1 inhibition assay, the homogeneous peptides 16F, 10, A5F, A5, and A6J were examined for their ability to bind to IgG. None of these peptides demonstrated positive binding to IgG under conditions where binding could be detected for a $K_{ass} > 1 \times 10^4$ $l.mol^{-1}$. These results preclude the binding of peptide to IgG as the mechanism by which the synthetic peptides inhibit the classical complement pathway.

Since peptide A5F exhibited the highest activity in the C1 inhibition assay, it was examined for its ability to bind to C1q. Four different concentrations between 5 and 40 μM of A5F were tested, but no positive binding was observed at any concentration even though positive binding to C1q could have been detected for a K_{ass} as low as 1×10^4 $l.mol^{-1}$. If A5F were inhibiting C1-mediated hemolysis as IgG does by binding to C1q, then the expected association constant for A5F would be 27 times the K_{ass} for IgG or approximately 5.4×10^5 $l.mol^{-1}$. Since the K_{ass} for A5F was less than 1×10^4 $l.mol^{-1}$, peptide A5F must be inhibiting C1-mediated hemolysis by another mechanism.

This finding is consistent with recent X-ray crystallographic data (55) that show that residues 275-279 are deeply buried in the interior of the β-pleated sheets of $C_{\gamma}2$ and not available for C1q binding. The inability of A5F to bind to C1q supports the idea that formylation of the pentapeptide A5 has resulted in a potent inhibitor of the classical complement pathway that does not act through binding to C1q but by a different mechanism. Since A5F does not bind to either IgG or C1q but does inhibit the classical pathway, it should be tested in an assay system that can directly measure C1 activation, such as the C1s activation system of Cooper and Ziccardi (88). Should A5F inhibit C1 activation in this assay, then its mechanism of activation would be narrowed to inhibition of C1r and/or C1s.

When peptides 16F, 10, A5, and A6J were examined for C1q binding, no binding to C1q was observed even though binding could have been detected with a k_{ass} as low as 1×10^4 $l.mol^{-1}$. If these peptides inhibit C1-mediated hemolysis by binding to C1q, then the expected association constant for peptides 16F, 10, and A6J would be approximately 1×10^4 $l.mol^{-1}$. This calculation is based on the results that the peptides have half the inhibitory activity of monomeric IgG and that monomeric IgG binds to C1q with an association constant of 2×10^4 $l.mol^{-1}$ (39).

Efforts to increase the sensitivity of the assay by increasing the concentration of C1q were not successful because of the limited solubility of C1q in physiological buffers. An alternative would be to synthesize dimers of the cationic peptides. If the correct spatial orientation of the ligands were achieved, binding would increase approximately as the square of the association constant of the monomer. Synthetic studies with various dimeric peptides could also provide data on the number of binding sites per C1q head, the ability to activate complement by crosslinking C1q heads, and the possibility of inhibiting complement efficiently without activation by binding a dimer to two sites on the same C1q head. If the cationic region of peptides 16F and 10 does bind to C1q, which is consistent with the availability of this region as shown by X-ray crystallography, this binding should be relatively specific for C1q because it involves the interaction of a cationic peptide with the cationic C1q protein (isoelectric point: 10.0 - 10.6 (89)).

G. Conclusions

The major goal of this project was to define the structural requirements of the C1q-binding site of IgG. The homogeneous synthetic peptides examined in this study were inhibitors of the classical complement pathway as measured by a hemolytic inhibition assay. However, the exact mechanism by which these peptides inhibit the classical pathway is not clear. It is difficult to speculate on the way in which A6J inhibits, since it was originally designed as an immunopharmacological agent and not designed to elucidate a biochemical mechanism. Since the exposed cationic segment of the open-loop region of the γ-chain (residues 281-290) posesses the inhibitory activity of one $C_{\gamma}2$ domain, this segment may be involved in binding to C1q. From the recent X-ray crystallographic data and from the equal activities of peptides 10 and 16F, the hydrophobic segment containing a buried tryptophan-277 (residues 275-279) clearly is not an integral part of the C1q-binding site of IgG. However, the formylated form of this hydrophobic segment was a potent inhibitor of the classical complement pathway. An understanding of its mode of action may give valuable insight into the structural requirements for another mechanism of complement inhibition.

BIBLIOGRAPHY

1. Wilson, C.B. (1976) in Textbook of Immunopathology (Miescher, P.A., and Müller-Eberhard, H.J., eds) 2nd Ed, pp. 529-554, Grune and Stratton, Inc., New York

2. Gocke, D.J., Hsu, K., Morgan, C., Bombardieri, S., Lockshin, M., and Christian, C.L. (1970) Lancet 2, 1149-1153

3. Mongan, E.S., Cass, R.M., Jacox, R.F., and Vaughn, J.H. (1969) Am. J. Med. 47, 23-35

4. Rose, N.R., and Wibetsky, E. (1956) J. Immunol. 76, 417-

5. Kunkel, H.G., Müller-Eberhard, H.J., Fudenberg, H. H., and Tomasi, T.B. (1961) J. Clin. Invest. 40, 117-129

6. Normansell, D.E. (1971) Immunochemistry 8, 593-602

7. Roitt, I.M., Doniach, D., Campbell, P.N., and Hudson, R.V. (1956) Lancet 2, 820-821

8. Koffler, D. (1975) in Pathobiology Annual: 1975 (Ioachim, H.L. ed) Vol. 5, pp. 221-247, Appleton-Century-Crofts, New York

9. Cochrane, C.G., and Dixon, F.J. (1976) in Textbook of Immunopathology (Miescher, P.A., and Müller-Eberhard, H.J. eds) 2nd Ed, pp. 137-156, Grune & Stratton, Inc., New York

10. Erickson, B.W., and Merrifield, R.B. (1976) in The Proteins (Neurath, H. and Hill, R.L., eds) 3rd Ed, Vol. II, pp. 257-527, Academic Press, New York

11. Taniuchi, H., and Anfinsen, C.B. (1968) J. Biol. Chem. 243, 4778-4786

12. Smyth, D.G., Stein, W.H., and Moore, S. (1963) J. Biol. Chem. 238, 227-234

13. Crestfield, A.M., Stein, W.H., and Moore, S. (1963) J. Biol. Chem. 238, 2413-2420

14. Crestfield, A.M., Stein, W.H., and Moore, S. (1963) J. Biol. Chem. 238, 2421-2428

15. Lin, M.C., Gutte, B., Moore, S., and Merrifield, R.B. (1970) *J. Biol. Chem.* *245*, 5169-5170

16. Gutte, B., Lin, M.C., Caldi, D.G., and Merrifield, R.B. (1972) *J. Biol. Chem.* *247*, 4763-4767

17. Ontjes, D.A., and Anfinsen, C.B. (1969) *Proc. Nat. Acad. Sci.* *64*, 428-435

18. Ontjes, D.A., and Anfinsen C.B. (1969) *J. Biol. Chem.* *244*, 6316-6322

19. Sanchez, G.R., Chaiken, I.M., and Anfinsen, C.B. (1973) *J. Biol. Chem.* *248*, 3653-3659

20. Lin, M.C., Gutte, B., Caldi, D.G., Moore, S., and Merrifield, R.B. (1972) *J. Biol. Chem.* *247*, 4768-4774

21. Hodges, R.S., and Merrifield, R.B. (1975) *J. Biol. Chem.* *250*, 1231-1241

22. Ehrlich, P., and Morgenroth, J. (1899) *Berlin. Klin. Wochenschr.* *36*, 6-9

23. Pope, C.G., (1939) *Brit. J. Exp. Path.* *20*, 132-149

24. Pope, C.G., (1939) *Brit. J. Exp. Path.* *20*, 201-212

25. Petermann, M.L. (1942) *J. Biol. Chem.* *144*, 607-616

26. Petermann, M.L. (1946) *J. Amer. Chem. Soc.* *68*, 106-113

27. Porter, R.R. (1959) *Biochem. J.* *73*, 119-126

28. Edelman, G.M., Heremans, J.F., Heremans, M., and Kunkel, H.G. (1960) *J. Exp. Med.* *112*, 203-223

29. Ishizaka, K., Ishizaka, T., and Sugahara, T. (1962) *J. Immunol.* *88*, 690-701

30. Utsumi, S. (1969) *Biochem. J.* *112*, 343-355

31. Kehoe, J.M., Fougereau, M., and Bourgois, A. (1969) *Nature* *224*, 1212-1213

32. Colomb, M., and Porter, R.R. (1975) *Biochem. J.* *145*, 177-183

33. Yasmeen, D., Ellerson, J.R., Dorrington, K.J., and Painter, R.H. (1976) *J. Immunol.* *116*, 518-526

34. Edelman, G.M., Cunningham, B.A., Gall, W.E., Gottlieb, P.D., Rutishauser, U., and Waxdal, M.D. (1969) Proc. Nat. Acad. Sci. 63, 78-85

35. Augener, W., Grey, H.M., Cooper, N.R., and Muller-Eberhard, H.J. (1971) Immunochemistry 8, 1011-1020

36. Ishizaka, T., Ishizaka, K., Salmon, S., and Fudenberg, H. (1967) J. Immunol. 99, 82-91

37. Isenman, D.E., Dorrington, K.J., and Painter, R.H. (1975) J. Immunol. 114, 1726-1729

38. Schur, P.H., and Christian, G.D. (1964) J. Exp. Med. 120, 531-545

39. Schumaker, V.N., Calcott, M.A., Spiegelberg, H., and Müller-Eberhard, H.J. (1976) Biochemistry 15, 5175-5181

40. Hyslop, N.E., Dourmashkin, R.R., Green, N.M., and Porter, R.R. (1970) J. Exp. Med. 131, 783-802

41. Jaton, J-C., Huser, H., Braun, D.G., Schlessinger, J., Pecht, I., and Givol, D. (1975) Biochemistry 14, 5312-5315

42. Goers, J.W., Ziccardi, R.J., Schumaker, V.N., and Glovsky, M.M. (1977) J. Immunol. 118, 2182-2191

43. Jaton, J-C., Huser, H., Riesen, W.F., Schlessinger, J., and Givol, D. (1976) J. Immunol. 116, 1363-1366

44. Guyer, R.L., Plotz, P.H., and Segal, D.M. (1978) submitted to Biochemistry

45. Peterson, P.A., Cunningham, B.A., Berggard, I., and Edelman, G.M. (1972) Proc. Nat. Acad. Sci. 69, 1697-1701

46. Isenman, D.E., Painter, R.H., and Dorrington, K.J. (1975) Proc. Nat. Acad. Sci. 72, 548-552

47. Sledge, C.R., and Bing, D.H. (1973) J. Biol. Chem. 248, 2818-2823

48. Isenman, D.E., Ellerson, J.E., Painter, R.H., and Dorrington, K.J. (1977) Biochemistry 16, 233-240

49. Horton, H.R., and Koshland, D.E. (1965) J. Am. Chem. Soc. 87, 1126-1132

50. Allan, R., and Isliker, H. (1974) Immunochemistry 11, 175-180

51. Allan, R., and Isliker, H. (1974) Immunochemistry 11, 243-248

52. Hurst, M.M., Volanakis, J.E., Hester, R.B., Stroud, R.M. and Bennet, J.C. (1974) J. Exp. Med. 140, 117-121

53. Deisenhofer, J., Colman, P.M., Hüber, R., Haupt, H. and Schwick, G. (1976) Hoppe-Seyler's Z. Physiol. Chem. 357, 435-445

54. Deisenhofer, J., Colman, P.M., Epp, O., and Hüber, R. (1976) Hoppe-Seyler's Z. Physiol. Chem. 357, 1421-1434

55. Deisenhofer, J. (1978) personal communication

56. Wolfenstein-Todel, C., Fragione, B., Prelli, F., and Franklin, E.C. (1976) Biochem. Biophys. Res. Commun. 71, 907-914

57. Johnson, B.J. and Thames, K.E. (1976) J. Immunol. 117, 1491-1494

58. Windbridge, G.C., and Jorgensen, E.C. (1971) J. Am. Chem. Soc. 93, 6318-6319

59. Shalteil, S. (1967) Biochem. Biophys. Res. Commun. 29, 178-183

60. Ondetti, M.A., Deer, A., Sheehan, J.T., Pluščec, J., and Kocy, O. (1968) Biochemistry 7, 4069-4075

61. Baba, T., Sugiyama, H. and Seto, S. (1973) Chem. Pharm. Bull. 21, 207-209

62. Erickson, B.W., and Merrifield, R.B. (1973) J. Am. Chem. Soc. 95, 3757-3763

63. Gisin, B.F., and Merrifield, R.B. (1972) J. Am. Chem. Soc. 94, 3102-3106

64. Schnabel, E. (1967) Justus Liebigs Ann. Chem. 702, 188-196

65. Gisin, B.F. (1973) Helv. Chim. Acta 56, 1476-1482

66. Gisin, B.F. (1972) Anal. Chim. Acta 58, 248-249

67. Merrifield, R.B. (1963) J. Amer. Chem. Soc. 85, 2149-2154

68. Erickson, B.W., and Krieger, D.E. (1977) in Antibodies in Human Diagnosis and Therapy (Haber, E., and Krause, R.M. eds) pp. 159-190 Raven Press, New York

69. Sakakibara, S., and Shimonishi, Y. (1965) Bull. Chem. Soc. Jap. 38, 1412-1413

70. Stewart, J.M., and Young, J.D. (1969) Solid Phase Peptide Synthesis p. 62, W.H. Freeman and Company, San Francisco

71. Ohno, M., Tsukamato, S., Makisumi, S., and Izumiya, N. (1972) Bull. Chem. Soc. Jap. 45, 2852-2855

72. Moore, S., and Stein, W.H. (1963) Methods Enzymol. 7, 819-831

73. Hugli, T.E., and Moore, S. (1972) J. Biol. Chem. 247, 2828-2834

74. Blackburn, P. (1978) personal communication

75. Salnikow, J., Liao, T-H., Moore, S., and Stein, W.H. (1973) J. Biol. Chem. 248, 1480-1488

76. Borsos, T., and Rapp, H.J. (1963) J. Immunol 91, 851-858

77. Freifelder, D. (1976) Physical Biochemistry: Applications to Biochemistry and Molecular Biology pp. 267-340, W.H. Freeman and Company, San Francisco

78. Rapp, H.J., and Borsos, T. (1970) Molecular Basis of Complement Action pp. 75-78, Appleton-Century-Crofts, New York

79. Knobel, H.R., Heusser, C., Rodrick, M.L., and Isliker, H. (1974) J. Immunol. 112, 2094-2101

80. Agnello, V., Winchester, R.J., and Kunkel, H.G. (1970) Immunology 19, 909-919

81. McPhie, P. (1971) Methods Enzymol. 22, 23-32

82. King, T.P. (1974) in Clinical Biochemistry: Principles and Methods (Curtius, H.Ch., and Roth,M. eds) pp. 195-208, de Gruyter, New York

83. Yamashiro, D., and Li, C.H. (1973) J. Org. Chem. 38, 2594-2597

84. Boackle, R.J., and Johnson, B.J. (1978) Fed. Proc. 37, 590 Abstr., p. 1377

85. Katsoyannis, P.G., Gish, D.T., Hess, G.P., and du Vingeaud, V. (1958) J. Am. Chem. Soc. 80, 2558-2562

86. Paul, R., and Kende, A.S. (1964) J. Am. Chem. Soc. 86, 4162-4166

87. Mojsov, S. (1978) personal communication

88. Cooper, N.R., and Ziccardi, R.J. (1977) J. Immunol. 119, 1664-1667

89. Lin, T-Y., and Fletcher, D.S. (1978) Immunochemsitry 15, 107-117